



UNIVERSITÀ DEGLI STUDI DI PAVIA
DOTTORATO IN SCIENZE CHIMICHE
E FARMACEUTICHE
XXX CICLO

Coordinatore: Chiar.mo Prof. Mauro Freccero

LIGHT-DRIVEN RELEASE OF ACIDS FOR
TECHNOLOGICAL APPLICATIONS

Tutore

Chiar.mo Prof. Maurizio Fagnoni

Tesi di Dottorato di

EDOARDO TORTI

a.a. 2016- 2017

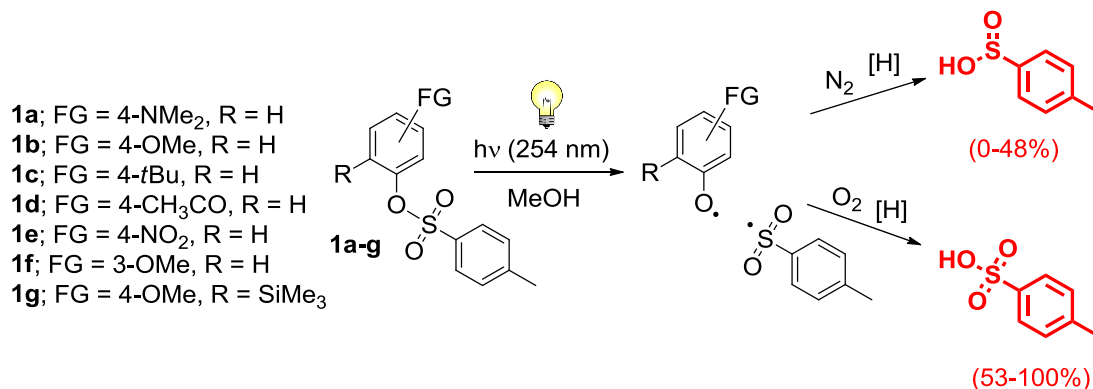
“Luminous beings are we...not this crude matter.”

Yoda - The Empire Strikes Back

Abstract

This thesis is focused mainly on the development of novel photoacid generators (PAGs), compounds able to release strong acids upon light absorption which find application as photoinitiators for cationic polymerization and in photolithography.

We first studied the possibility to use simple aryl tosylates as PAGs. With the only exception of **1e** (photostable), irradiation of tosylates **1a-g** in the absence of oxygen (N₂ saturated solutions) resulted in the formation of different photoproducts along with only poor yields of *p*-toluenesulfinic acid (0-48%, see Scheme I). In O₂ saturated media, however, strong *p*-toluenesulfonic acid was released in moderate to high yields (53-100%), moving from electron-rich to electron-poor tosylates. The photochemical behavior was consistent with a homolytic cleavage of the ArO-S bond with the formation of a radical pair. Under oxygenated conditions, trapping of the generated *p*-toluenesulfonyl radical by O₂ occurred and CH₃C₆H₄SO₃H was liberated in solution. The studied tosylates were successfully tested also as photoinitiators for the cationic polymerization of an epoxy based hybrid organic-inorganic material, confirming their suitability as PAGs.

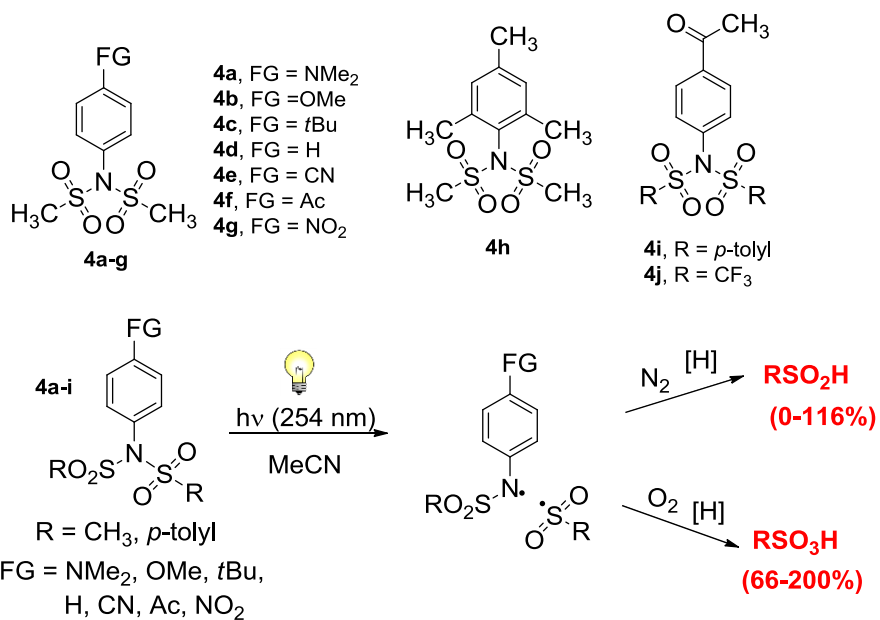


Scheme I. Mechanism of acids photorelease from aryl tosylates.

We focused then on systems potentially able to generate two or more equivalents of acid for one equivalent of PAG. Accordingly we studied the photochemistry of *N*-arylsulfonimides **4a-j** (Scheme II). Except for **4g** (photostable), irradiation of **4a-i** in N₂ saturated acetonitrile resulted in the formation of *N*-arylsulfonamides, anilines and thia-Fries rearrangement products, along with weak sulfinic acids (0-116%). In contrast, in O₂ saturated media strong sulfonic acids were released in high yields (up to 2 equivalents for one equivalent of **4a-i**), confirming our initial hypothesis. Again, the yields of acid released became higher moving from electron-rich to electron-poor aromatics and the obtained results were justified by a mechanism based on the homolytic cleavage of the ArN-S bond with the formation of a radical pair. In addition, in the present case, each of the two ArN-S bonds can be photocleaved. A different behavior was observed from irradiation of **4j**: in this case, after the formation of a sulfonyl radical, SO₂ is lost from the latter to produce a F₃C• radical. Thus no strong acid was released but the trifluoromethyl radical generated was however used to perform photochemical trifluoromethylations of (hetero)aromatic compounds.

N-arylsulfonimides were likewise tested as photoinitiators for cationic polymerization of the epoxy-based hybrid organic-inorganic material employed also for tosylates and they were found to be as efficient as commercially available PAG (DPST, see Chart I). Subsequently, micrometric patterns were achieved using one of these compounds (**4f**), thus proving their suitability in photolithographic applications.

Going on with the project, we switched from conventional UV lithography to extreme ultraviolet lithography (EUVL), a next generation technique which employs extreme ultraviolet (EUV) radiation ($\lambda \sim 13$ nm) to pursue a better resolution of the obtained lithographic patterns.



Scheme II. *N*-arylsulfonimides studied and their photochemical behavior.

Thus, we synthesized two pentafluorophenyl sulfonates (**1h,i**, see Chart I), PAGs specifically designed to properly work with this radiation. These new PAGs were tested as cationic initiators for EUV promoted polymerization of the usual epoxy-based material and **1h** behaved much better than commercial DPST. We then performed lithographic experiments by using EUV irradiation: films of the hybrid epoxy-based material containing **1h** were exposed and patterns with feature size down below 100 nm were successfully obtained with extremely low EUV dose (6 mJ/cm²).

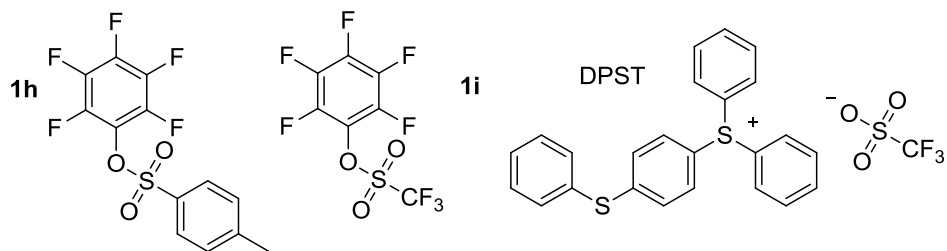


Chart I. Compounds tested PAGs for EUV lithography (DPST is a commercially available PAG).

Lastly, as part of a research carried on at the Masaryk University (Brno, Czech Republic), we tried to enlarge the field of application of PAGs. Accordingly, we used other non-ionic photoacid generators (based on the *p*-hydroxyphenacyl protecting group) as phototriggers for the oxidation of Fe²⁺ ion by persulfate, in combination with a supramolecular host-guest system.

Index

1	Introduction	1
1.1	<i>Photorelease, caged protons and photoacid generators.</i>	1
1.2	<i>Diaryliodonium and triarylsulfonium salts.</i>	2
1.3	<i>Cationic photopolymerization.</i>	4
1.4	<i>Photoacid Generators in photolithography.</i>	5
1.5	<i>Non-ionic photoacid generators.</i>	7
1.6	<i>Aryl sulfonates as non-ionic photoacid generators.</i>	10
1.7	<i>Aim of the thesis.</i>	11
2	Aryl tosylates as non-ionic photoacid generators	13
2.1	<i>Introduction.</i>	13
2.2	<i>Results.</i>	15
2.3	<i>Discussion.</i>	25
2.3.1	<i>Photochemistry of aryl tosylates.</i>	25
2.3.2	<i>Applications in cationic photopolymerization.</i>	29
2.4	<i>Conclusion.</i>	29
3	<i>N</i>-arylsulfonimides: photochemistry and applications as PAGs for photolithography	31
3.1	<i>Introduction.</i>	31
3.2	<i>Results.</i>	32
3.2.1	<i>Photochemical experiments on 4a-j.</i>	32
3.2.2	<i>Photochemical experiments on 5a-j and 6a,b.</i>	40
3.2.3	<i>Laser flash photolysis (LFP) and EPR experiments.</i>	42
3.2.4	<i>Photopolymerization and photopatterning experiments.</i>	47
3.3	<i>Discussion.</i>	50
3.3.1	<i>Photochemistry of compounds 4a-j.</i>	50
3.3.2	<i>Applications in cationic polymerization and photolithography.</i>	53
3.4	<i>Conclusion.</i>	54
4	Aryl sulfonates for EUV lithography	55

4.1	<i>Introduction.</i>	55
4.2	<i>Results and discussion.</i>	56
4.2.1	Design and synthesis of photoacid generators.	56
4.2.2	EUV promoted polymerization of hybrid organic-inorganic materials.	59
4.2.3	EUV promoted patterning experiments.	63
4.3	<i>Conclusion.</i>	67
5	Phototriggered oxidation of Fe²⁺ by release of HI	68
5.1	<i>Introduction.</i>	68
5.2	<i>Results and discussion.</i>	69
5.3	<i>Conclusion.</i>	82
6	Photoinduced trifluoromethylation of aromatics by an N-arylsulfonimide	83
6.1	<i>Introduction.</i>	83
6.2	<i>Results and discussion.</i>	85
6.3	<i>Conclusion.</i>	93
7	Conclusion	94
8	Experimental Section	96
8.1	<i>Experimental details regarding chapter 2.</i>	96
8.1.1	General Information.	96
8.1.2	Synthesis of aryl tosylates 1a-g .	97
8.1.3	Preparative irradiations.	99
8.1.4	Use of aryl tosylates in polymerization processes.	101
8.2	<i>Experimental details regarding chapter 3.</i>	102
8.2.1	General Information.	102
8.2.2	Synthesis of <i>N</i> -arylsulfonamides 5a-j .	104
8.2.3	Synthesis of <i>N</i> -arylsulfonimides 4a-j .	107
8.2.4	Preparative irradiations.	110
8.2.5	Photopolymerization and photopatterning experiments with sulfonimides.	114
8.3	<i>Experimental details regarding chapter 4.</i>	115
8.3.1	General Information.	115

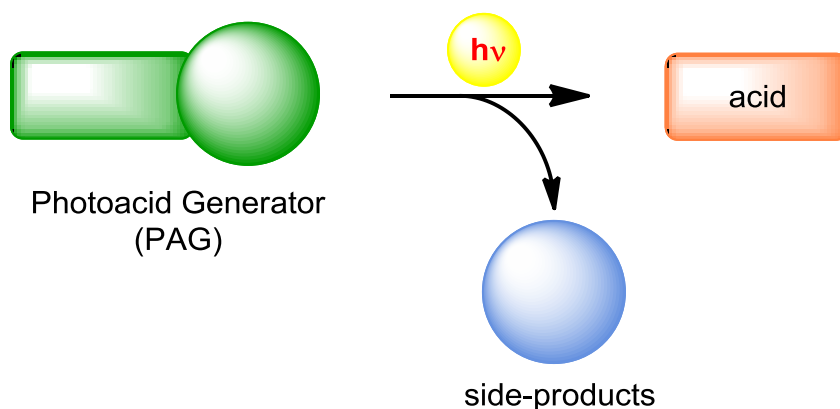
8.3.2	Synthesis of photoacid generators 1d , 1i and 1j .	116
8.3.3	Synthesis of hybrid organic-inorganic matrices.	117
8.3.4	Polymerization and patterning experiments.	117
8.3.5	Determination of PAGs reduction potentials.	120
8.4	<i>Experimental details regarding chapter 5.</i>	121
8.4.1	General Information.	121
8.4.2	Syntheses.	122
8.4.3	Photochemical experiments on 11a and 11b .	125
8.4.4	Experiments on phototriggered oxidation of Fe ²⁺ .	127
8.4.5	Determination of the Fe ²⁺ concentration by 1,10-phenanthroline.	128
8.5	<i>Experimental details regarding chapter 6.</i>	129
8.5.1	General Information.	129
8.5.2	Synthesis of sulfonimide 4j and sulfonamide 5j .	131
8.5.3	General procedures for photochemical trifluoromethylations.	131
8.5.4	Compounds synthesized by photochemical trifluoromethylations.	132
9	Acknowledgements	138
10	References	139

1 Introduction

1.1 Photorelease, caged protons and photoacid generators.

Caged compounds are light-sensitive probes which encapsulate chemically or biologically active substances to be *photoreleased*, that means liberated by irradiation.^[1] In practice they are compounds made initially inactive by the presence of a photolabile protecting group which can be cleaved by irradiation, to give the desired species. These systems are usually developed for the photorelease of drugs and biomolecules for medicinal and biological applications where temporal and spatial control over the concentration of the active species is required.

There is however a particular class of caged compounds involved in the liberation of completely different substances. These are the so-called photoacid generators (PAGs), compounds able to release acid species upon light absorption (Scheme 1.1). In particular, these systems are commonly exploited to release very strong Brønsted acids (e.g. $\text{CH}_3\text{SO}_3\text{H}$, $\text{CF}_3\text{SO}_3\text{H}$, HSbF_6 , HPF_6 , HBF_4 , etc.).^[2]



Scheme 1.1. Photorelease of acids from photoacid generators.

In view of the nature of the generated acids, PAGs are not usually employed in biology but they find application in polymer and material chemistry as a sort of “caged protons” to be used whenever a well-defined, precise and confined increase of acidity is needed.

1.2 Diaryliodonium and triarylsulfonium salts.

One of the first class of photoacid generators to be developed (and maybe the most employed one) is given by photoactive diaryliodonium and triarylsulfonium salts.^[3] Some of these PAGs are depicted in the Chart 1.1 as examples.

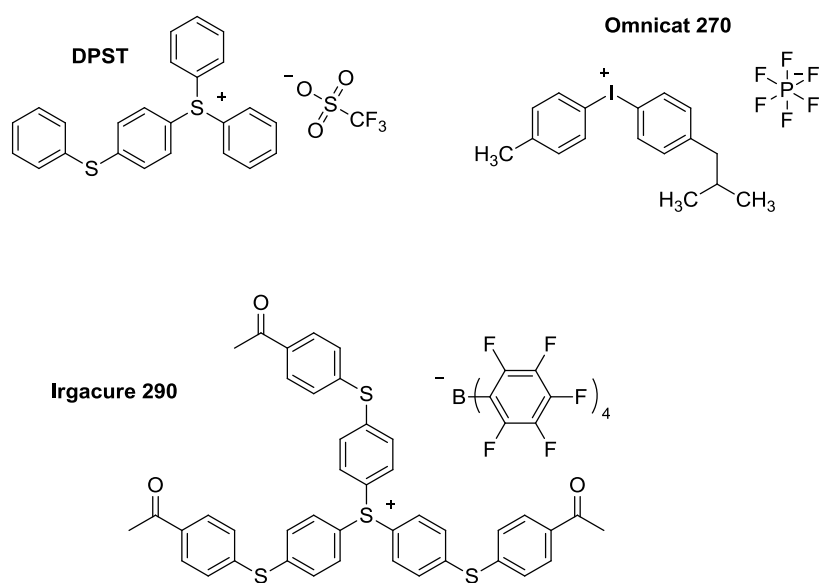


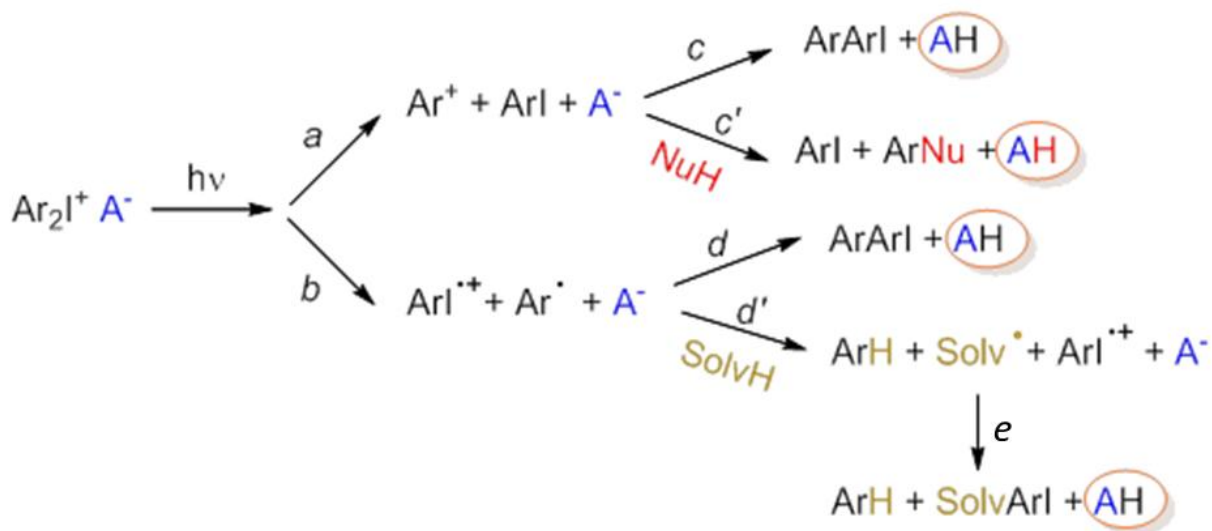
Chart 1.1. Commercially available ionic photoacid generators supplied by Sigma-Aldrich (DPST), iGM Resins (Omnicat 270) and BASF (Irgacure 290).

The mechanism of acid generation from these ionic compounds is shown in the Scheme 1.2 for the case of iodonium salts.^[4] When the salt is irradiated, heterolysis of one Ar-I bond occurs from the singlet excited state (*path a*) to give an aryl cation (Ar^+) and an aryl iodide (ArI). Ar^+ can then

either attack ArI bringing to biaryl ArArI (*path c*) or undergo solvolysis to ArNu (*path c'*), in the case the reaction takes place in a nucleophilic medium (NuH). However both of the reactions bring eventually to proton photorelease, with the subsequent formation of the acid AH.

Alternatively, photoinduced homolysis of Ar-I bond can occur (from either the singlet or triplet excited state, *path b*), giving radical Ar[•] and radical-cation ArI^{•+}. The two intermediates could then react in two different ways. Indeed they can either recombine to form biaryl ArArI (*path d*) or Ar[•] can abstract hydrogen from the reaction medium (SolvH) to give the aromatic compound ArH and the radical Solv[•] (*path d'*). Finally ArI^{•+} and Solv[•] react with each other to give SolvArI (*path e*). Both *path d* and *path d'*, however, bring again to proton release. Thus the photoinduced homolytic cleavage generates acids AH as well.

Triarylsulfonium salts photorelease acids with an analogous mechanism, with the only difference that, in this case, a C-S bond is photocleaved instead of a C-I bond.^[5]



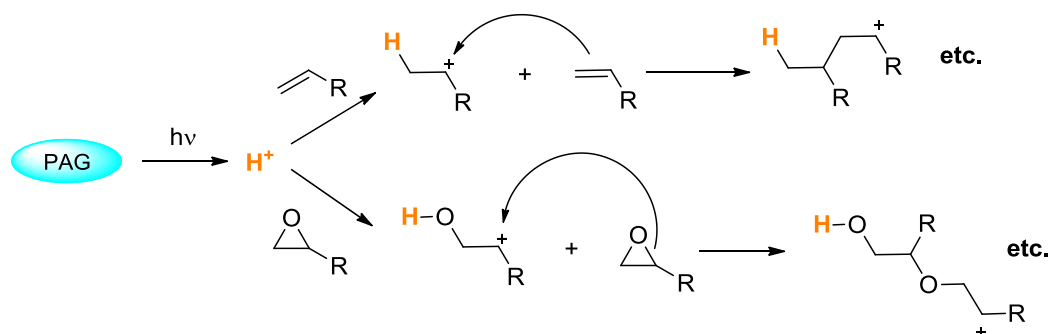
Scheme 1.2. Mechanism of acid photogeneration from diaryliodonium salts.

1.3 *Cationic photopolymerization.*

As mentioned above, PAGs such as iodonium and sulfonium salts find wide application in material science and, in particular, for photopolymerization.^[3b,6] The latter is a technique which employs light irradiation to promote chemical reactions, starting the polymerization process.^[6b] It is used in all the situations where very high precision in the realization of the final device is desired: it allows indeed better control over the process, compared to other polymerization strategies. Moreover it provides a number of ecological (and economical) advantages over traditional thermal curing techniques, including low material costs, solvent-free formulations and room temperature treatments.^[6a,b]

Photopolymerization requires the use of photosensitive initiators, able to release reactive species only upon light (usually UV-light) exposition. Thus photopolymerization can be divided in either radical or cationic polymerization, depending on the nature of the photoreleased reactive intermediate. The former is surely better known for its widespread use in dental materials realization^[7] but the latter offers the notable advantage of not being inhibited by oxygen: this condition eliminates the need for high irradiation intensities and for the use of an inert atmosphere during curing.^[6c,8]

Hence the importance of photoacid generators in photopolymerization is easily understood, as they are the commonly employed photoinitiators in cationic polymerization process.^[3b,6] Indeed the strong acids released by PAGs irradiation readily react with acid-sensitive monomers present in the reaction mixture to give a cationic intermediate. The latter then attacks a second monomer extending the polymer chain and giving another active cation able to further propagate the process (Scheme 1.3).^[6b]



Scheme 1.3. Mechanism of cationic photopolymerization of olefins and epoxy rings.

Many different monomers can be successfully polymerized by this technique, ranging from olefins (such as styrenes and vinyl ethers) to cyclic ethers, lactones and epoxy rings.^[3b,6b,c] For this reason, besides dentistry,^[9] cationic photopolymerization is employed in many other fields, for example to realize inject inks, adhesives, coatings and devices for composites and silicones industry.^[3b,6c,10]

1.4 Photoacid Generators in photolithography.

The peculiar behavior of PAGs make them suitable not only as photoinitiators for cationic polymerization, but also in other important technological applications where the controlled release of acid is a crucial step, such as 3D printing,^[11] super-hydrophobic coating^[12] and biopolymerization.^[13]

However the second field where proton photorelease has been applied more consistently is microelectronic industry, in photolithographic techniques used to achieve micro and nano-structures on integrated circuits, MEMS and other optoelectronic devices. In detail photolithography consists in the selective light exposure of chosen areas of a photosensitive material deposited on silicon (or semiconductor) substrates, in order to obtain chemical changes

which modify the solubility of the exposed material. Then development with a proper solvent able to dissolve either the irradiated (positive development) or the non-irradiated areas (negative development) and a subsequent etching process give the desired pattern on the silicon wafers (Figure 1.1).

The photosensitive systems are usually polymer matrices and are called photoresists.^[2a,c,d,14] The role of PAGs in photoresists is instead to be the real photoreactive species: they promote acid-catalyzed reactions in the system after irradiation, thus bringing to desired structural modifications.^[2a,c,d,15]

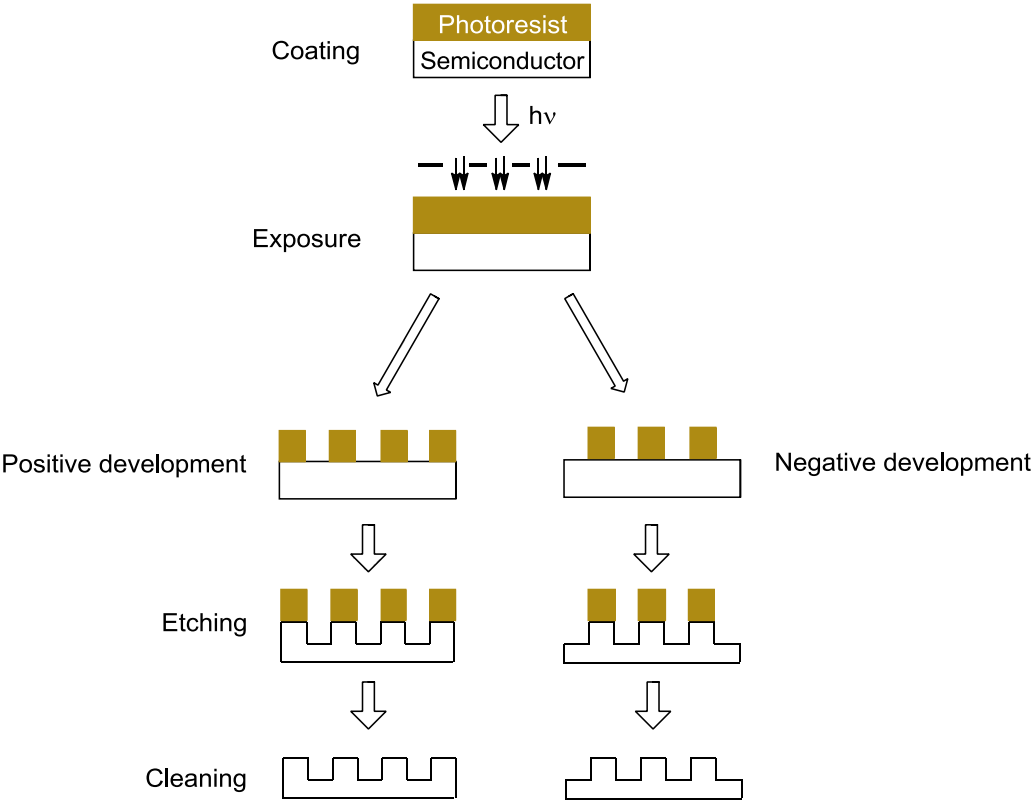
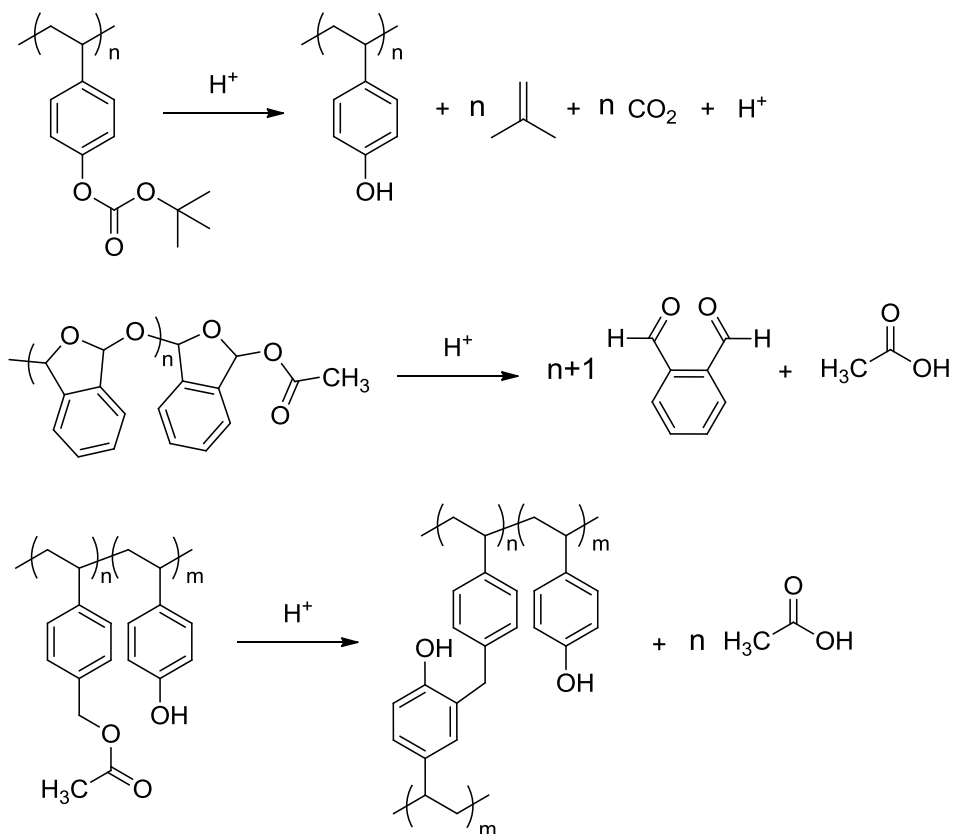


Figure 1.1. Picture describing a general photolithographic process (illustration based on a figure presented in the Ref. 14c)

Some examples of commonly employed photoresists and reactions in which they are involved (mainly removals of protecting groups, polymer degradations and crosslinking reactions) are given in the Scheme 1.4.^[2a,c,d,14b,c,15]



Scheme 1.4. Examples of widely used photoresists.

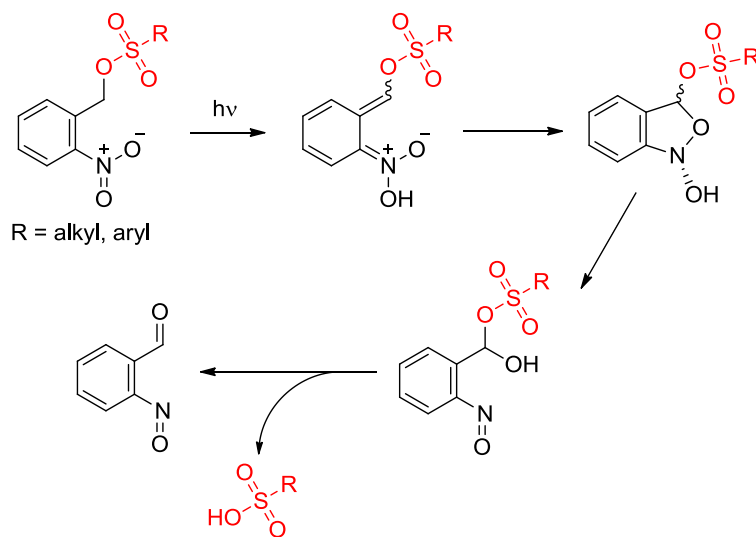
1.5 Non-ionic photoacid generators.

Albeit diaryliodonium and triarylsulfonium salts are very common in photolithographic applications due to their high efficiency (up to $\Phi = 0.9$) and thermal stability,^[2b,3b] they usually display poor solubility in polymer matrices used in photoresists, causing problems such as loss of reproducibility or phase separations.^[2c,16] Moreover, their syntheses require the use of peracids, transition metal catalysts, dehydrating agents and other hazardous reagents.^[17] Thus the design of

new more soluble and eco-friendly non-ionic PAGs is a crucial issue for materials chemistry. Accordingly, a great variety of new PAGs able to photorelease mainly sulfonic acids was developed.^[2b]

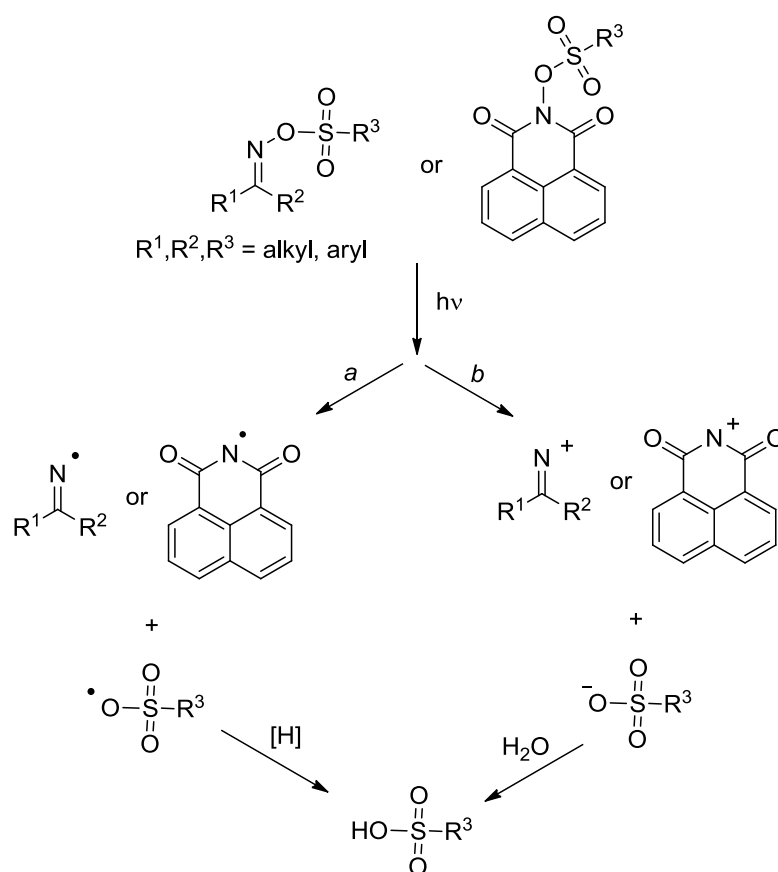
Among them, 2-nitrobenzyl esters of sulfonic acids are a milestone. Indeed, even if the 2-nitrobenzyl photoremovable protecting group is well known for its use in organic synthesis^[18] and for the photorelease of biomolecules (e.g. aminoacids, peptides, nucleotides),^[1,19] its chemistry was successfully applied also to release sulfonic acids for lithographic purposes.^[20] In fact the peculiar photoinduced intramolecular *o*-nitrobenzyl rearrangement on these sulfonates affords a nitrosobenzaldehyde along with the desired sulfonic acid (Scheme 1.5).^[21]

Despite based on a robust photochemistry, the quantum yields of acid generation in polymer films (not exceeding $\Phi = 0.3$) are lower than those observed for iodonium and sulfonium salts.^[20]



Scheme 1.5. Photorelease of sulfonic acids from the photorearrangement of 2-nitrobenzyl sulfonates.

Hence other non-ionic PAGs were developed ^[22] and good results in the photorelease of sulfonic acids were obtained with iminosulfonates ^[23] and imidosulfonates. ^[24] Indeed, after irradiation, both of them give mainly homolytic cleavage of N-O bond, generating a sulfoniloxy radical which, upon hydrogen abstraction, brings to the desired sulfonic acid (see Scheme 1.6, *path a*).^[25,26] Photoheterolysis of N-O bond can likewise occur and this reaction pathway becomes predominant in the case of the release of perfluoroalkylsulfonic acids (Scheme 1.6, *path b*).^[25a,26c]

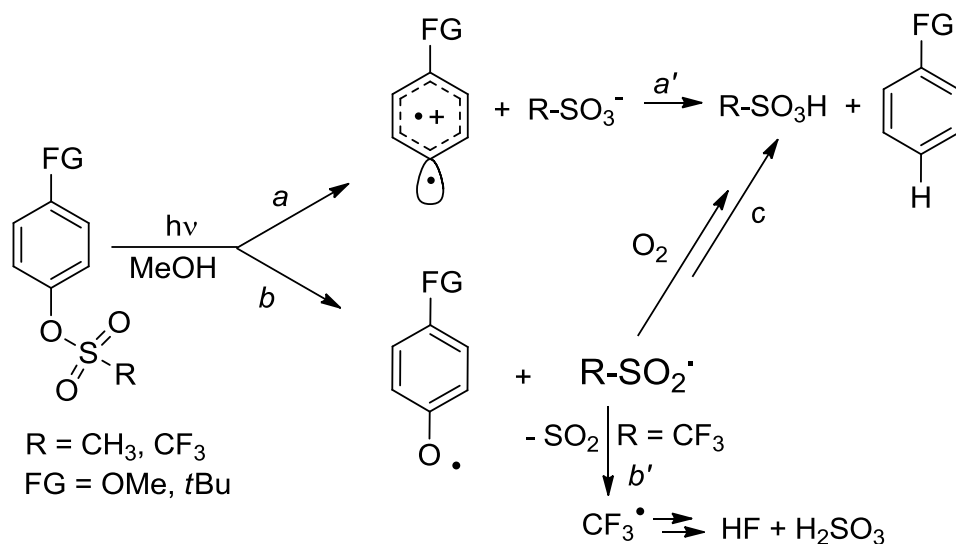


Scheme 1.6. Main mechanisms of sulfonic acid photorelease from iminosulfonates and imidosulfonates. *Path b* is predominant when $\text{R}^3 = \text{CF}_3$.

1.6 Aryl sulfonates as non-ionic photoacid generators.

The search for better non-ionic PAGs was carried out also in our research group. In particular our initial goal was to develop new PAGs with an efficiency comparable to that of iminosulfonates and imidosulfonates but with a simpler molecular structure, thus getting compounds easier and cheaper to be synthesized. In fact few years ago we demonstrated that very simple aryl sulfonates such as mesylates and triflates are able to release sulfonic acid in very high yield (> 90%) and therefore they can be applied as alternative non-ionic photoacid generators.^[27]

As depicted in the Scheme 1.7 two mechanisms for the acid photorelease compete, namely, heterolysis of the Ar–OS bond (*path a*) and homolysis of the ArO–S bond (*path b*), depending on the substituent FG present on the aromatic ring and on the sulfonic moiety.



Scheme 1.7. Competitive pathways in the photorelease of acids from (substituted) aryl mesylates and triflates.

In the former case, a sulfonic acid is released directly after heterolysis (*path a'*), whereas in the latter case trapping of the generated RSO_2^\cdot radical by oxygen present in the reaction medium ^[28] leads to the formation of RSO_3H (*path c*). Notably the presence of molecular oxygen is crucial in the case of aryl triflates because, otherwise, fragmentation of $\text{CF}_3\text{SO}_2^\cdot$ occurs (*path b'*) and, since only *path b* is active for these compounds, just weak acids, such as HF and H_2SO_3 , can be obtained. However both *path a* and *path b* are feasible for the liberation of strong sulfonic acids.

1.7 Aim of the thesis.

The main research project behind the present thesis was oriented to develop innovative and efficient non-ionic PAGs based on simple molecular structures, whose synthesis was clean and cost (and time) effective. The second target of the project was to apply the newly made PAGs in technological applications, mainly for photolithography but also as initiators for cationic polymerization. Thus results found during the project are reported in the next chapters of this thesis.

In addition, studies about different applications of photoacid generators were likewise carried on. In particular, the photorelease of acids such as hydrogen iodide to perform phototriggered oxidations in supramolecular host-guest systems is reported. Furthermore, the peculiar photochemistry of some of the newly synthesized PAGs was exploited to perform radical reactions for organic synthesis: results obtained are described in the last chapter of the thesis.

In detail, the thesis is divided in the following chapters:

- **Chapter 2: Aryl tosylates as non-ionic photoacid generators.** This chapter describes the photochemistry of differently substituted aryl tosylates and their application as PAGs for cationic polymerization.

- **Chapter 3: *N*-arylsulfonimides: photochemistry and applications as PAGs for photolithography.** This chapter describes the photochemistry of novel PAGs, namely *N*-arylsulfonimides, and their use in photolithography.
- **Chapter 4: Aryl sulfonates for EUV lithography.** This chapter is devoted to the development of some specifically designed aryl sulfonates to be used as PAGs for extreme ultraviolet lithography, a next generation lithographic technique.
- **Chapter 5: Phototriggered oxidation of Fe²⁺ by release of HI.** This chapter focuses on the photorelease of HI to trigger the oxidation of Fe²⁺ by S₂O₈²⁻ in the presence of a macrocyclic cage.
- **Chapter 6: Photoinduced trifluoromethylation of aromatics by an *N*-arylsulfonimide.** This chapter show the application of an *N*-arylsulfonimide in organic synthesis, to perform radical trifluoromethylation of (hetero)aromatics.

2 Aryl tosylates as non-ionic photoacid generators

2.1 Introduction.

Starting from the good results obtained with aryl mesylates and triflates,^[27] we decided at first to enlarge this previous research testing other kinds of aryl sulfonates as non-ionic photoacid generators. Thus we focused on aryl tosylates, since they are crystalline compounds readily prepared from inexpensive reagents and they are more stable toward hydrolysis than other commonly used sulfonates (such as triflates and mesylates already tested). In addition, aryl tosylates have shown a higher thermal stability than the corresponding mesylates when heated in a poly-(4-hydroxystyrene) matrix.^[29] Furthermore the photorelease of *p*-toluenesulfonic acid (PTSA) from nitrobenzyl tosylates,^[20b,f,g] imidotosylates^[26c,28a] and iminotosylates^[25a] have been extensively studied and some commercially available PAGs are currently based on the structure of iminotosylates (e.g. Irgacure 121).

Conversely the photochemistry of aryl tosylates was rarely investigated^[30] and, to the best of our knowledge, the use of aryl tosylates as PAGs has been tested only with *o*-arenesulfonyloxyanilide derivatives, where photorelease of PTSA was found to be almost quantitative, albeit with a very low efficiency (Φ_{-1} ca. 0.05).^[30a]

For this reasons aryl tosylates were believed to be worth to be investigated and the aim of the work presented in this chapter was the exploration of the photochemistry of some substituted phenyl tosylates, as well as the evaluation of their potential use as photoinitiators for acid-induced polymerization.

Regarding this second target, the system chosen for polymerization experiments was an innovative epoxy-based hybrid organic-inorganic matrix,^[31] obtained via a sol-gel process.^[32]

Indeed the preparation of such a kind of system proceeds by hydrolysis and condensation reactions of organically modified alkoxides with formulas $\text{RSi}(\text{OR}')_{4-n}$, obtained by acid or basic catalysis. The presence of a non-hydrolysable Si–C bond provides a stable linkage between the organic unit and the oxide matrix, resulting in an inorganic tridimensional network with pendant, reactive moieties (e.g. double bonds or, as in the present case, acid sensitive epoxy rings) which could lead to further cross-linking, as schematically depicted in Figure 2.1.^[31]

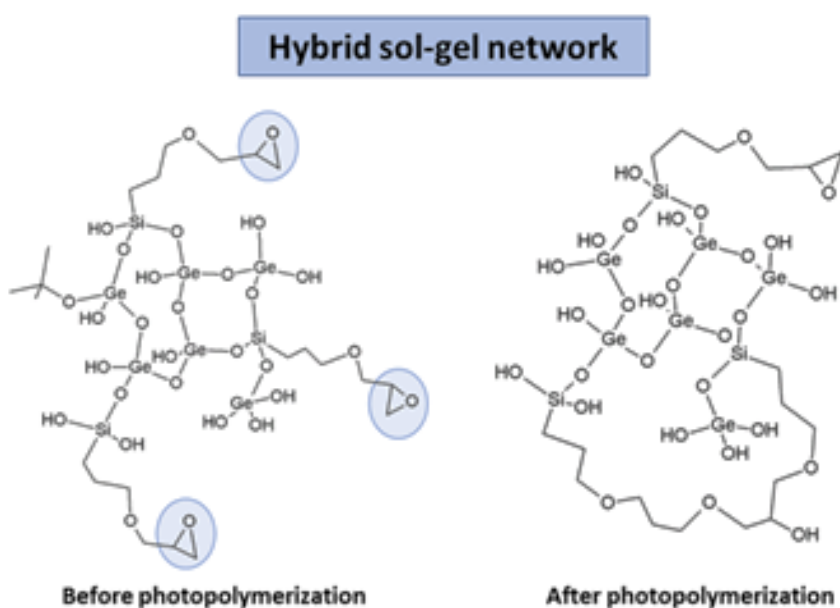


Figure 2.1. Example of an epoxy-based hybrid sol-gel network before and after UV-induced polymerization.

These matrices were selected because they have many advantages over the traditional photoresists: high thermal resistance, mechanical strength and chemical endurance, together with the possibility to tune their refractive index. All these features make them suitable also for “one-step” photolithographic processes, where no etching step is required and the material itself can be used as the final device just after irradiation.^[31]

Results obtained about the photochemistry of tested aryl tosylates and about their application as photoinitiators for cationic polymerization are described and discussed below.^[33]

2.2 Results.

A series of phenyl sulfonates substituted with both electron-donating and electron-withdrawing groups (**1a-f**, see Chart 2.1) were examined. The silylated derivative **1g** was also tested because it was previously demonstrated in our group that the presence of silicon-based substituents was able to influence the photoreactivity of aryl sulfonates.^[34] These substrates were synthesized from the corresponding phenols.^[35]

First the absorption and emission properties of tosylates **1a-g** were studied. Two absorption maxima in the UV region around 260-290 nm ($\epsilon > 5000 \text{ M}^{-1} \text{ cm}^{-1}$) and 220-240 nm ($\epsilon > 10^4 \text{ M}^{-1} \text{ cm}^{-1}$) were observed for compounds **1a-c** and **1e-g** (see below for right absorption maxima, Table 2.2), whereas compound **1d** exhibited single significant absorption at 239 nm ($\epsilon = 17800 \text{ M}^{-1} \text{ cm}^{-1}$).

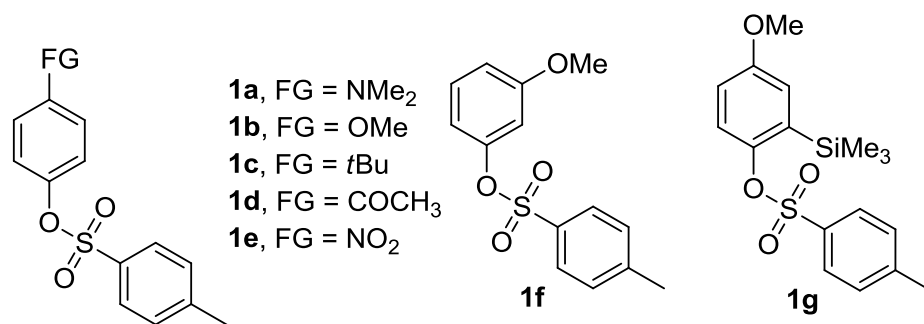
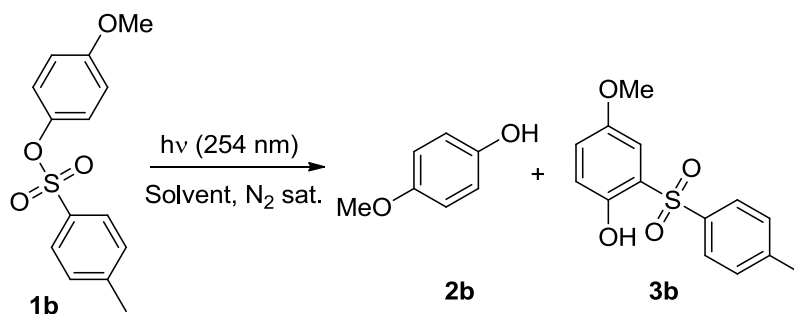


Chart 2.1. Aryl tosylates studied in the present work.

Photochemical investigation started with 4-methoxyaryl tosylate **1b** (Table 2.1), including the measurement of the disappearance quantum yield (Φ_{-1}). This turned out to be modest in all of the solvents tested ($\Phi_{-1} = 0.07$ - 0.14). Photolysis of **1b** under UV irradiation ($\lambda = 254$ nm, chosen on the basis of the absorption spectra) caused an exclusive ArO-S bond cleavage and 4-methoxyphenol **2b** and *o*-tosylphenol **3b** (a photo-Fries adduct) were formed in variable amounts depending on the solvent employed. Compound **3b** was the only product formed in cyclohexane, whereas the amount of **2b** increased with proticity (methanol, 2-methoxyethanol) or with the presence of easily cleavable C-H bonds (see for instance the case of THF). No products arising from Ar-OS bond cleavage, such as anisole or 1,4-dimethoxybenzene, were detected, contrary to what was observed for the other methoxyphenyl sulfonates previously studied.^[27] Irradiation in neat acetone (a triplet sensitizer) caused likewise the complete consumption of **1b**, forming **2b** as the main product. The same experiment carried out in oxygenated acetone led to no **1b** consumption. The photolyzed solution in methanol was subjected to potentiometric titration and ionic chromatography analyses, revealing that 4-tolylsulfonic acid was liberated in modest yield (*ca.* 40%).

Table 2.1. Irradiation of Aryl Tosylate **1b** in neat solvents.^[a]

Solvent	Φ_{-1}	2b , yield %	3b , yield %
Cyclohexane	-	4	68
CH ₂ Cl ₂ ,	0.08 ^[b]	12	33
CH ₃ COOCH ₂ CH ₃	-	26	36
THF	-	39	24
CH ₃ COCH ₃	-	30	10
CH ₃ CN,	0.13 ^[b]	24	30
CH ₃ OCH ₂ CH ₂ OH	0.07 ^[b]	34	29
CH ₃ OH	0.14 ^[b]	41	28

^[a] A nitrogen-saturated solution of **1b** (10⁻² M) in the chosen solvent irradiated at 254 nm (4×15 W Hg lamps, 2h) until a >80% consumption of **1b** was achieved. Product yields derived by GC analyses and calculated on the basis of the amount of **1b** consumed. ^[b] Disappearance quantum yield (Φ_{-1}) measured on a 10⁻² M **1b** solution in the chosen solvent ($\lambda = 254$ nm, 1×15W Hg lamp) by using potassium ferrioxalate as actinometer.

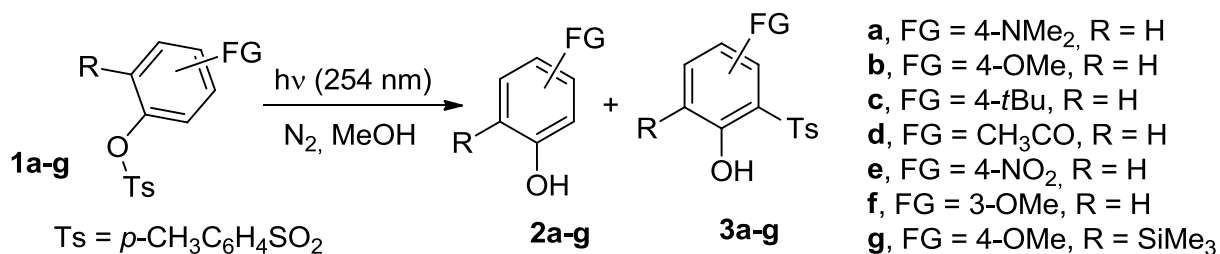
We proceeded then to investigate the photorelease of acids from tosylates **1a-g** in methanol under both nitrogen- and oxygen-saturated conditions (Table 2.2). Under deaerated conditions, the Φ_{-1} measured was in the 0.1-0.15 range except for **1d**, to which the acetyl group imparted a higher photoreactivity ($\Phi_{-1} = 0.29$), and **1e** which was virtually photostable under these conditions (Table 2.2). It is notable that the presence of a trimethylsilyl group made the tosylate more photoreactive (compare the Φ_{-1} value of **1b** with **1g**, Table 2). Noteworthy, the disappearance

quantum yield ($\Phi_{.1}$) values for **1b** and **1d** were not affected by the presence of oxygen (Table 2.2).

Cleavage of the sulfonyl group upon UV light absorption led either to phenols **2** or to photo-Fries adducts **3**, in analogy to what had been observed for **1b**. Formation of **3** was exclusive when a strong electron-donating group (FG = NMe₂) was present, negligible with electron-withdrawing groups (e.g. MeCO, Table 2.2) or of the same order as **2** with less strongly donating groups (FG = OMe, *t*Bu). Photocleavage of the ArO-S bond occurred independently of the nature and the position of the substituents present on the aromatic ring (except for the case of unreactive **1e**). The formation of the photo-Fries products, on the contrary, depended on position, as shown by the different results from isomeric **1b** and **1f** (no Fries adduct in the latter case).

As for the release of acid, potentiometric titration and ionic chromatography analyses were likewise carried out on the photolyzed solutions, showing that *p*-toluenesulfinic acid was formed in variable amounts in nitrogen saturated methanol, with the single exception of tosylate **1d**, for which a mixture of *p*-toluenesulfinic acid and PTSA was observed. As expected, the higher was the amount of phenol **3** formed, the smaller was the amount of acid released (Table 2.2).

On the other hand, under oxygenated conditions, a large amount of PTSA was released depending on the tosylate used (up to quantitative for **1d**) and the corresponding sulfinic acid was found only as a minor product in the case of **1b**. The lowest yield of released PTSA was found in the photolysis of **1a** (Table 2.3).

Table 2.2. Irradiation experiments on aryl tosylates **1a-g** in neat nitrogen purged methanol.

	λ_{\max} (nm), ϵ/L (mol ⁻¹ cm ⁻¹) ^[a]	Φ_{-1} ^[b]	Photoproducts, yield % ^[c,d]	H ⁺ , yield % ^[c,e]	Acids, yield % ^[c,f]
1a	231, 8241	0.11	3a , 100	[g]	[g]
	264, 10287				
1b	317, 1171	0.14 ^[h]	2b , 41 3b , 28	40	CH ₃ C ₆ H ₄ SO ₂ H, 38
	227, 21190				
	274, 2423				
1c	227, 15060	0.14	2c , 52 3c , 18	50	CH ₃ C ₆ H ₄ SO ₂ H, 48
	263, 1230				
1d	232, 28320	0.29 ^[h]	2d , 73	67	CH ₃ C ₆ H ₄ SO ₂ H, 45 CH ₃ C ₆ H ₄ SO ₃ H, 29
1e	227, 7980	< 0.01	[i]	[g]	[g]
	264, 6350				
1f	224, 20940	0.11	2f , 52	49	CH ₃ C ₆ H ₄ SO ₂ H, 47
	273, 3057				
1g	228, 17100	0.21	2g , 21 3g , 18	32	CH ₃ C ₆ H ₄ SO ₂ H, 22
	285, 2010				

^[a] Maximum absorption wavelength and molar absorption coefficient. ^[b] Disappearance quantum yield measured on a 10⁻² M **1a-g** solution in nitrogen saturated MeOH (λ = 254 nm, 1×15 W Hg lamp) by using potassium ferrioxalate as actinometer. ^[c] A 10⁻² M solution of tosylates **1a-g** in nitrogen saturated MeOH irradiated for 2 h at 254 nm (4×15 W Hg lamps) until total consumption of **1a-g**. ^[d] GC yields. ^[e] Determined by potentiometric titration. ^[f] Determined by HPLC ion chromatography analyses. ^[g] No acid released. ^[h] A similar Φ_{-1} value was measured under oxygen saturated conditions. ^[i] No photoproducts detected by GC analysis.

Table 2.3. Amount and type of acid released upon irradiation of **1a-g** in oxygen saturated methanol.^[a]

ArOTs	H ⁺ , yield % ^[b]	Acids, yield % ^[c]
1a	46	CH ₃ C ₆ H ₄ SO ₃ H, 53
1b	82	CH ₃ C ₆ H ₄ SO ₃ H, 82 ^[d]
1c	96	CH ₃ C ₆ H ₄ SO ₃ H, 90
1d	100	CH ₃ C ₆ H ₄ SO ₃ H, 100
1e	[e]	[e]
1f	99	CH ₃ C ₆ H ₄ SO ₃ H, 95
1g	84	CH ₃ C ₆ H ₄ SO ₃ H, 77

^[a] A 10⁻² M solution of tosylates **1a-g** in oxygen saturated methanol irradiated for 2 h at 254 nm (4×15 W Hg lamps) until total consumption of **1a-g**. ^[b] Determined by potentiometric titration. ^[c] Determined by means of HPLC ion chromatography analyses. ^[d] CH₃C₆H₄SO₂H (< 4%) was likewise formed. ^[e] No consumption of **1e** was observed.

Some mechanistic studies were carried out with tosylates **1b** and **1d** as well as the photostable **1e**. Laser flash photolysis at 266 nm of an argon-saturated solution of **1b** (ca. 10⁻⁴ M) in methanol revealed the rapid formation (within a few ns) of two intense absorption bands with $\lambda_{\text{max}} = 330$ nm and 410 nm respectively, with a weaker, broad absorption located at longer wavelengths (580-700 nm, Figure 2.2a). The time evolution of the absorption bands indicated the presence of different transient species, with the predominant contribution from a long lived intermediate ($\tau = 24 \mu\text{s}$, $k = 1.5 \times 10^{10} \text{ M}^{-1} \text{ s}^{-1}$) in both bands. Kinetic analysis revealed the presence of a second short-lived ($\tau = 4.1 \mu\text{s}$) species absorbing at 330 nm.

Shifting to an oxygen-saturated solution resulted in a slight modification of the transient absorption profile, with quenching of that portion of the 330 nm absorption attributable to the short lived species (see Figure 2.2a), while the kinetics of the remaining absorption bands

remained almost unchanged (Figure 2.2b). Notably the residual broad band at 580-700 nm was observed even 150 μs after the laser pulse, in both nitrogen- and oxygen-saturated solutions.

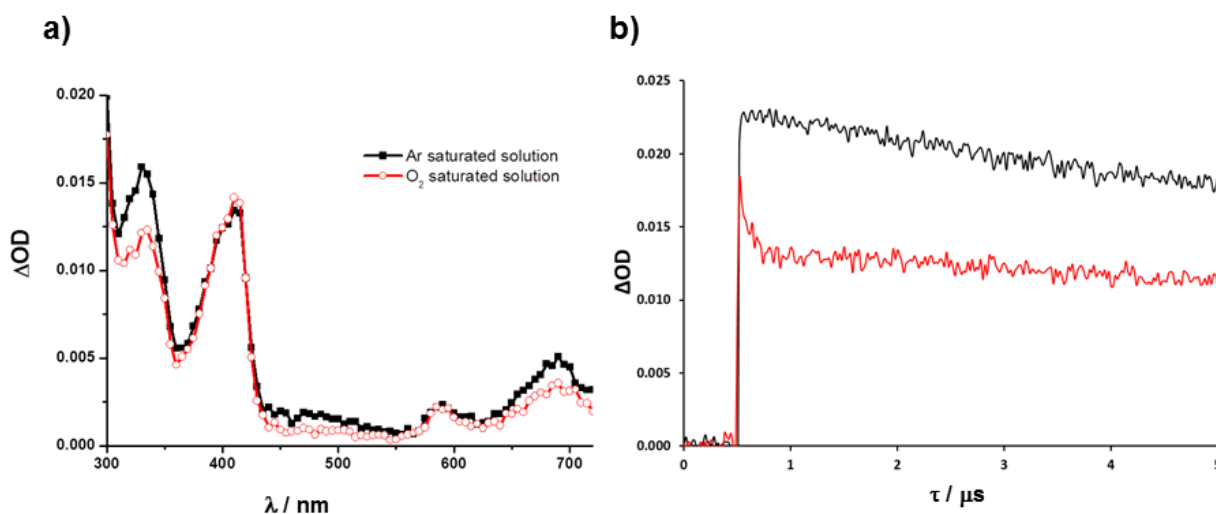


Figure 2.2. Transient absorption spectra of a solution of **1b** (10^{-4} M) in: a) Argon saturated methanol and O_2 saturated methanol recorded 0.1 μs after a 20 ns laser pulse ($\lambda = 266$ nm); b) Profile of the absorbance change observed at 330 nm for a solution of **1b** in argon saturated (black) and O_2 saturated (red) methanol.

With acetyl derivative **1d** (*ca.* 10^{-4} M in methanol, see Figure 2.3) again two absorption bands ($\lambda_{\text{max}} = 330$ nm and 410 nm) along with a broad signal (580-700 nm, Figure 2.3a) were detected under argon-saturated conditions. Kinetic analysis revealed the presence of three different transient species, for which the longest lived ($\tau = 33$ μs) represented the main contributors to both maxima, whereas two short-lived bands were observed at 340 ($\tau = 2.9$ μs) and 420 nm ($\tau = 0.7$ μs), respectively. The shortest-lived species was found to be also the main contributor to the broad absorption band at 580-700 nm.

Shifting to an oxygen saturated solution resulted in the quenching of the two short lived intermediates (see Figures 2.3b and 2.3c), whereas no significant effects were observed for the longest lived species. Conversely, no significant transient species were observed with the nitroderivative **1e**.

As mentioned in the introduction, results obtained in solution encouraged us to test the efficiency of photoactive aryl tosylates **1a-d** and **1f-g** in cationic photoinduced polymerization processes. Thus the tests were carried out in a hybrid organic-inorganic photoresist containing acid-sensitive epoxy functionalities (G8Ge2) obtained via acid-catalyzed condensation of 3-glycidoxypropyltrimethoxysilane (GPTMS) and germanium tetraethoxide (TEOG) in 2-methoxyethanol, (molar ratio GPTMS/TEOG: 80:20).^[31c] The synthesized aryl tosylates were then incorporated in the G8Ge2 system and the resulting sol was spin-coated on silicon substrates. The films obtained were then exposed to UV light (by a Hg-Xe UV spot light source) at increasing doses and the structural modifications induced by aryl tosylates were investigated by means of FT-IR analysis.

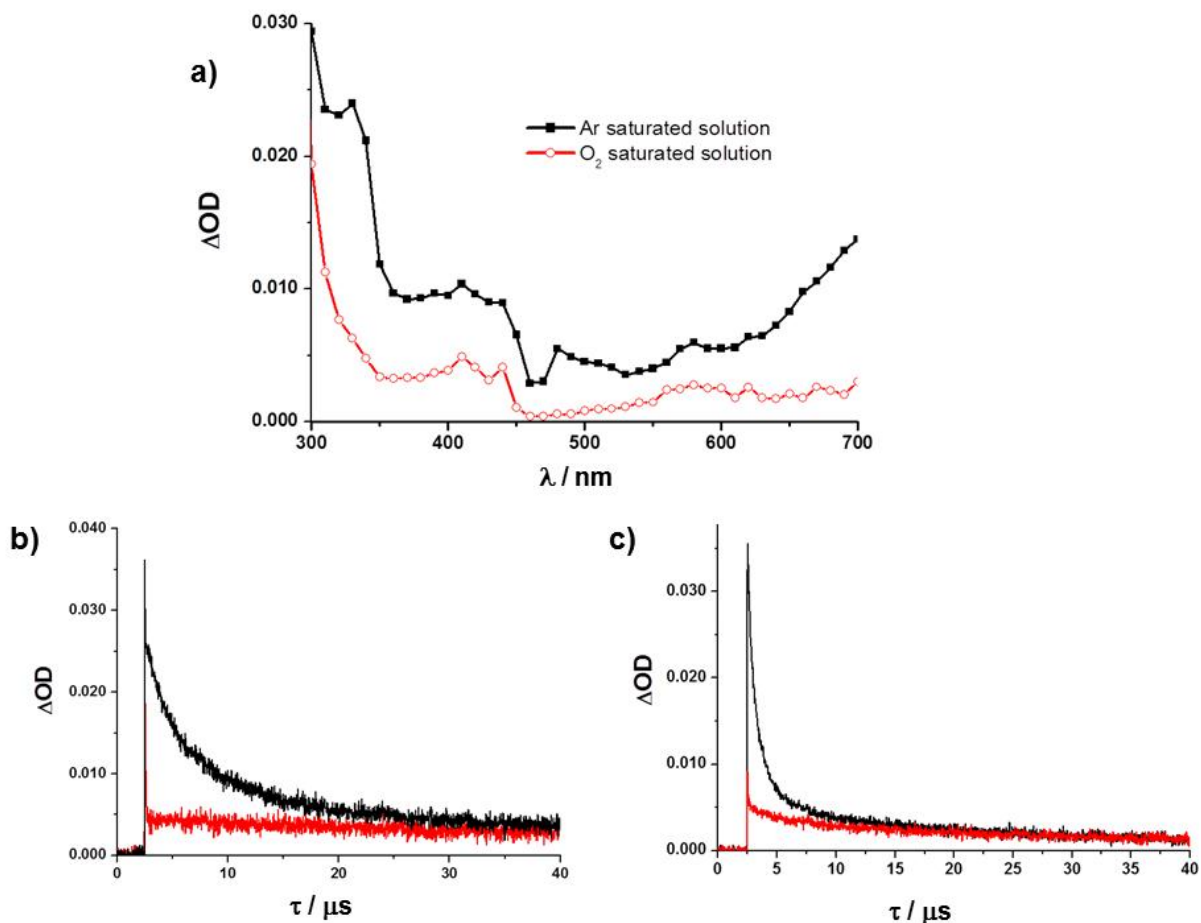


Figure 2.3. Transient absorption spectra of a solution of **1d** (10⁻⁴ M) in: a) Argon saturated methanol and O₂ saturated methanol recorded 0.1 μs after a 20 ns laser pulse (λ = 266 nm); Profile of the absorbance change observed at b) 340 nm and c) at 420 nm for a solution of **1d** in argon saturated (black) and O₂ saturated (red) methanol.

In particular the area under the signals at 3060 and 3000 cm⁻¹, assigned to C-H stretching of the epoxy moiety, were chosen to evaluate the degree of polymerization (see Figure 2.4a).^[36] As shown in Figure 2.4a for the G8Ge2/**1d** system, UV irradiation caused an absorbance decrease in the two bands. This indicates a gradual ring opening of the epoxy moiety and consequent polymerization induced by photo-generated acid molecules.^[31c]

Hence it was found that the degree of photopolymerization induced by phenyl tosylates **1a-d** roughly followed (at least within the first three minutes of UV exposure, Figure 2.4b) the amount of PTSA photoreleased under oxygenated conditions (with **1d** the best and **1a** the worst of the series, see Table 2.3).

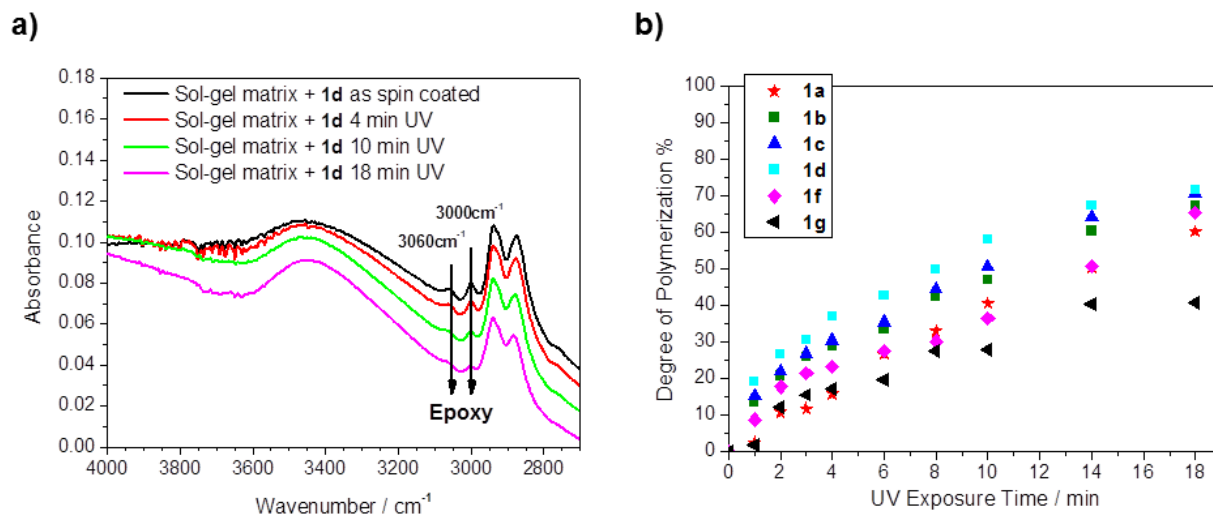


Figure 2.4. a) FTIR spectra in the 4000-2600 cm⁻¹ region of G8Ge2 films containing 1% molar concentration of **1d**, before and after UV irradiation. b) Degree of photopolymerization of epoxy groups versus UV curing time. Experiments performed on G8Ge2 films containing 1% molar addition **1a-d**, **1f-g** (calculated measuring the area under 3060 cm⁻¹ band).

Notably a degree of polymerization above 60% was achieved in all cases (except **1g**) after 18 minutes of UV exposure time. Moreover a blank experiment revealed that no polymerization took place when UV-curing was carried out in the absence of **1a-g**.

2.3 Discussion.

2.3.1 Photochemistry of aryl tosylates.

Differently to what observed in the case of aryl triflates and mesylates,^[27] for the substrates examined in this paper no heterolysis of the Ar-OS bond took place and the homolytic cleavage of the ArO-S bond was the exclusive reaction pathway. Thus a phenoxy (**I**) / *p*-toluenesulfonyl (**II**) radical pair is readily formed just after irradiation of aryl tosylates (see Scheme 2.1, *path a*). A similar behavior had been already observed in 1966 by Havinga studying the photochemistry of phenyl 4-methylbenzenesulfonate.^[37]

Laser flash photolysis (LFP) analyses confirmed the proposed photoreactivity. Indeed, as seen above, transient absorption spectra of **1b** show two significant absorption bands at 330 and 410 nm (Figure 2.1a). The oxygen-sensitive signal dominating at 330 nm was recognized as the 4-methylbenzenesulfonyl radical **II**, as previously suggested,^[28a,b] whereas the 4-methoxyphenoxy radical **Ib** can be confidently attributed to the long-lived intermediate with a maximum at 410 nm (and to the portion at 330 nm absorption not quenched by oxygen).^[38] In the case of **1d**, however, LFP revealed the presence of an additional transient, assigned to triplet ³**1d** (absorption at 420 and 580-700 nm), accompanying the two radicals absorbing at 330 and 420 nm.

Photo-Fries reactions are known to arise mainly from excited singlets, although triplets have occasionally been invoked.^[39] Regarding the derivatives studied in the present work cleavage of the ArO-S bond in the excited singlet state is the exclusive pathway upon direct irradiation. A triplet is not involved since no oxygen quenching of the photocleavage for **1b** and **1d** was observed (see Table 2.2). Moreover, as for compound **1d**, none of the photoreactivity normally observed from triplet aromatic ketones (e.g. hydrogen abstraction) was found even in an excellent hydrogen donating solvent such as methanol. Thus triplets have a role only when the cleavage from the singlets does not take place, as in the case of **1e**, where efficient intersystem crossing

Looking at the fate of the photogenerated radical pair, the resulting phenoxy and sulfonyl radical intermediates can follow two competing pathways in N₂-saturated solvents. The first is the escape from the solvent cage and subsequent hydrogen abstraction from the medium to give phenol **2** and *p*-toluenesulfinic acid (*paths c, c'*). The other possibility is direct recombination of the two radicals bringing to the formation of the Fries rearrangement product **3**, via the cyclohexanedione intermediate **III** (*paths d, d'*). Indeed the residual, persistent absorption at 300-350 nm and at 600-700 nm (see Figure 2.1a) found in LFP experiments on **1b** could be assigned to **III**, in analogy to what has already been reported about the photo-Fries rearrangement of naphthyl^[42] and phenyl acetates.^[43]

With the single exception of the nitroaryl tosylate **1e**, all of the sulfonates examined showed comparable photoreactivity in solution ($\Phi_{-1} = 0.11-0.29$, the highest value measured for tosylate **1d**), but different product distributions. We reasoned that the stability of the phenoxy radical **I** and, accordingly, the O-H bond dissociation energy (BDE) of **2**, could have a role in determining the fate of the reaction, driving it to either *paths c, c'* or *paths d, d'* (Scheme 2.1). As is apparent from Table 2.4, the lower is the O-H BDE of phenols **2** (e.g. 321.3 kJ mol⁻¹ in the case **2a**) the higher is the amount of the Fries adduct **3** obtained from the corresponding tosylates **1**, whereby formal hydrolysis to **2** is the sole reaction allowed for electron-withdrawing substituted tosylates, with stronger O-H bonds for the corresponding phenols (e.g. BDE = 380.3 kJ mol⁻¹ for **2d**).

Thus the recombination to **III** (*paths d, d'*) is favored for electron-rich tosylates such as amino derivative **1a** (making the photoinduced release of acid even negligible). On the other hand, although the presence of electron-withdrawing groups is desirable to maximize the yield of acid generation, moving to a very electron-poor tosylates (e.g. nitro derivative **1e**) completely inhibits the overall photoreactivity.

Table 2.4. Comparison of the products distribution observed in the irradiation of tosylates **1a-f** in methanol with the O-H BDE values of phenols **2a-f**.

O-H BDE for 2 (kJ mol ⁻¹) ^[a]	Ar-OTs	Photoproducts 2 : 3
321.3	1a	0 : 100
349.3	1b	60 : 40
364.3	1c	74 : 26
371.3	1f	100 : 0
380.3	1d	100 : 0
396.3	1e	- ^[b]
371.3	PhOTs	-

^[a] Experimental values reported in literature.^[44] ^[b] No significant consumption of **1e** observed.

A peculiar case is represented by **1g**. As previously observed in related sulfonate esters (mesylates, triflates),^[34b] the presence of a silicon based substituent *ortho* to the sulfonate moiety significantly enhanced the overall photoreactivity. The same behavior was found here, although the cleavage shifted from heterolysis of an Ar-OS bond (in the case of mesylates and triflates)^[34b] to ArO-S homolysis (in the case of tosylate).

Finally, moving again to the photochemical mechanism, the presence of oxygen was discovered to promote efficient trapping of the ArSO₂[•] radical **II** (Scheme 2.1, *path e*) before it could recombine with **I**. Thus PTSA is obtained via the corresponding peroxy-sulfonyl radical **IV**.^[28a,b] Both experimental and spectroscopic data exclude SO₂ loss from **II** to afford phenyl radical **V** (*path f*), contrary to results previously reported for arylsulfonyl radicals in acetonitrile.^[28a,b]

2.3.2 Applications in cationic photopolymerization.

Most of the aryl tosylates tested showed to be suitable PAGs for the release of PTSA to be used for the cationic ring opening of epoxy groups in sol-gel systems. When compounds **1a-d** and **1f-g** were incorporated in the photoresists, the efficiency of organic cross-linking of the G8Ge2 acid labile moieties depended on the tosylate used, the most favourable case being acetyl derivative **1d**.

Noteworthy the polymerization of the epoxy moiety is important also for the lithographic process. Indeed it involves the formation of an organic network covalently bonded to the inorganic component, with the development of an interpenetrated organic-inorganic hybrid structure which causes a densification of the exposed area. Thus the evaluation of the degree of polymerization reached by the systems represents also a good method to evaluate the efficiency of the tested substrates as PAGs for photolithography. Hence it can be said that the studied compounds look suitable also for future applications in microelectronic technologies.

Finally, differently to other aryl sulfonates^[27] where competing pathways affected the yield and the quality of the generated acids (see Scheme 1.7), photodecomposition of aryl tosylates proceeds via an unambiguous mechanism, and strong PTSA is the only acid produced by irradiation in oxygenated solutions, making them even much more promising photoinitiators.

2.4 Conclusion.

Summing up, the photochemistry of the substituted phenyl tosylates proceeds exclusively via ArO-S bond homolytic cleavage to generate a phenoxy/sulfonyl radical pair. Depending on the reaction conditions, either *p*-toluenesulfonic or *p*-toluenesulfonic acid can be released, the latter obtained exclusively under oxygenated conditions. Notably acids are photoreleased even in the solid state and this feature highlights the potential of aryl tosylates as a promising class of non-

ionic PAGs, able to promote the cationic polymerization of epoxy groups in hybrid sol-gel photoresists. Thus they could be exploited for photo(nano)lithography on sol-gel materials which play important roles in the realization of many devices.^[45]

3 *N*-arylsulfonimides: photochemistry and applications as PAGs for photolithography

3.1 Introduction.

In the last chapter it was shown that aryl tosylates are able to photorelease very high amounts of *p*-toluenesulfonic acid (up to 100% yield), being potentially suitable as PAGs for photolithography. However in that case, as well as in the case of the other sulfonates tested in the past,^[27] only one equivalent of acid could be obtained per equivalent of PAG. In few cases, nonetheless, PAGs able to generate more than one equivalent of acid, via either a multiphoton^[46] or a one-photon process,^[47] have been reported. This last situation is obviously desirable since it allows to reach higher amounts of acid photogenerated without any increase in the PAG concentration.

Herein the work on a new class of non-ionic PAGs, namely *N*-arylsulfonimides **4a-j** (Chart 3.1), potentially able to release more than one equivalent of strong sulfonic acids is presented.^[48] The idea behind this research was that each of the two N-S bonds could be potentially cleaved after irradiation, thus bringing to a double amount of sulfonic acids.

Compounds belonging to sulfonimides class were recently investigated as potential inhibitors of tryptophan-2,3-dioxygenase in cancer therapy,^[49] as hepatitis C virus inhibitors^[50] and as herbicides.^[51] However, to the best of our knowledge, the potentialities of sulfonimides as PAGs have been preliminary investigated only by Sasaki *et al.*, who reported the release of variable amounts of sulfonic and sulfinic acids (depending on the reaction conditions) from both alkyl and phenyl substituted sulfonimides.^[52]

Thus the photochemistry of different *N*-arylsulfonimides bearing different aromatic substituents (**4a-j**) was initially deeply investigated, focusing especially on the quality and the amount of acidic species photoreleased. Then the application of these compounds in materials science was explored. Accordingly, they were tested as photoinitiators in the polymerization of the same epoxy-based hybrid organic-inorganic system employed for aryl tosylates (see the previous chapter) and used afterwards to achieve micrometric patterns on the same materials by UV photolithography.^[53] Results obtained are described and discussed below.

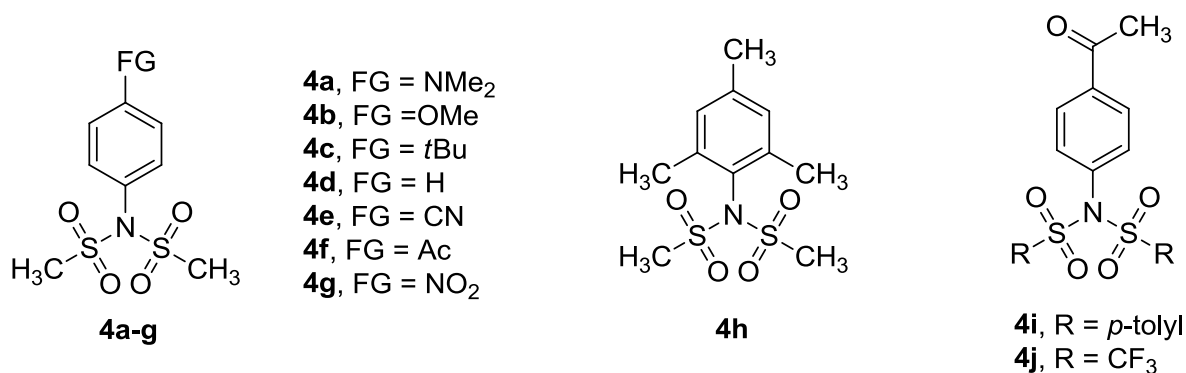


Chart 3.1. *N*-arylsulfonimides studied in this work.

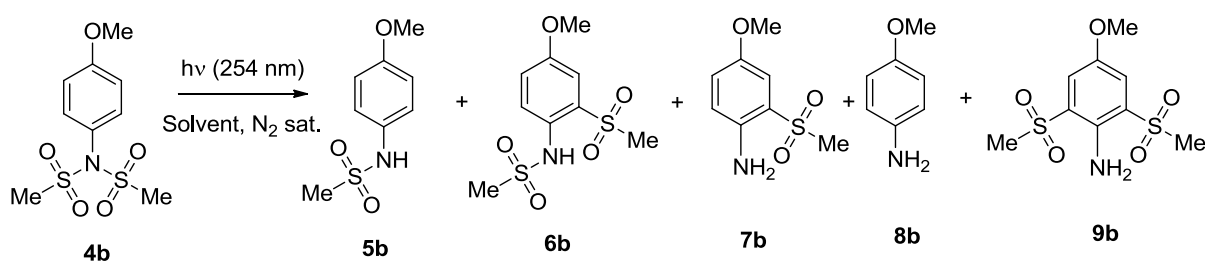
3.2 Results.

3.2.1 Photochemical experiments on 4a-j.

The examined sulfonimides were easily prepared from the corresponding anilines by condensation with sulfonylating reagents (see the Experimental Section chapter for details). Preliminary irradiation experiments ($\lambda = 254$ nm, 2h) were carried out on compound **4b** in medium to polar solvents under deaerated conditions (Table 3.1). A good photoreactivity for such substrate was observed in tetrahydrofuran, ethyl acetate and acetonitrile ($\Phi_{\cdot 1}$ in the 0.1-0.2 range). The presence of protic solvents (MeOH or water) did not increase the consumption of **4b**

that was photostable in acetone. The products distribution obtained was quite complex and all of the compounds formed arose from the cleavage of the N-S bond, as in the case of desulfonylated derivatives **5b** and **8b**, or from a photo-Fries rearrangement (products **6b**, **7b** and **9b**). The presence of a protic medium increased the amounts of the desulfonylated adducts (Table 3.1).

Table 3.1. Irradiation of sulfonimide **4b** in neat solvents.^[a]



Solvent	Φ_{-1} ^[b]	Products, yield % ^[c]	Desulf/Fries ^[d]
AcOEt	0.14	5b , 25; 6b , 26; 8b , 9; 9b , 16	44/56
THF	0.08	5b , 29; 6b , 5; 8b , 10; 9b , 16.	64/36
MeCN	0.21	5b , 22; 6b , 12; 8b , 11; 9b , 20	50/50
MeCN/MeOH (1:1)	0.16	5b , 33; 6b , 6; 8b , 30; 9b , 14	75/25
MeCN/H ₂ O (1:1)	0.10	5b , 30; 6b , 7; 8b , 16; 9b , 11	70/30
Acetone	< 0.01	[e]	[e]

^[a] Conditions: A solution of **4b** (10^{-2} M, nitrogen saturated) in the chosen solvent irradiated for 2h at 254 nm (4×15 W Hg lamps). ^[b] Disappearance quantum yield (Φ_{-1}) measured on a N₂ saturated 10^{-2} M **4b** solution in the chosen solvent ($\lambda = 254$ nm, 1×15 W Hg lamp). ^[c] Yields determined by HPLC analyses and calculated on the basis of the amount of consumed **4b**. In each case, **7b** was detected in < 1% yield. ^[d] Ratio between the yields of compounds **5b**, **8b** versus photo-Fries adducts **6b**, **7b**, **9b**. ^[e] No consumption of **4b** was observed and no photoproduct was detected by HPLC analyses.

With these results in hand we extended the investigation to the other sulfonimides **4a-j**. As for the photophysical properties (see Tables 3.2, 3.3, 3.4 and 3.5), compounds **4a-j** showed two

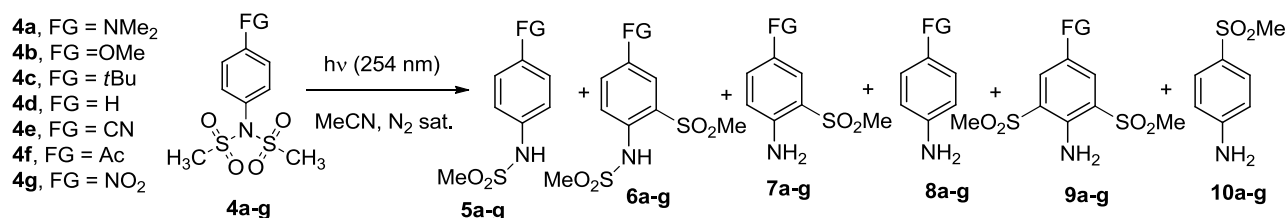
absorption maxima in the UV regions around 250-300 nm and 210-240 nm with the only exceptions of **4g** and **4i** which exhibited a single absorption band at 260 and 240 nm, respectively.

Thus photochemical experiments were performed using a 254 nm radiation source and the investigation started with methanesulfonimides **4a-g**. In view of the satisfactory Φ_{-1} value obtained for **4b**, irradiations on **4a-g** were carried out in deaerated (nitrogen-saturated) acetonitrile. As depicted in Table 3.2, a complex mixture of desulfonylated derivatives **5**, **8** and Fries adducts **6**, **7**, **9** resulted, along with sulfonyl anilines **10**. All of the sulfonimides **4a-g** were consumed with a disappearance quantum yield $\Phi_{-1} > 0.1$, with the amino and acetyl derivatives **4a**, **4f** being the most reactive in the series (Φ_{-1} ca. 0.3). The only exception was **4g**, almost photostable.

In analogy to what done for tosylates,^[33] potentiometric titration and ionic chromatography analyses were performed on the resulting solutions. Methanesulfinic acid was the only acid formed and its amount was comparable to the sum of the amounts of desulfonylated products **5**, **7**, **8** and **10**.

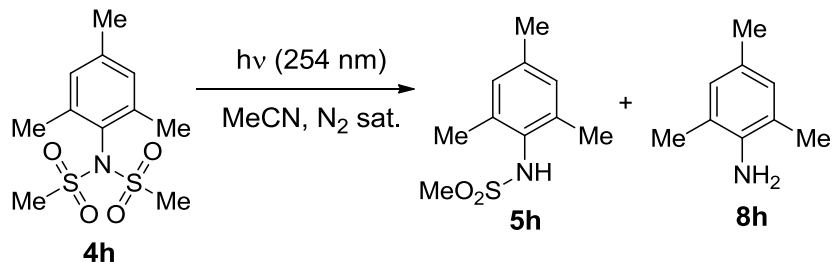
In order to hamper the formation of Fries adducts and to increase the release of acids, we tested then methanesulfonimide **4h**, in which the *ortho* and *para* positions bear methyl groups. As expected, no Ar-S bonds were formed in the reaction and only compounds **5h** and **8h** were obtained, along with a 71% yield of CH₃SO₂H (Table 3.3).

Table 3.2. Irradiation of methanesulfonimides **4a-g** in MeCN.^[a]



4	λ_{\max} (nm), ϵ (M ⁻¹ cm ⁻¹) ^[b]	Φ_{-1} ^[c]	Conversion %	Products, yield % ^[d]	H ⁺ , yield % ^[e]	Acids, yield % ^[f]
4a	273, 26988 305, 3771	0.31	100	6a , 82; 9a 10	0	CH ₃ SO ₂ H, < 1
4b	233, 16260 272, 2249	0.21	91	5b , 22; 6b , 12; 8b , 11; 9b , 20	46	CH ₃ SO ₂ H, 45
4c	222, 14894 254, 3342	0.09	75	5c , 21; 7c , 55; 8c , 12	99	CH ₃ SO ₂ H, 96
4d	210, 8493 262, 621	0.10	76	5d , 32; 8d , 14; 10d , 9	75	CH ₃ SO ₂ H, 74
4e	232, 18730 274, 1509	0.10	83	5e , 17; 7e , 53; 8e , 22	125	CH ₃ SO ₂ H, 116
4f ^[g]	242, 14061 288, 2498	0.28	40	5f , 80; 7f , 8; 8f , 7	^[h]	^[h]
4f	242, 14061 288, 2498	0.28	100	5f , 36; 7f , 18; 8f , 18; 10d , 4	98	CH ₃ SO ₂ H, 93
4g	214, 6084 260, 11513	<0.01	0	^[i]	0	^[j]

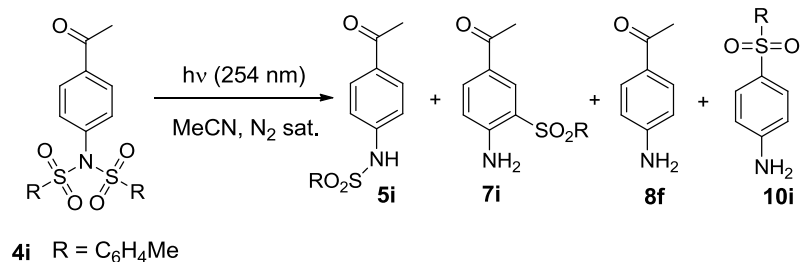
^[a] Conditions: A solution of **4a-g** (10⁻² M, nitrogen saturated) in MeCN irradiated for 2h at 254 nm. ^[b] Maximum absorption wavelength and molar absorption coefficient. ^[c] Disappearance quantum yield measured on a nitrogen purged 10⁻² M **4a-g** solution in MeCN ($\lambda = 254$ nm). ^[d] Determined by either HPLC or GC analyses and calculated on the basis of the amount of consumed **4a-g**. ^[e] Determined by potentiometric titration and calculated on the basis of the amount of consumed **4a-g**. ^[f] Determined by HPLC ion chromatography analyses and calculated on the basis of the amount of consumed **4a-g**. ^[g] 15 min irradiation. ^[h] Not determined. ^[i] No photoproducts detected. ^[j] No acid released.

Table 3.3. Irradiation of methanesulfonimide **4h** in MeCN.^[a]

λ_{max} (nm), ϵ ($\text{M}^{-1} \text{cm}^{-1}$) ^[b]	Φ_{-1} ^[c]	Conversion %	Products, yield % ^[d]	H^+ , yield % ^[e]	Acids, yield % ^[f]
204, 46154					
222, 8640 269, 573	0.13	86	5h , 56; 8h , 9	72	$\text{CH}_3\text{SO}_2\text{H}$, 71

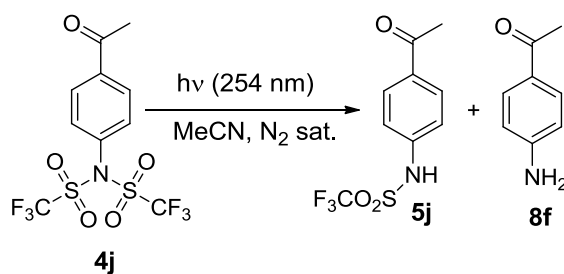
^[a] Conditions: A solution of **4h** (10^{-2} M, nitrogen saturated) in MeCN irradiated for 2h at 254 nm. ^[b] Maximum absorption wavelength and molar absorption coefficient. ^[c] Disappearance quantum yield measured on a nitrogen purged 10^{-2} M **4h** solution in MeCN ($\lambda = 254$ nm). ^[d] Determined by GC analysis and calculated on the basis of the amount of consumed **4h**. ^[e] Determined by potentiometric titration and calculated on the basis of the amount of consumed **4h**. ^[f] Determined by HPLC ion chromatography analysis and calculated on the basis of the amount of consumed **4h**.

Finally we tested acetylated *p*-toluenesulfonimide **4i** and trifluoromethanesulfonimide **4j** (for results see Tables 3.4 and 3.5, respectively). In both cases the Φ_{-1} value was in the same order of that observed for methanesulfonimide **4f** (*ca.* 0.25). The photochemical behavior of **4i** was very similar to that of **4f** (and likewise included ipso-substituted adduct **10i**) and a good amount of *p*-toluenesulfonic acid (along with traces of acetic acid) was detected by chromatographic analyses. On contrast, no Fries rearrangement was observed in the case of compound **4j**, and a mixture of weak acids (H_2SO_3 and HF) was released in place of expected $\text{CF}_3\text{SO}_2\text{H}$ (Table 3.2). Gaseous fluoroform (CHF_3) and hexafluoroethane were revealed in this photolyzed solution by means of IR and GC-MS analyses.^[27,54]

Table 3.4. Irradiation of sulfonimide **4i** in MeCN.^[a]

	λ_{\max} (nm), ϵ (M ⁻¹ cm ⁻¹) ^[b]	Φ_{-1} ^[c]	Conversion %	Products, yield % ^[d]	H ⁺ , yield % ^[e]	Acids, yield % ^[f]
4i	240, 32496	0.24	100	5i , 17; 7i , 38; 8f , 28; 10i , 13	128	CH ₃ C ₆ H ₄ SO ₂ H, 116; CH ₃ COOH, 11

^[a] Conditions: A solution of **4i** (10⁻² M, nitrogen saturated) in MeCN irradiated for 2h at 254 nm. ^[b] Maximum absorption wavelength and molar absorption coefficient. ^[c] Disappearance quantum yield measured on a nitrogen purged 10⁻² M **4i** solution in MeCN ($\lambda = 254$ nm). ^[d] Determined by HPLC analysis. ^[e] Determined by potentiometric titration. ^[f] Determined by HPLC ion chromatography analysis.

Table 3.5. Irradiation of sulfonimide **4j** in MeCN.^[a]

	λ_{\max} (nm), ϵ (M ⁻¹ cm ⁻¹) ^[b]	Φ_{-1} ^[c]	Conversion %	Products, yield % ^[d]	H ⁺ , yield % ^[e]	Acids, yield % ^[f]
4j	239, 18151 280, 1655	0.22	100	5j , 5; 8f , 78	319	H ₂ SO ₃ , 123; HF, 44

^[a] Conditions: A solution of **4j** (10⁻² M, nitrogen saturated) in MeCN irradiated for 2h at 254 nm. ^[b] Maximum absorption wavelength and molar absorption coefficient. ^[c] Disappearance quantum yield measured on a nitrogen purged 10⁻² M **4j** solution in MeCN ($\lambda = 254$ nm). ^[d] Determined by GC analysis. ^[e] Determined by potentiometric titration. ^[f] Determined by HPLC ion chromatography analysis.

Photolysis of compounds **4a-j** was then repeated under oxygenated conditions. As it is apparent from Table 3.6, the presence of oxygen did not affect the Φ_{-1} value. The scenario dramatically changed, however, analyzing the amount and the nature of the acids released.

Table 3.6. Irradiation of sulfonimides **4a-j** in MeCN under oxygenated condition.^[a]

4	Φ_{-1} ^[b]	Conversion % ^[c]	H ⁺ , yield % ^[d]	Acids, yield % ^[e]
4a	0.29	100	72	CH ₃ SO ₃ H, 66
4b	0.21	92	149	CH ₃ SO ₃ H, 154
4c	0.08	74	172	CH ₃ SO ₃ H, 178
4d	0.08	70	157	CH ₃ SO ₃ H, 154
4e	0.10	80	190	CH ₃ SO ₃ H, 182
4f	0.28	100	199	CH ₃ SO ₃ H, 192
4f ^[f]	-	100	195	CH ₃ SO ₃ H, 185
4g	< 0.01	< 1	< 1	[g]
4h	0.22	96	186	CH ₃ SO ₃ H, 182
4i	0.23	100	195	CH ₃ C ₆ H ₄ SO ₃ H, 200; CH ₃ COOH, < 1
4j	0.22	100	698	H ₂ SO ₃ , 175; HF, 330

^[a] Conditions: Solutions of **4a-j** (10⁻² M, oxygen saturated) in MeCN irradiated for 2h at 254 nm. ^[b] Measured on a 10⁻² M **4a-j** solution in oxygen purged MeCN ($\lambda = 254$ nm). ^[c] Determined by HPLC or GC analyses. ^[d] Determined by potentiometric titration of the photolysed solution with aqueous NaOH. ^[e] Determined by HPLC ion chromatography analyses. ^[f] Reaction carried out on an oxygen equilibrated solution. ^[g] No acid released.

Indeed, methanesulfonic acid (up to two equivalents) was formed from compounds **4a-h** and, similarly, a quantitative amount of *p*-toluenesulfonic acid was released from **4i**. In the case of **4f**,

the result obtained in air-equilibrated solution is very similar to that observed under oxygenated conditions. Compound **4j** gave the same acids formed in deaerated conditions, albeit in a higher amount.

In order to have a deep insight on the mechanism, we monitored the evolution of the photoproducts distribution obtained from compound **4b** under deaerated conditions after different irradiation times (see Figure 3.1). As apparent, compounds **5b** and **6b** were initially formed, but their concentration settled to almost constant values during the irradiation, with the concomitant accumulation of anilines **8b** and **9b**.

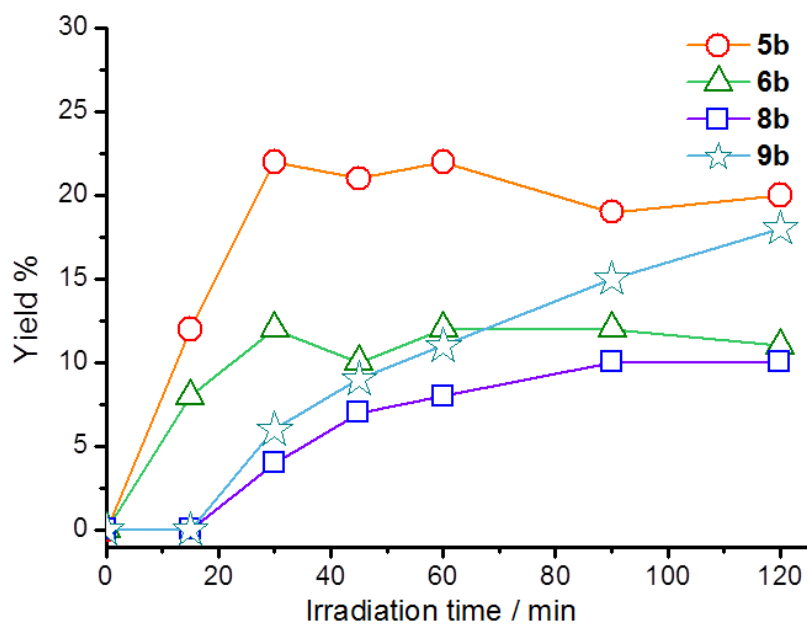


Figure 3.1. Photoproducts obtained from irradiation of a nitrogen saturated 10^{-2} M solution of **4b** in acetonitrile at 254 nm (4×15 W Hg lamps). Product yields measured by HPLC analysis and calculated on the basis of the initial concentration of **4b**.

A similar behavior was found for **4f**. In this case, sulfonamide **5f** was obtained in 80% yield after 15 min irradiation. A prolonged photolysis (2 h) caused the consumption of **5f** in favor of the formation of anilines **7f**, **8f** and **10d** (Table 3.2).

3.2.2 Photochemical experiments on 5a-j and 6a,b.

In order to point out the presence of secondary photochemical paths, our investigation proceeded with the exploration of sulfonamides **5** and Fries adducts **6** in MeCN, as detailed in Table 3.7. Compounds **5b-j** and **6a,b** usually showed Φ_{-1} values lower than the corresponding sulfonimides, with notable exceptions for **5e** ($\Phi_{-1} = 0.2$) and **5j** ($\Phi_{-1} = 0.4$). Again, the presence of oxygen did not significantly affect the efficiency of the consumption.

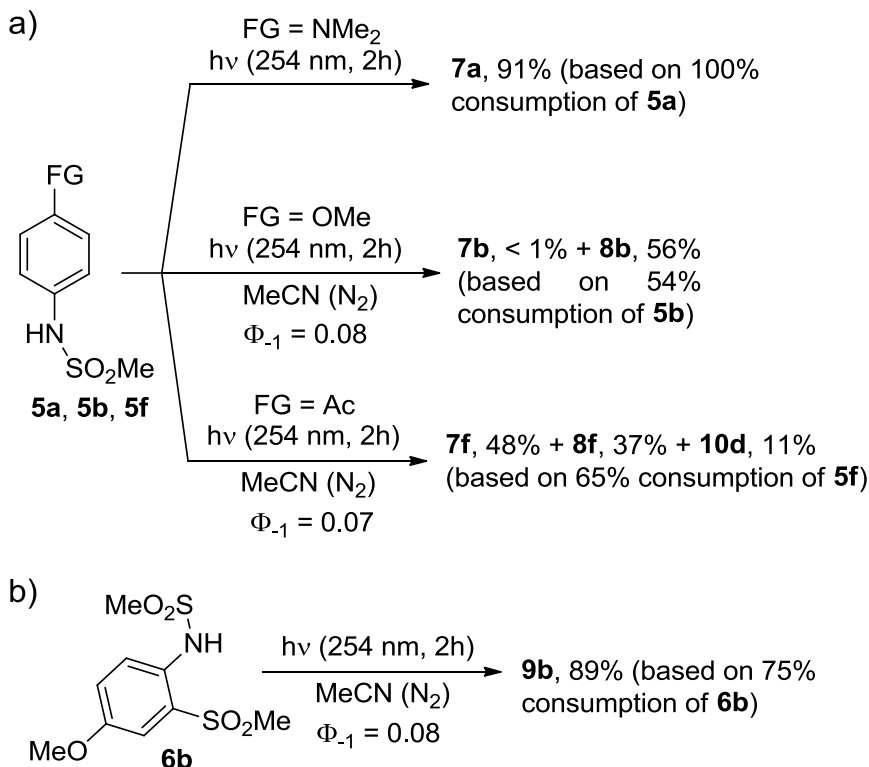
Table 3.7. Irradiation of compounds **5a-j** and **6a,b** in MeCN.

Compound	$\lambda_{\text{max}}, \epsilon \text{ (M}^{-1} \text{ cm}^{-1}\text{)}^{[a]}$	$\Phi_{-1}^{[b]}$
5a	265, 20508; 308, 2233	<i>n.d.</i> ^[c]
5b	231, 13181; 282, 2014	0.06 (0.09)
5c	227, 11981; 274, 610	0.08
5d	224, 9303; 272, 430	0.07
5e	252, 22525; 309, 481	0.20
5f	216,8371; 268, 16157	0.07 (0.08)
5g	220, 7015; 306, 11783	< 0.01
5h	201, 34106; 223, 5175	0.06
5i	220, 18727; 271, 21171	0.15
5j	254, 17585; 309, 967	0.40
6a	214, 16488; 276, 18057; 344, 2988	0.04
6b	209, 34641; 242, 13884; 305, 4306	0.08 (0.08)

^[a] Maximum absorption wavelength and molar absorption coefficient (in MeCN). ^[b] Determined on nitrogen saturated solutions (in parenthesis the value under oxygenated conditions) in MeCN ($\lambda = 254 \text{ nm}$). ^[c] Not measured in the specific case.

Regarding the distribution of photoproducts irradiation experiments were performed on nitrogen saturated solutions of model sulfonamides **5a**, **5b** and **5f**, in the same conditions employed for **4a-j**. Photolysis of **5a** gave Fries-adduct **7a** (91% yield) as the only photoproduct (Scheme 3.1a). An almost selective conversion of **5b** to anisidine **8b** was observed (Scheme 3.1a), whereas in the case of **5f** a mixture of Fries adduct **7f** and desulfonylated aniline **8f**, along with a minor amount of ipso-substituted product **10d**, was obtained.

Lastly, irradiation of the Fries adduct **6b** gave exclusively compound **9b** in 89% yield (Scheme 3.1b).



Scheme 3.1. Irradiation of **5a**, **5b**, **5f** and **6b** (10^{-2} M, nitrogen saturated) in MeCN.

3.2.3 Laser flash photolysis (LFP) and EPR experiments.

Compounds **4b** and **4f** were further examined by means of time resolved absorption spectroscopy. LFP experiments at 266 nm of a nitrogen-saturated solution of **4b** (5×10^{-4} M) in acetonitrile revealed the formation of two intense absorptions located at 300-340 nm and at 440-460 nm (Figure 3.2a). The time evolution of the transient spectrum pointed out the presence of different transient species, with the predominant contribution of a long lived intermediate ($\tau = \text{ca. } 100 \mu\text{s}$) in both absorption bands. However, two short-lived intermediates characterized by a lifetime of $\tau = 6$ and $1.8 \mu\text{s}$ were also identified at 300-340 and 440-460 nm respectively (see Figures 3.2b and 3.2c). When the same experiments were repeated in an oxygen saturated solution, a modification of the transient absorption profile was observed, with both of the short

lived species quenched, and a modest lowering in the intensity of the remaining absorption bands resulted (Figure 3.2).

Analogous results were obtained in the case of acetyl derivative **4f** (5×10^{-4} M in MeCN), where again two absorption bands ($\lambda_{\text{max}} = 300\text{-}340$ nm and $450\text{-}480$ nm) were detected under nitrogen-saturated conditions. However, in this case only two transient species contributed to both bands: a short lived ($\tau = 1.8$ μs) and a long lived ($\tau = 100$ μs) intermediate, with the former quenched in the presence of oxygen (see Figure 3.3).

Turning to compound **4i** (10^{-4} M in MeCN), an absorption spectrum with a strong maximum located in the $300\text{-}340$ nm region was observed, along with a weaker absorption band at ca. $440\text{-}470$ nm (Figure 3.4a). Kinetic analysis pointed out the presence of a long lived intermediate (τ ca. 100 μs) that is the main contributor to both maxima. However, as in the case of **4b**, we also found the presence of two oxygen sensitive species characterized by a lifetime of ca. 1.8 and 9.4 μs , the former present in both maxima, whereas the latter contributing significantly only to the absorption in the $300\text{-}340$ nm region (Figures 3.4b and 3.4c).

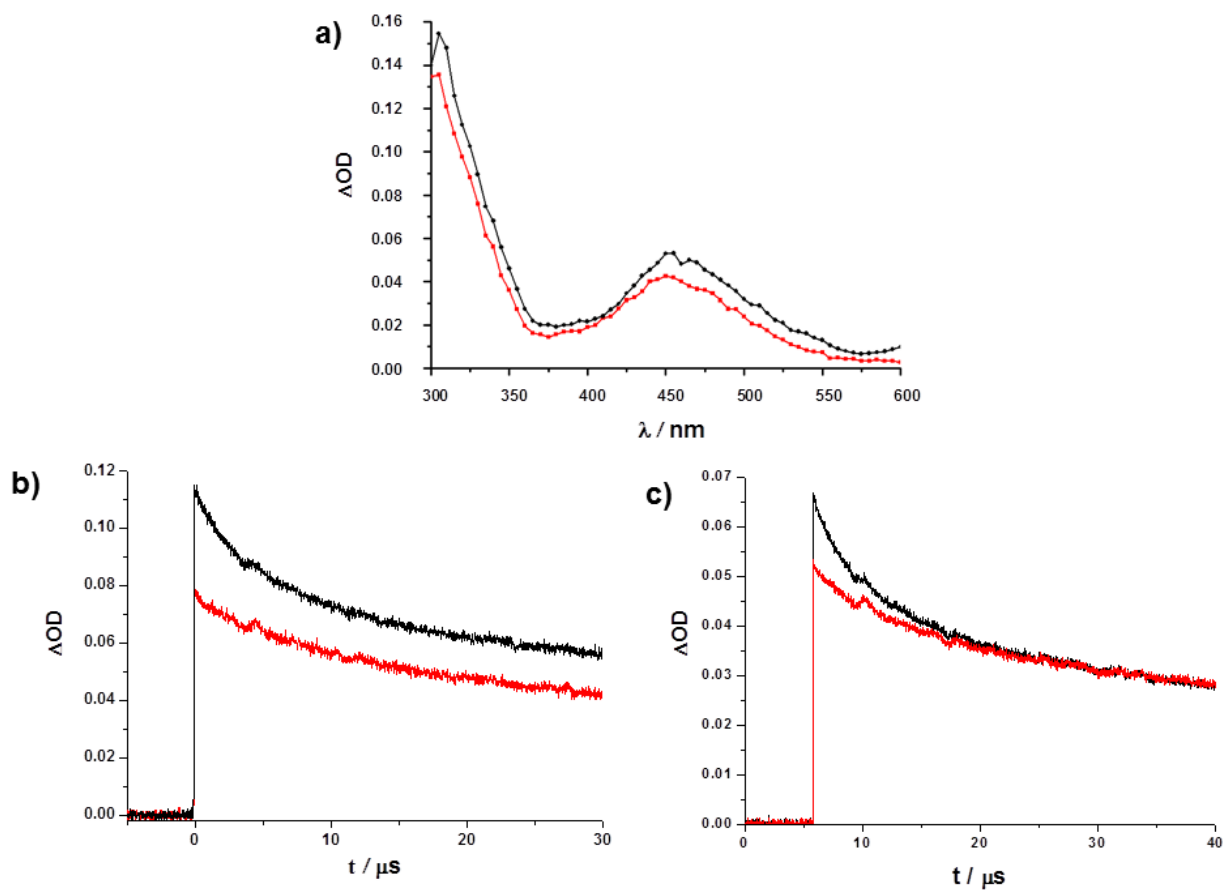


Figure 3.2. Transient absorption spectra of a solution of **4b** ($5 \times 10^{-4} \text{ M}$) in: a) nitrogen-saturated (black) and oxygen-saturated (red) acetonitrile, recorded 6 μs after a 7 ns laser pulse ($\lambda = 266 \text{ nm}$); Profile of the absorbance change observed at b) 340 nm and c) at 450 nm for a solution of **4b** in nitrogen-saturated (black) and oxygen-saturated (red) acetonitrile.

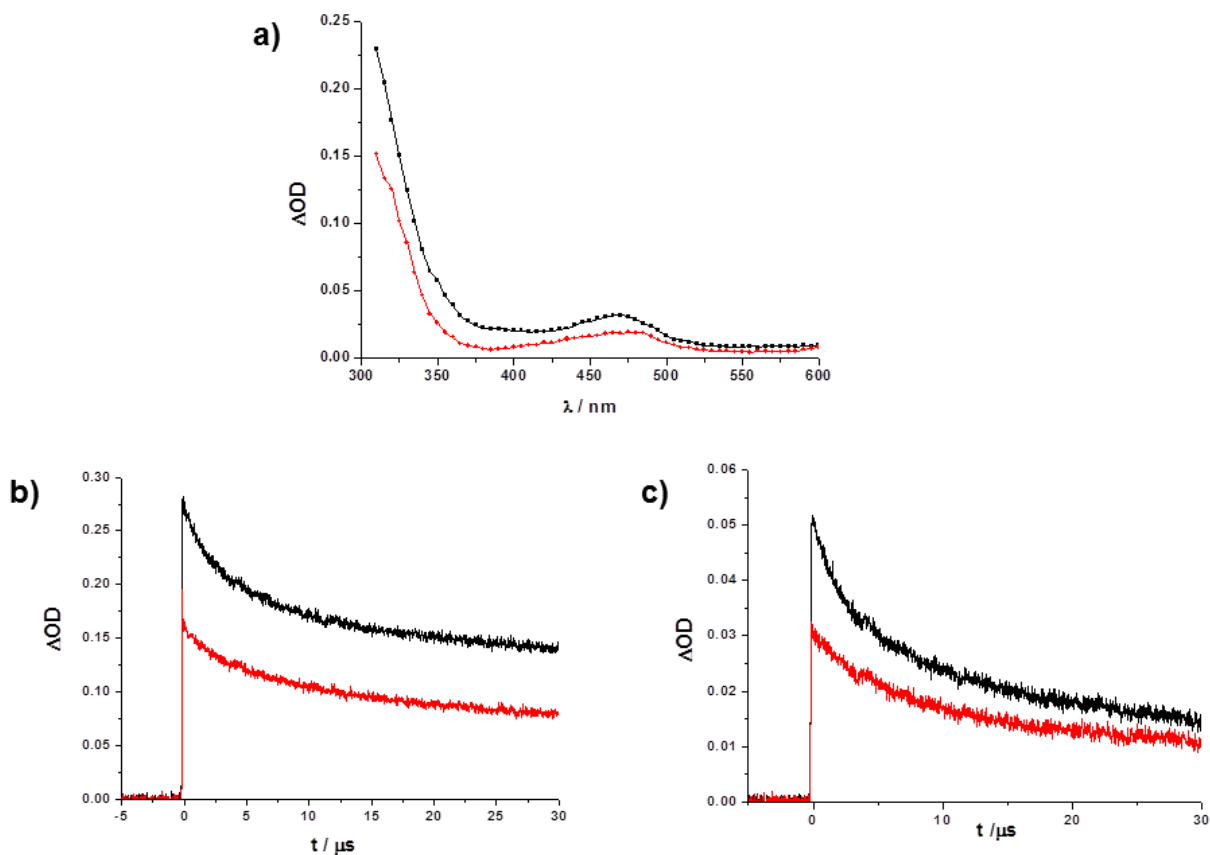


Figure 3.3. Transient absorption spectra of a solution of **4f** (5×10^{-4} M) in: a) nitrogen-saturated (black) and oxygen-saturated (red) acetonitrile, recorded 6 μ s after a 7 ns laser pulse ($\lambda = 266$ nm); Profile of the absorbance change observed at b) 315 nm and c) at 470 nm for a solution of **4f** in nitrogen-saturated (black) and oxygen-saturated (red) acetonitrile.

Electron paramagnetic resonance (EPR) analyses were performed on solutions of **4f**, **4i** and **4j** in deaerated benzonitrile. As for compounds **4f** and **4i**, two species with similar g values (2.006 ± 0.0005) were observed during irradiation of the samples by a high pressure Hg lamp (Figures 3.5a and 3.5b). Analyses of **4f** carried out in the presence of spin trap *N-tert-butyl- α -phenylnitrone* (PBN) resulted in an amplification of the generated species giving a signal with

hyperfine coupling constants of 13 G (a_N) and $3 \text{ G} \pm 0.5 \text{ G}$ (a_H). In the case of **4j**, a weak signal was observed only when irradiating the sample in the presence of 2-methyl-2-nitrosopropane (MNP) as spin trap, although in an amount below the limit of quantification (Figure 3.5c).

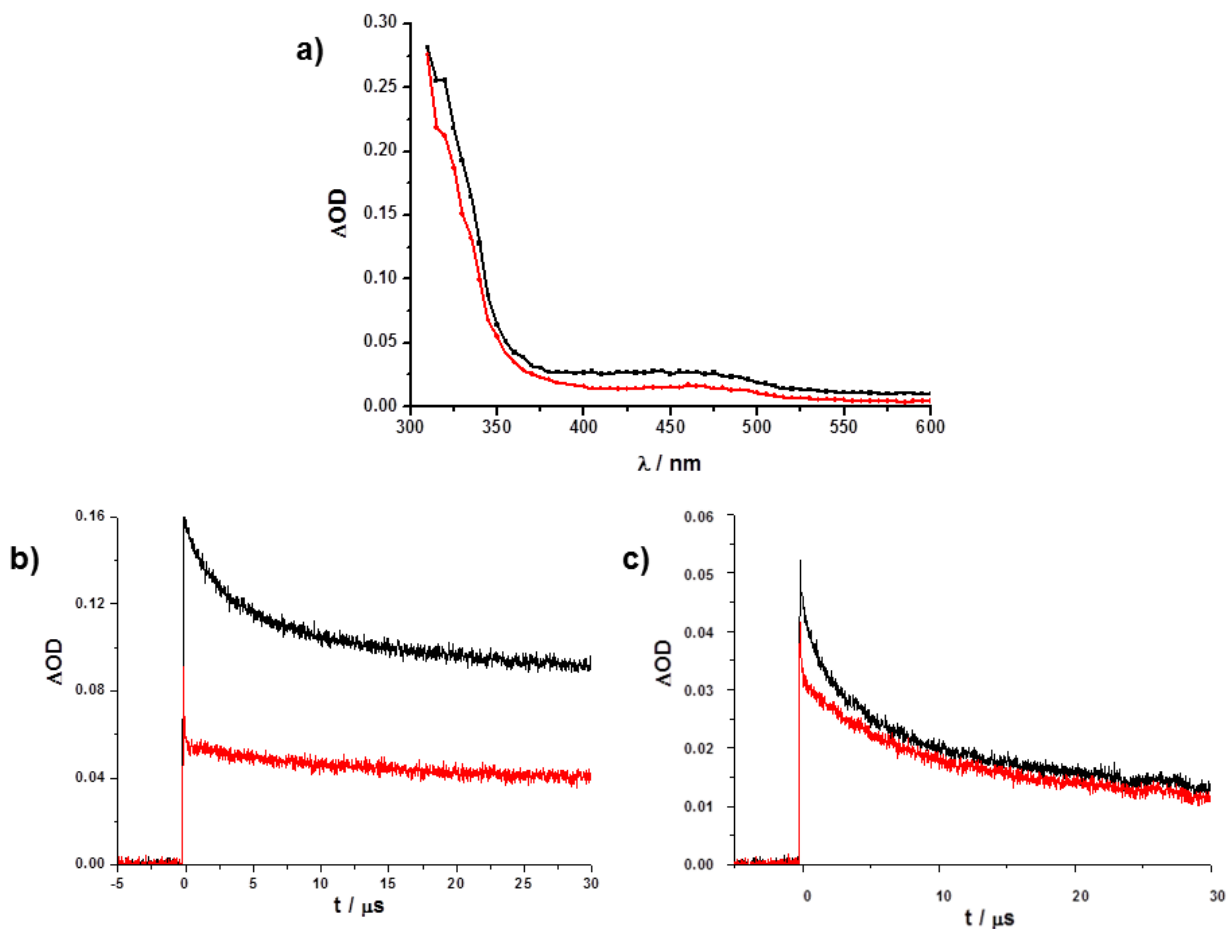


Figure 3.4. Transient absorption spectra of a solution of **4i** ($1 \times 10^{-4} \text{ M}$) in: a) nitrogen-saturated (black) and oxygen-saturated (red) acetonitrile, recorded 6 μs after a 7 ns laser pulse ($\lambda = 266 \text{ nm}$); Profile of the absorbance change observed at b) 340 nm and c) at 460 nm for a solution of **4i** in nitrogen-saturated (black) and oxygen-saturated (red) acetonitrile.

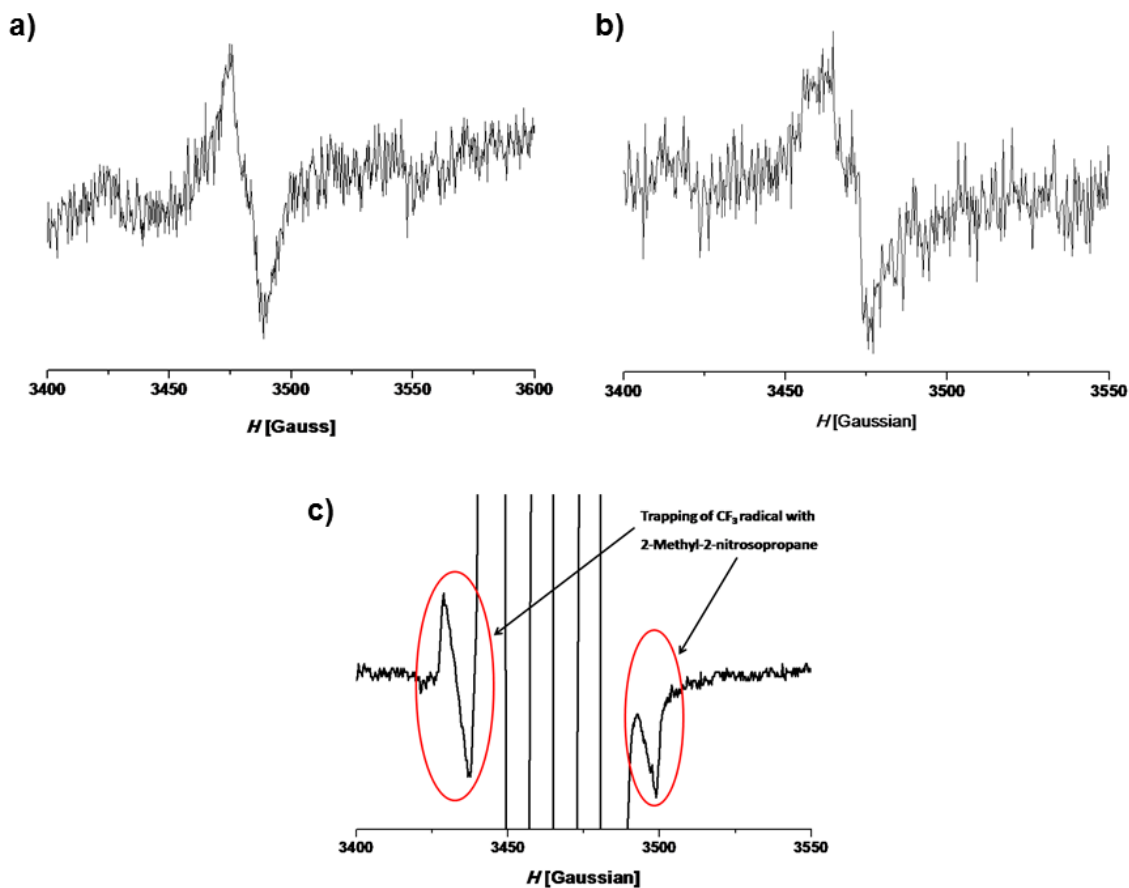


Figure 3.5. a) EPR spectrum recorded during photolysis of **4f** in nitrogen-saturated benzonitrile. b) EPR spectrum recorded during photolysis of **4i** in nitrogen-saturated benzonitrile. c) EPR spectrum recorded during photolysis of **4j** in nitrogen-saturated benzonitrile, in the presence of 2-methylnitrosopropane (MNP) 10^{-1} M.

3.2.4 Photopolymerization and photopatterning experiments.

Polymerization experiments were performed by using the same method employed for aryl tosylates.^[33] Thus experiments were carried out on the same hybrid organic-inorganic material (G8Ge2) containing the different substrates, namely methanesulfonimides compounds **4b**, **4e**, **4f** (chosen as model compounds), tosyl derivative **4i** and trifluoromethanesulfonimide **4j**. Spin-coated films (1 μm thickness) of the resulting sol-gel system were irradiated at increasing UV

doses (with a Hg-Xe lamp) and the structural modifications induced by the tested compounds were investigated by FT-IR analysis. Again the area under the signals at 3060 and 3000 cm^{-1} was analyzed to determine the degree of polymerization.

The degree of photopolymerization induced by the irradiated methanesulfonimides **4b**, **4e** and **4f** (Figure 3.6a) was compared to that obtained employing 4-phenylthiophenyl)diphenylsulfonium triflate (DPST, a commercial PAG, see Chart 1.1). Even though not efficient as DPST, the tested compounds were responsible for a good degree of polymerization (more than 60% for **4f**).

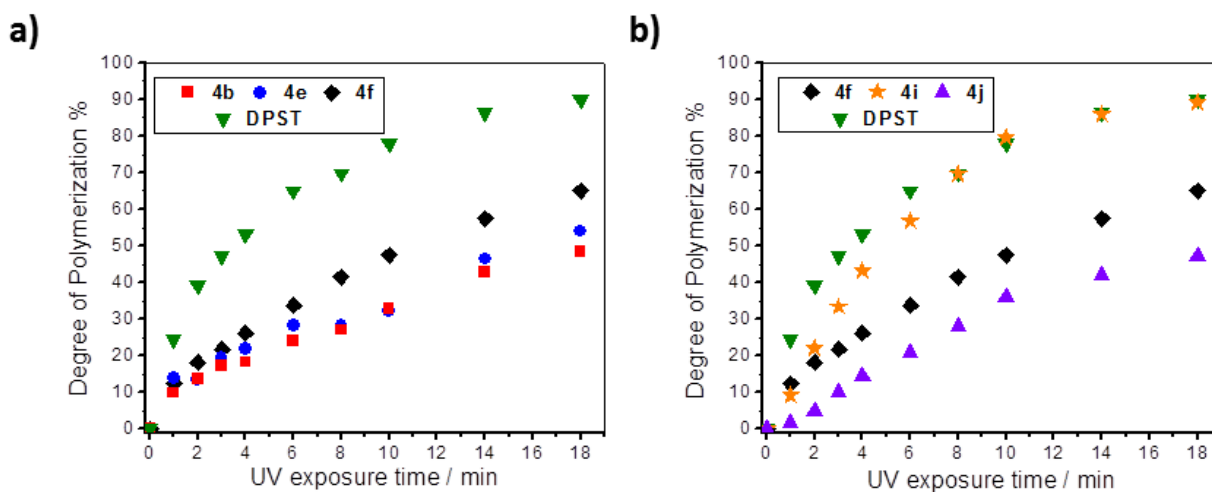


Figure 3.6. a) Photopolymerization degree of epoxy groups vs UV curing time reached by G8Ge2 films containing 1% molar **4b,e,f** (calculated measuring the area under 3060 cm^{-1} band). A comparison with the polymerization degree reached using DPST under the same conditions is provided. b) Photopolymerization degree obtained when using PAGs **4f,i,j** used under the same conditions of Figure 3.6a (comparison with DPST is shown).

A dramatic effect was observed when moving from *N*-arylmethanesulfonimides to *p*-toluenesulfonyl derivatives since a higher polymerization degree was observed in the latter case (compare the performance of compound **4f** with **4i** in Figure 3.6b). Moreover the degree of

polymerization found for compound **4i** is quite similar to that of commercial DPST. On the contrary, trifluoromethanesulfonimide **4j** behaved as a modest photoinitiator (see Figure 3.6b). To evaluate the possible application of *N*-arylsulfonimides as PAGs in photolithography, compound **4f** (which gave average results in photoinduced polymerization) was tested as photoinitiator in photopattern experiments. For this aim, G8Ge2 sol-gel films containing 1% **4f** were exposed to UV light for 1-3 min through a quartz mask with different geometries. The irradiated films were then developed in an acidic alcoholic solution. As shown in Figure 3.7, different microstructures characterized by features resolutions between 10 and 100 μm were successfully achieved. Notably, as expected, the system behaves as a negative tone resist, remaining in the UV exposed areas, due to the increasing crosslinking degree and to the consequent decrease in solubility of the irradiated regions.

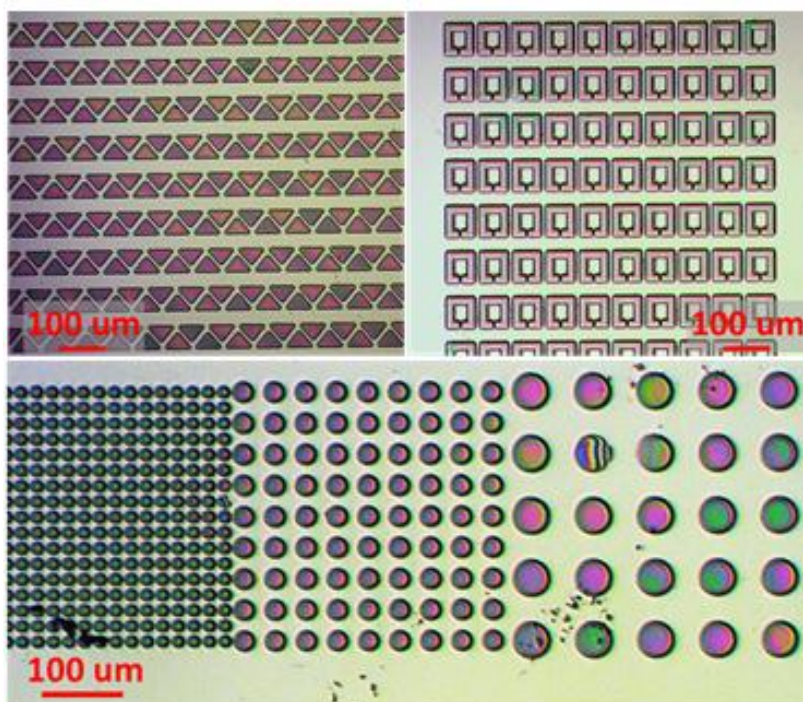
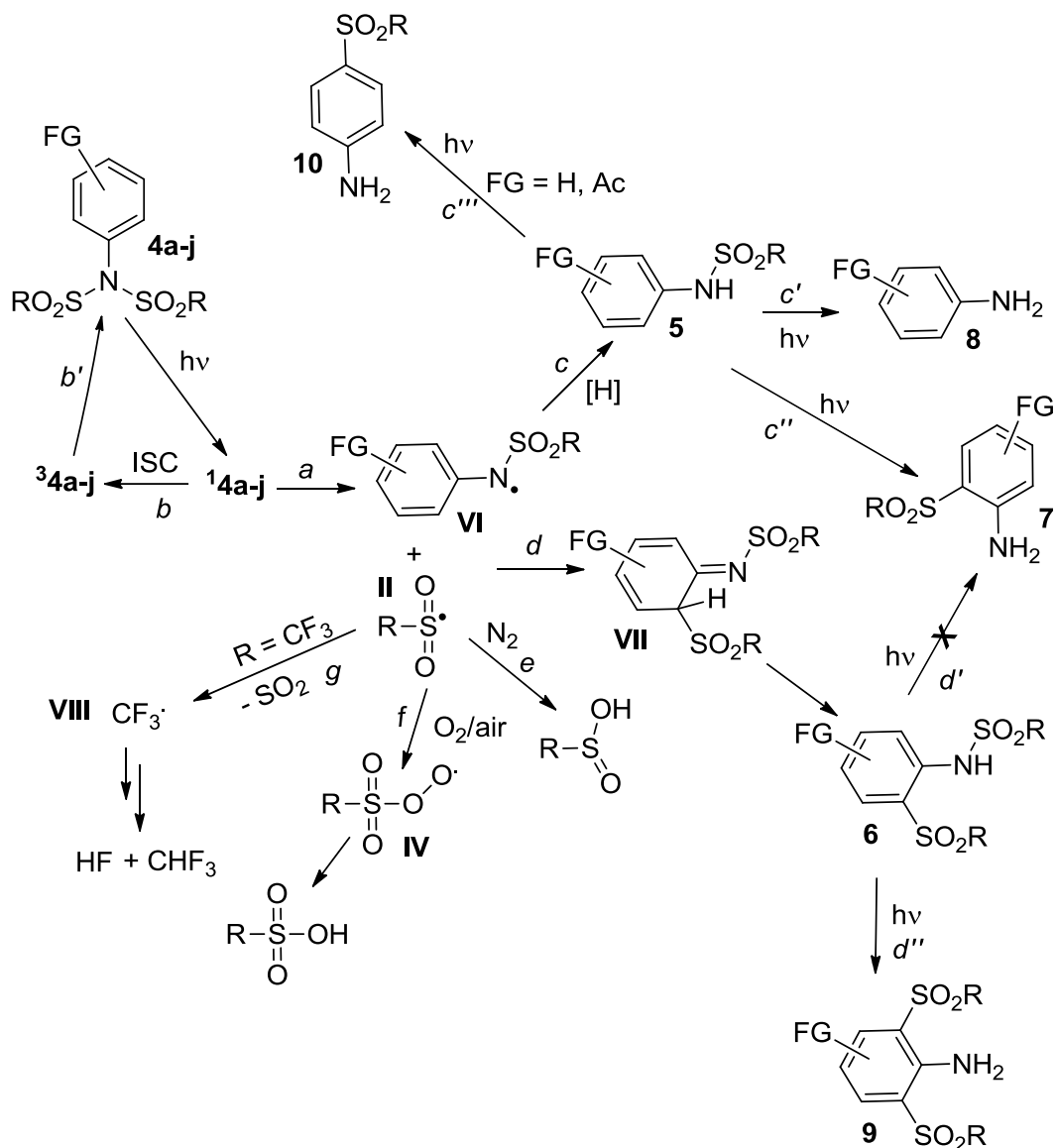


Figure 3.7. Optical microscopy images of patterns gained by UV lithography. The epoxy based sol-gel system G8Ge2, with 1% PAG **4f**, was used as the photosensitive material.

3.3 Discussion.

3.3.1 Photochemistry of compounds 4a-j.

A tentative mechanism for the photoreactivity of *N*-arylsulfonimides (not too dissimilar to the one proposed for **1a-g**) is shown in Scheme 3.2.



Scheme 3.2. Mechanism for the photochemical reactivity of *N*-arylsulfonimides **4a-j**.

Irradiation of **4a-j** causes their excitation to the singlet excited state $^1\mathbf{4a-j}$. Then, homolytic fragmentation of one of the N-S bonds (*path a*) takes place from $^1\mathbf{4a-j}$ to afford sulfamido (**VI**) and sulfonyl (**II**) radicals. The presence of such species is strongly supported by both time resolved absorption and EPR spectroscopy techniques. In particular, the long lived species found in transient spectra with absorption maxima in the 300-340 nm and 440-480 nm regions were assigned to **VI**, whereas methanesulfonyl and *para*-toluenesulfonyl radicals **II** were characterized as the short lived (6 and 9.4 μs respectively), oxygen sensitive signals in the 300-340 nm region.^[55] The presence of such sulfur centered radicals was further confirmed by EPR analyses on **4f** where the g factor value obtained for methanesulfonyl radical (2.006 ± 0.0005) is in accordance with the literature data (Figure 3.5a).^[56]

The very short lived transient species at 440-460 nm for **4b** can be safely assigned to its triplet state, by comparison with the absorption spectra of triplet state of anisidine.^[57] Similarly, the 2 μs long, oxygen sensitive, signals at 300-340 and 440-480 nm seen studying **4f** and **4i** were assigned to $^3\mathbf{4f}$, $^3\mathbf{4i}$ (Figures 3.3 and 3.4).^[58] However, the insensitivity of the photoreactions of **4a-j** to oxygen (compare the similar Φ_{-1} values reported in Tables 3.2-3.6), and the observed photostability of **4b** in acetone (Table 3.1), exclude a fragmentation from this state (*paths b, b'*). Noteworthy, despite the presence of the acetyl substituent in derivatives **4f**, **4i**, **4j** could increase the rate of Inter System Crossing (making the triplet state accessible) no alteration of the reaction mechanism was observed. Once generated, radicals **VI**, **II** can follow two competing pathways, namely recombination to yield Fries rearrangement products **6** or escape from the solvent cage. In the former case, formation of **6** (*path d*) proceeds through intermediate **VII**.^[59] On contrast, sulfonamides **5** arise from hydrogen abstraction by radical **VI** from the reaction medium (*path c*). The competition between these two pathways depends on the functional groups present on the aryl moiety and on the reaction media. In analogy to aryl tosylate, compound **6** is formed

preferentially in less polar solvents (Table 3.1) and in the presence of electron-donating aromatic substituents (NMe₂, OMe; Table 3.2).

As previously reported,^[60] the obtained *N*-arylsulfonamides are likewise photoactive, and both desulfonylation to the corresponding anilines and formation of anilines **8** (*path c'*) and Fries rearrangement (**7**, *path c''*) can be observed. The last pathway is favored for electron-rich sulfonamides, as in the case of **5a**, which gave exclusively Fries-adduct **7a** upon irradiation. On the other hand, when irradiating non substituted **4d**, the photo-Fries rearrangement from the primary photoproduct **5d** resulted in the formation of either aniline **8d** or *p*-substituted compounds **10d** (*path c'''*).

Compounds **10** were likewise obtained as minor products from acetyl derivatives **4f**, **4i**. In the latter case, we suggest that *path c'''* is still involved and an aromatic ipso-substitution occurs with the subsequent release of acetic acid (see Table 3.4). The radical induced displacement of an acyl group was previously observed for 2-acetylbenzothiazoles^[61] and acylpyridines.^[62] Moreover, the photosubstitution of a chlorine atom for a sulfonyl group has been likewise reported in the photo-Fries rearrangement of *N*-chlorophenylsulfonamides, where a chlorine cation is supposed to be lost at the end of the process.^[60a] The photoreactivity of photoproducts **6a,b** is instead limited to rearranged anilines **9a,b** (*path d''*), while desulfonylation to compounds **7** (*path d'*) seems to have no role (see Scheme 3.1b).

As for the release of acid, under deaerated conditions the corresponding weak sulfinic acids are mainly released (Scheme 3.2, *path e*). However, as seen in the previous chapter, the presence of oxygen prevents any Fries rearrangement and drives the process to the formation of radicals **IV** which are precursors of sulfonic acids (*path f*). Thus, in the case of sulfonimides **4b-f,h,i**, a strong acid is always photoreleased in high yields (over 100%, Table 3.6). Paradigmatic is the case of

compound **4i**, where 2 equivalents of *p*-toluenesulfonic acid were obtained from each mole of starting substrate.

Interestingly, no triflic acid was released upon irradiation of triflimide **4j** under oxygenated conditions. This is due to the facile SO₂ loss (detected as H₂SO₃ by ion chromatography) from trifluoromethanesulfonyl radical **II** (*path g*).^[27,63] Secondary processes of the resulting trifluoromethyl radicals F₃C[•] (**VIII**) lead to the formation of fluoroform, hexafluoroethane and to the liberation of HF.^[27] The presence of such radical was confirmed by the EPR analyses on **4j**. Indeed, the weak signal observed during irradiation in the presence of MNP spin trap can be assigned to F₃C[•] species (Figure 3.5c), according to the literature data.^[64]

3.3.2 Applications in cationic polymerization and photolithography.

Results depicted in Figure 3.6 are very clear. First of all it must be underlined that the good degrees of polymerization reached show that sulfonimides are able to efficiently photorelease a strong acid even in solution and that the latter is capable of promoting cationic polymerization in the solid state.

Furthermore, looking at the methanesulfonimides series, the highest degree of polymerization was achieved by **4f**, which also released the highest amount of CH₃SO₃H in solution (see Table 3.6). Thus the trend observed for acid release in solution roughly reflects the efficiency of the tested substrates in the solid state, with compound **4b** which appears to be the worst in the series.

The behavior shown by **4i** is noteworthy. It indeed behaved better than the corresponding methanesulfonimide **4f** and, matching the efficiency of DPST, seriously represents a valid and cheap alternative to commercially available PAGs for cationic polymerization. Moreover its performance indicates that the quality of the generated acid (in the present case PTSA instead of CH₃SO₃H) have a huge consequence in the photopolymerization of this kind of hybrid organic-

inorganic materials. Thus bad results obtained with trifluoromethanesulfonimide **4j** can be likewise explained by its inability to release strong sulfonic acids.

Regarding photopatterning experiments, micrometric patterns with good resolution were obtained through UV lithography of films containing **4f**, pointing out the potential of *N*-arylsulfonimides as PAGs for the preparation of new hybrid sol-gel photoresists for micro- and nanolithography.

3.4 Conclusion.

In conclusion a new class of non-ionic photoacid generators was developed. These compounds, namely *N*-arylsulfonimides, are able to release, upon irradiation, up to two equivalents of strong sulfonic acids (methanesulfonic and *p*-toluensulfonic acids) for each mole of photoactive substrate. They can be easily prepared from the corresponding commercially available anilines and their absorption properties and photochemical behaviors can be simply tuned by choosing the suitable substituent. *N*-arylsulfonimides were exploited also as photoinitiators in the cationic photopolymerization of epoxy rings in a hybrid sol-gel material. Even in this case the chemical modification of the benzene ring or the proper choice of the sulfonyl groups can further improve the photopolymerization efficiency, making it comparable to that of commercial photoacid generators. In reason of this behavior, the developed PAGs were also adequate to achieve micrometric photopatterns. Thus future applications in microelectronics and materials science are desirable.

4 Aryl sulfonates for EUV lithography

4.1 Introduction.

While studying novel photoresists and developing new photoacid generators for photolithography, it must be considered that, even if the sensitivity of the system is a crucial point, the entire research process should be oriented to the achievement of well resolved patterns. Indeed, according to Moore's law, integrated circuits features size should be increasingly reduced^[65] and there is a growing demand from microelectronic industry to improve the resolution of photolithographic patterns. Since the minimum feature size is proportional to the irradiation wavelength,^[2a,14b] the simplest way to increase the resolution is to use more energetic radiation. In particular, extreme ultraviolet lithography (EUVL), an extension of the conventional photolithography, is presently considered one of the most promising technologies. The short wavelength of the extreme ultraviolet (EUV) radiation employed ($\lambda = 10\text{-}15\text{ nm}$) markedly improves the resolution, with features size even below 32 nm.^[66] Nonetheless, such a different technique requires special irradiation sources and, moreover, proper optical setups^[67a,d,e] and specifically designed resists are needed.^[67]

Interestingly, looking at these newly developed photoresists, hybrid organic-inorganic materials have been successfully employed for EUVL applications,^[68] thus allowing a convenient combination of the two different technologies. On the other hand, when we focus on photoacid generators, it must be underlined that, besides iodonium and sulfonium salts, even simple aryl sulfonates (e.g. triflates and nonaflates) have been successfully employed as cost-effective PAGs for EUV lithography in traditional styrene/acrylate polymer matrices.^[69]

Hence our initial goal to use simple molecules as new PAGs for UV lithography was extended even to EUVL techniques and the first application of aryl sulfonates as PAGs for EUVL in a hybrid organic-inorganic material is shown in the present chapter. In particular the work, aiming to improve the performance of the hybrid photoresist, was oriented on the specific design of aryl sulfonates for a proper response to EUV radiation, as described below.

4.2 Results and discussion.

4.2.1 Design and synthesis of photoacid generators.

Aryl sulfonates **1h** and **1i** (see Chart 4.1) were synthesized and studied as potential PAGs for EUV lithography. Their synthesis was achieved simply by reaction of 2,3,4,5,6-pentafluorophenol with, respectively, *p*-toluenesulfonyl chloride and trifluoromethanesulfonic anhydride. The commercial PAG DPST and the tosylate **1d** were likewise tested for the sake of comparison (see below).

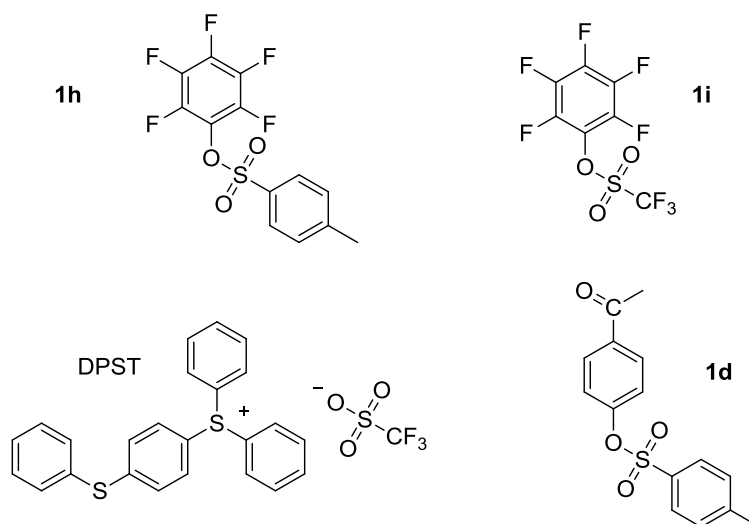


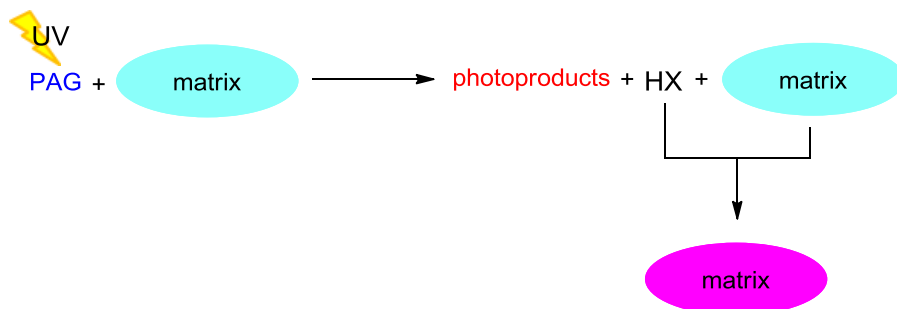
Chart 4.1. Compounds tested as photoacid generators for EUV lithography.

The choice for these two compounds was justified by the particular role of PAGs in EUV lithography. Indeed, as seen in the Introduction chapter, in conventional UV lithography an exclusive direct excitation of photoinitiators occurs and the role of the photoresist polymer matrix is only to react with acids released by the PAGs (Scheme 4.1). On the contrary, in the EUVL technique, the matrix itself may have a crucial role in the absorption of the EUV radiation,^[70] causing the emission of photoelectrons and secondary electrons. Trapping of the released electrons from PAGs brings then to their decomposition and the concomitant release of acidic species able to react with the matrix modifying its structure (Scheme 4.1).^[71]

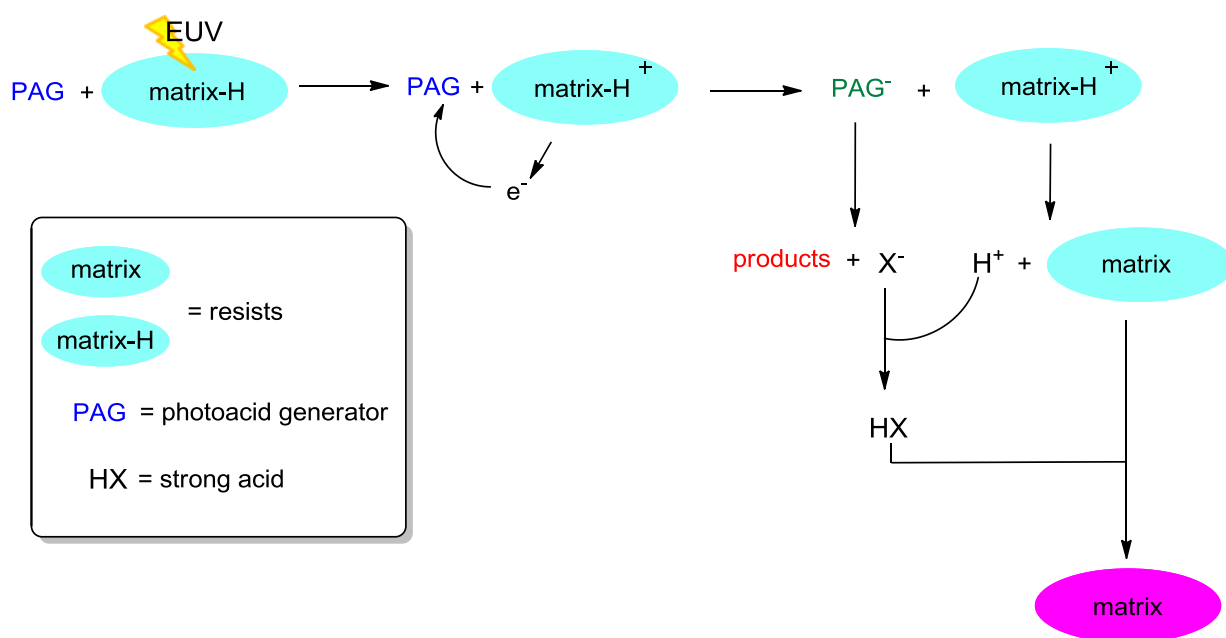
Keeping these considerations in mind, the peculiar structure of **1i** seemed convenient for its use as a potential PAG for EUV. Indeed it was previously demonstrated that irradiation of **1i** in the presence of electron-rich aromatics gives a photoinduced electron transfer where **1i** releases strong triflic acid upon electron capture.^[72] Thus, to have a better indication on the capability of **1i** to take electrons, cyclic voltammetry experiments (in *N,N*-dimethylformamide, DMF) were carried out to determine its reduction potential. It was found that **1i** is a quite reducible compound ($E^{0'} \approx -1.50$ V vs. Ag/AgCl, 3 M NaCl), thus potentially suitable for EUVL.

The suitability was suggested also by the fact that the presence of many fluorine atoms on **1i** skeleton has a twofold role. Indeed fluorine atoms, besides making the aromatic more prone to accept electrons, have also an high absorption cross section in the EUV region.^[70] The latter point is an added bonus since, in some cases, the direct excitation of PAGs by EUV radiation was claimed to have a role in the acid generation.^[73]

UV photolithography



EUV lithography (EUVL)



Scheme 4.1. Mechanism of acid generation and reactivity in UV and EUV promoted lithography.

1h was chosen instead to bypass a possible drawback of **1i**. In fact, EUV patterning must be performed in vacuum (see the experimental section chapter) but **1i** is a quite volatile liquid ($T_{\text{eb.}} = 40\text{ }^{\circ}\text{C}$ at 0.5 torr),^[74] as well as the triflic acid released, and might be eliminated during the experiment. Conversely, **1h** has a similar reduction potential ($E^{0'} \approx -1.60\text{ V}$ vs. Ag/AgCl, 3 M NaCl), but is a much less volatile solid which could release a high boiling *p*-toluensulfonic acid.

4.2.2 EUV promoted polymerization of hybrid organic-inorganic materials.

Two different silica-based hybrid organic-inorganic materials bearing acid-sensitive epoxy functionalities were selected and synthesized to perform the polymerization experiments, namely G8Ge2 (already employed for tests on aryl tosylates and sulfonimides, see chapters 2 and 3) and GB (see Chart 4.2 for a comparison). The two materials were chosen aiming to test PAGs in matrices with a different grade of transparency. In G8Ge2, in fact, 20% of silicon atoms are substituted with germanium: since Ge has an absorption cross sections in the EUV region significantly higher than Si,^[70] G8Ge2 is far less transparent than GB.

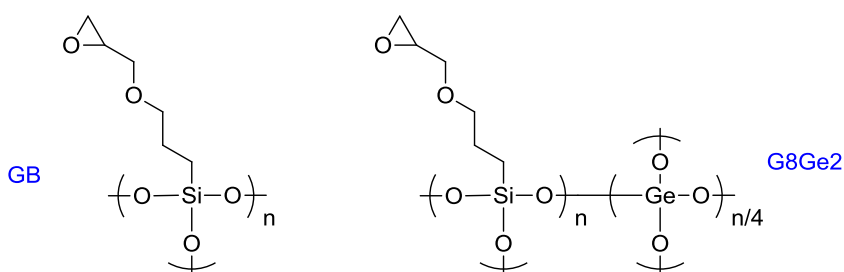


Chart 4.2. Hybrid organic-inorganic sol-gel materials employed for polymerization experiments.

To carry out polymerization tests, spin-coated films (100-150 nm thickness) of the synthesized matrices (containing **1h** and **1i**, 1% molar concentration with respect to the epoxy groups) were irradiated in low-pressure xenon environment ($P = 10^{-2}$ mbar plus 10^{-5} mbar of residual air) at increasing EUV doses (25-400 mJ/cm^2). The EUV radiation source was a Xe discharge produced plasma (DPP) emitting radiation in the 10-20 nm region.

Performances of each combination of PAGs and hybrid matrices were tested and, for every experiment, a blank of the same matrix not containing the photoacid generator was irradiated in parallel. This was done to estimate the effects of PAGs in the polymerization processes,

minimizing the errors deriving from fluctuations of the EUV radiation source. Furthermore (4-phenylthiophenyl)diphenylsulfonium triflate (DPST) was likewise tested to have a comparison with a commercially available PAG. The choice for this ionic PAG was motivated by the fact that triarylsulfonium salts are commonly used as EUVL initiators.^[75] Furthermore we determined that DPST is quite easy to be reduced ($E^{0'} \approx -1.10$ V vs. Ag/AgCl, 3 M NaCl), making it very prone to trap secondary electrons.

Similarly to what seen in the previous chapters, structural modifications induced by photoacid generators on GB and G8Ge2 were investigated by FT-IR analysis. However, in this case, the area under the signals at 910 and 855 cm^{-1} , belonging to the C–O stretching of the oxirane moiety,^[76] was measured to determine the degree of polymerization instead of that under bands at 3060 and 3000 cm^{-1} . The choice was determined by the use of GB system, for which the former measurement is more appropriate.^[31c]

Results obtained from the EUV induced polymerization experiments were interesting. The degrees of polymerization induced by aryl sulfonate **1h** and commercial DPST in GB as a function of the EUV dose are reported, respectively, in Figure 4.1a and Figure 4.1b. As above mentioned, these data were compared with results obtained from GB films not containing the chosen PAG and irradiated in parallel.

First of all it is evident from the graphs that GB films, even when photoinitiators were not present, were able to reach degrees of polymerization of about 60% with modest EUV doses (between 150 and 200 mJ/cm^2). Such results indicate that the proposed hybrid organic-inorganic epoxy-based materials have an inner potentiality toward EUV lithography. However the presence of **1h** allowed to reach a much faster polymerization: at low doses, the degrees of polymerization achieved with **1h** were double than those obtained without it (see Figure 4.1a). This result indicates that **1h** can induce further crosslinking reactions within the epoxy moieties. On the

contrary, Figure 4.1b shows that DPST was not able to substantially improve the polymerization of the GB films. Since **1h** gave positive results where a commercial, more reducible PAG failed, it is apparent that the specific design of related aryl sulfonates is a good starting point to have proper initiators for high-performance hybrid organic-inorganic resists suitable for EUV.

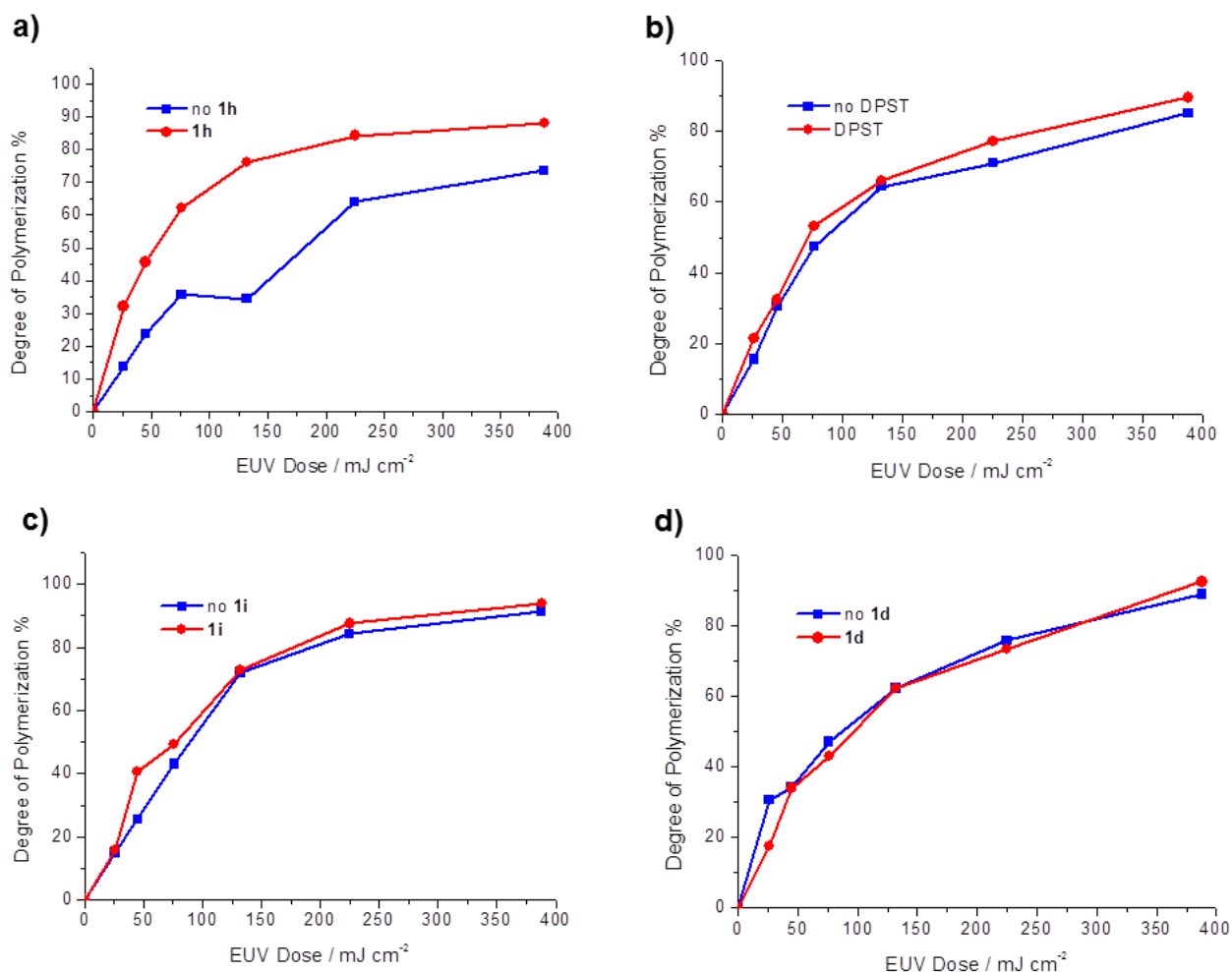


Figure 4.1. Polymerization degree of epoxy groups vs. EUV irradiation dose released (calculated measuring the area under 910 cm⁻¹ band). Experiment performed on GB films containing: a) 1% molar **1h**; b) 1% molar DPST; c) 1% molar **1i**, d) 1% molar **1d**. Comparisons with the polymerization degree reached by blank GB films irradiated in parallel and not containing the different PAGs are provided.

A different situation occurred for **1i**. Indeed, it behaved similarly to DPST and was not able to give improvements in the polymerization of GB (see Figure 4.1c). As expected, its volatility could decrease its real concentration in the resist, reducing its performances as initiator.

Similar results were obtained from tests performed on G8Ge2 matrix. Again very high degrees of polymerization were obtained independently on the presence or absence of PAGs and **1h** appeared as the only one among the tested initiators able to significantly improve the polymerization efficiency (see Figure 4.2). However, in this case the effect of **1h** was far less evident and the different absorption of the EUV radiation by GB and G8Ge2 seems to modify the reactivity of **1h**, which had a much more active role in the most transparent matrix.

In order to have more insights on the role of **1h** in the process we examined a fluorine-free tosylate (**1d**, see Chart 4.1), by repeating polymerization experiments on a GB film. **1d** was chosen for the comparison because it showed a similar reducibility ($E^{0'} \approx -1.60$ V vs. Ag/AgCl, 3 M NaCl) with respect to **1h** and gave good results as PAG for UV photopolymerization of epoxy-based hybrid organic-inorganic materials (see the chapter 2 on aryl tosylates).

However, no substantial differences between the degrees of polymerization reached by the tested film and its blank (not containing **1d**) were observed (see Figure 4.1d). Thus, the use of simple aryl tosylates is not sufficient to have chemically amplified resists and the need for specific perfluoroaryl sulfonates as PAGs for EUVL is apparent.

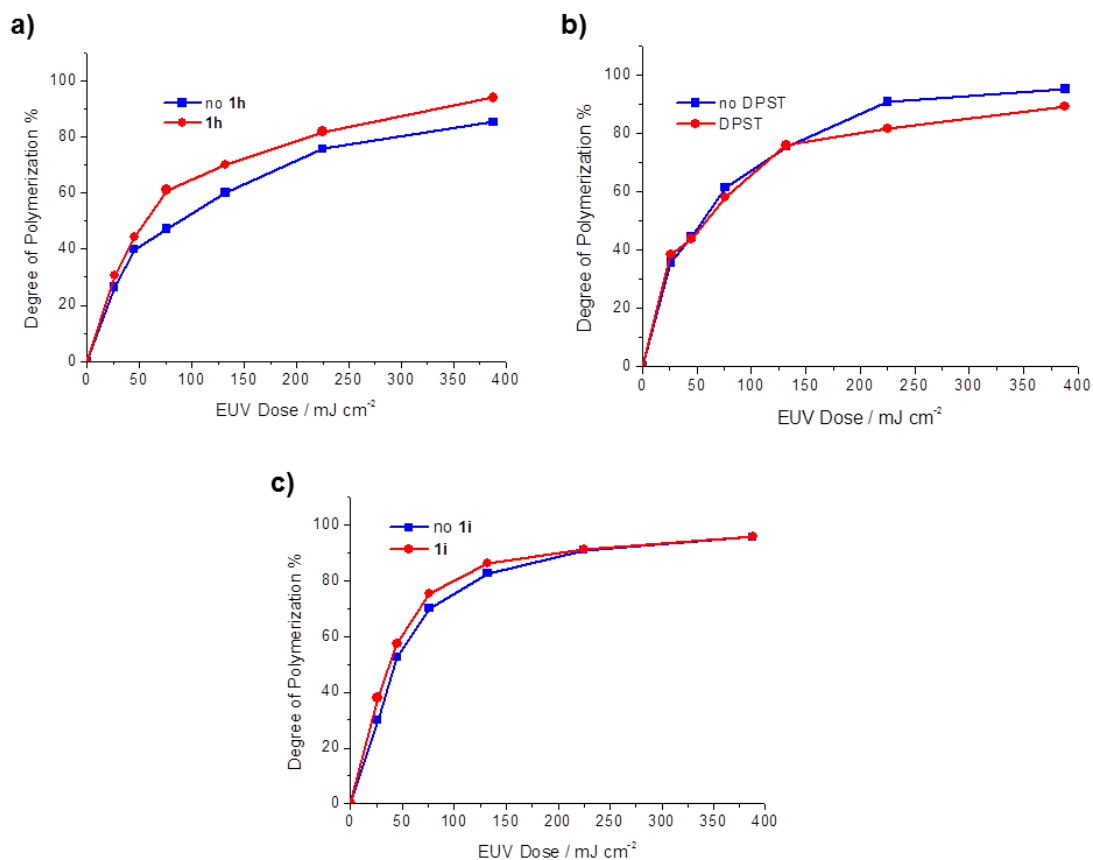


Figure 4.2. Polymerization degree of epoxy groups vs. EUV irradiation dose released (calculated measuring the area under 910 cm^{-1} band). Experiment performed on G8Ge2 films containing: a) 1% molar **1h**; b) 1% molar DPST; c) 1% molar **1i**. Comparisons with the polymerization degree reached by blank G8Ge2 films irradiated in parallel and not containing the different PAGs are provided.

4.2.3 EUV promoted patterning experiments.

Once demonstrated that the system GB + **1h** gave very good results in polymerization experiments, we decided to test it in real application for EUV lithography by performing pattern experiments. In detail, GB sol-gel films (100-150 nm thickness) containing 1% molar **1h** (with respect to epoxy groups) were exposed to EUV radiation using the DPP source combined with a contact EUV lithography (CEUVL) setup. CEUVL, compared with other EUVL techniques, like

the projection tools, is a laboratory-scale system, much less expensive and easy-to-use, although limited on the achievable spatial resolution to $\sim 0.1 \mu\text{m}$.^[77]

The resists were irradiated with doses between 5 and 100 mJ/cm^2 through masks composed by a Si_3N_4 membrane covered with absorbing gold patterns of different geometries.^[78]

Briefly, the irradiation setup was arranged to have DPP radiation source 17 cm far from the samples to be irradiated and the mask positioned between the two at only 3 μm from the sample (see Figure 4.3). Zirconium filters were added as well in front of the mask to select radiation with wavelengths between 10 and 20 nm among those emitted from the Xe plasma.^[79] Another important tool employed was a debris mitigation system (DMS),^[80] needed to protect the mask from debris coming from the source and specifically developed for the setup exploited. It was composed by two main elements: a permanent magnet dipole able to deflect ionic particles and a rotating structure (RS, placed between the source and the samples to be patterned) to stop particulate debris.

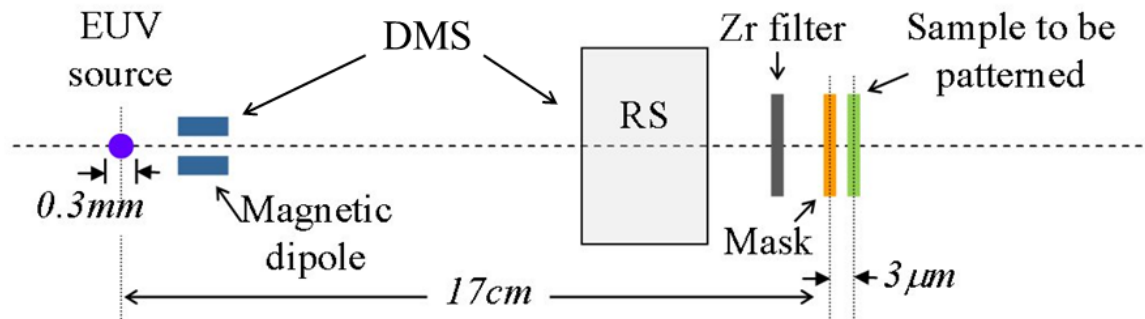


Figure 4.3. Experimental setup for contact EUVL exposures: the magnetic dipole and the rotating structure (RS) form the debris mitigation system (DMS).

Once the GB films containing **1h** had been irradiated they were developed by a NaOH solution (see Experimental Section) which dissolved the unexposed area and left the irradiated one on the substrates (the system behaved as a negative tone resist).

As shown in Figure 4.4, different microstructures characterized by feature resolutions below 1 μm were successfully achieved with doses of only 6-11 mJ/cm^2 . In particular, the detailed optical microscope observation of chessboards depicted in Figure 4.4b, obtained with a 11 mJ/cm^2 EUV dose, shows that squares of 1 μm side with sharp edges were easily obtained (Figure 4.4c). Moreover the SEM (Scanning Electron Microscope) analysis of the circular patterns shown in Figure 4.4d allowed to observe resolved details around 100 nm in size.

The latter observation is interesting since the expected optical resolution should follow the formula $R \sim \sqrt{\lambda \cdot G}$, where R is the optical resolution, λ (~ 13 nm) is the average radiation wavelength and G (~ 3 μm) is the gap between the mask and the resist.^[78,81] However the observed resolution was better than the expected one of about 0.2 μm : the improved lithographic resolution was caused by the non-linearity of the resist response, thus giving further evidence of the role of **1h** to start the polymerization process.

Lastly, the low EUV dose needed to properly expose the selected resist, together with a low concentration of the photoinitiator used (only 1% molar), could enable the system to impact on industrial applications.

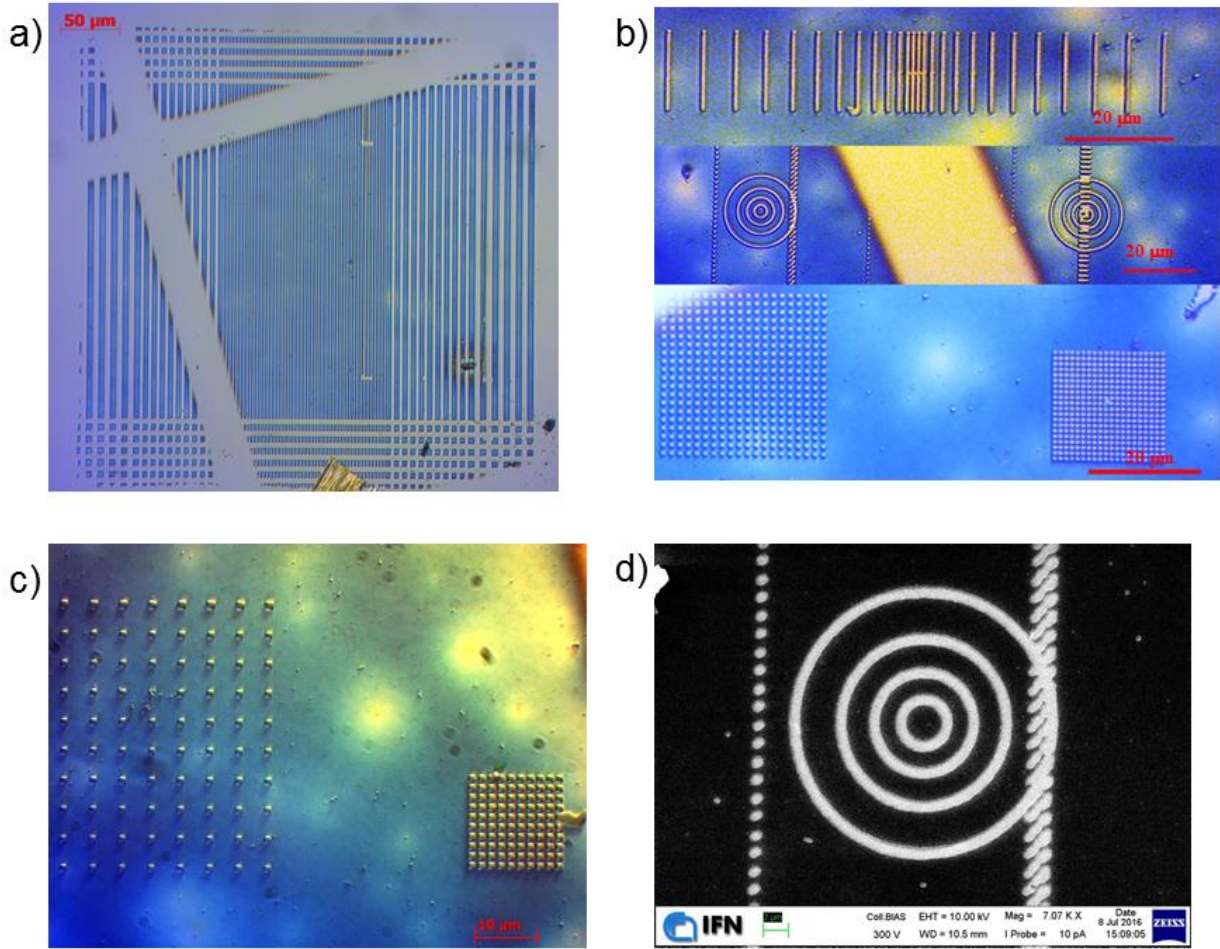


Figure 4.4. Examples of structures obtained by contact EUVL on films of GB + 1% **1h**. a) Optical microscope observation of pattern obtained with a 6 mJ/cm^2 EUV dose. Patterned lines have a step-growing period from the center to the borders of $3 \mu\text{m}$, $5 \mu\text{m}$ and $10 \mu\text{m}$. b) Optical microscope observations of patterns obtained with different masks by a 11 mJ/cm^2 EUV dose. Chessboards in the bottom pattern have periods of $2 \mu\text{m}$ (the one on the left) and $1 \mu\text{m}$ (the one on the right). c) Optical microscope observation of details of the chessboards depicted in Figure 4.4b. d) SEM image of detailed circular patterns shown in Figure 4.4b. The biggest of the four concentric circles is $20 \mu\text{m}$ in diameter.

4.3 *Conclusion.*

In the present chapter it was demonstrated that specifically designed electron-poor perfluoroaryl sulfonates such as **1h** can be employed as initiators for EUV promoted cationic polymerization of epoxy rings in sol-gel materials. Furthermore, regarding the tested system, the developed compound was found to be a better PAG than the commercially available DPST usually exploited for UV and EUV lithographic applications.

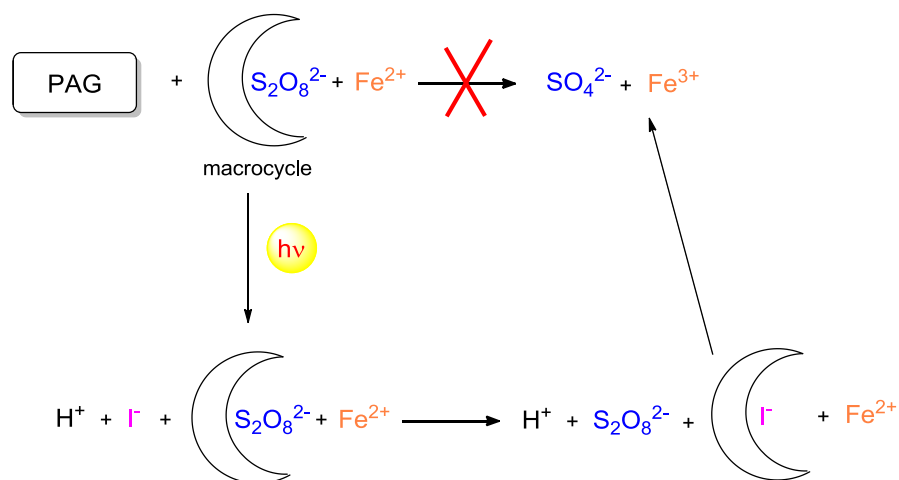
It is worth noticing that a resist composed by the silica based hybrid material GB and PAG **1h** was successfully patterned by very low EUV doses (about 10 mJ/cm²) in a contact EUVL setup, gaining resolved feature sizes down to 100 nm. Thus, in reason of the high efficiency of the GB + **1h** system and of the cost-effectiveness of the photoinitiator, the developed system seems very attractive for applications in microelectronic industry and it represents maybe the best result obtained in the whole research project.

5 Phototriggered oxidation of Fe²⁺ by release of HI

5.1 *Introduction.*

The previous chapters were devoted to the release of strong sulfonic acids from non-ionic photoacid generators. Such compounds were in fact considered as “caged protons” to be liberated upon irradiation. Thus the attention went mainly on the yields and efficiency in the release of H⁺ ions, while the conjugate bases (e.g. sulfonate anions) were selected only to ensure acidity to promote polymerization and photolithographic processes. The sole focus on the efficiency of the photorelease is, however, a peculiarity of PAGs. Indeed, for all the other caged compounds, the nature of the released species is as important as the photoreactivity of the labile moiety and, rather, a chosen protecting group can be exploited to liberate many different biomolecules and drugs.^[1,19,82]

In the present chapter we present a research project carried on at the Department of Chemistry (Faculty of Science) of the Masaryk University (Brno, Czech Republic), under the supervision of Prof. Petr Klán. This is a sort of crossover between the two approaches described above: the photorelease of a very strong acid where the counter-anion nature is crucial to perform technological applications. In fact we developed a system to phototrigger the oxidation of Fe²⁺ by S₂O₈²⁻ (Scheme 5.1).^[83] In detail, this known redox process^[84] was initially inhibited by trapping persulfate into a macrocyclic cage which shielded its reactivity. Then we irradiated PAGs able to photorelease strong HI to make the reaction to start. Indeed iodide had a higher affinity toward the macrocycle than S₂O₈²⁻, thus, once released, it could replace the latter into the macrocycle cavity, making it free to react and oxidize Fe²⁺. By this way we obtained a controlled the oxidation of Fe²⁺ to Fe³⁺.



Scheme 5.1. Oxidation of Fe^{2+} by $\text{S}_2\text{O}_8^{2-}$ phototriggered by photoacid generators in the presence of a macrocyclic cage.

The studied redox process is important because it brings to the formation of a Fenton's like reagent used in environmental chemistry,^[85] in molecular biology^[86] and as initiator in emulsion polymerization.^[87] Furthermore, the possibility to have spatial and temporal control over the reaction using a light-triggered system is an added value. For these reasons we embarked in this project and results obtained are described in the following.

5.2 Results and discussion.

The system used to sequentially encapsulate persulfate and iodide anions was **BU** (see Chart 5.1), a water soluble macrocycle belonging to the family of bambusurils, which are non-ionic receptors for anions such as I^- , ClO_4^- and SCN^- .^[88] To use this compound in the phototrigger, however, it was necessary, first, that its affinity toward I^- was higher than toward $\text{S}_2\text{O}_8^{2-}$. Thus association constants K_a between **BU** and the two anions (1:1 complexes) were calculated by isothermal titration calorimetry (ITC) and were found to be $K_a = (1.3 \pm 0.1) \times 10^7 \text{ M}^{-1}$ for I^- and $K_a = (8.3 \pm$

$0.1) \times 10^6$ for $S_2O_8^{2-}$, in water. Notably the obtained value for the complex with I^- , besides verifying the higher affinity between **BU** and iodide, is also the highest ever observed for a non-ionic receptor in water, including other bambusuril derivatives.^[88c]

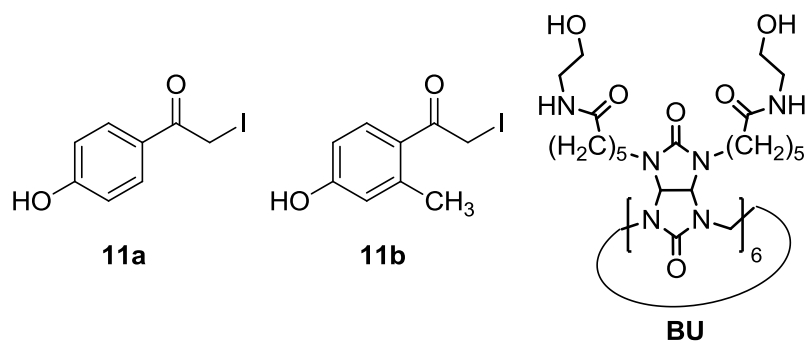


Chart 5.1. Photoacid generators **11a,b** and macrocyclic cage **BU**.

Nonetheless we had to demonstrate likewise that the association between **BU** and persulfate was tight enough to prevent early oxidation of Fe^{2+} in the dark. Furthermore we needed to check also that the difference in affinities between the macrocycle and the two anions was sufficient to give the replacement of $S_2O_8^{2-}$ by I^- and the subsequent oxidation of Fe^{2+} . Accordingly a water solution containing $S_2O_8^{2-}$, Fe^{2+} and **BU** was titrated adding tetrabutylammonium iodide (TBAI) and the titration was followed by UV-visible absorption spectroscopy. Indeed Fe^{3+} ion in water has a characteristic absorption band between 250 and 400 nm^[89] while Fe^{2+} is substantially transparent in this region,^[90] making absorption spectroscopy the proper technique to follow the process. As depicted in Figure 5.1a, a shoulder in the 200-450 nm region increasingly developed after additions of TBAI. Thus the oxidation of Fe^{2+} to Fe^{3+} as a consequence of the addition of I^- was demonstrated.

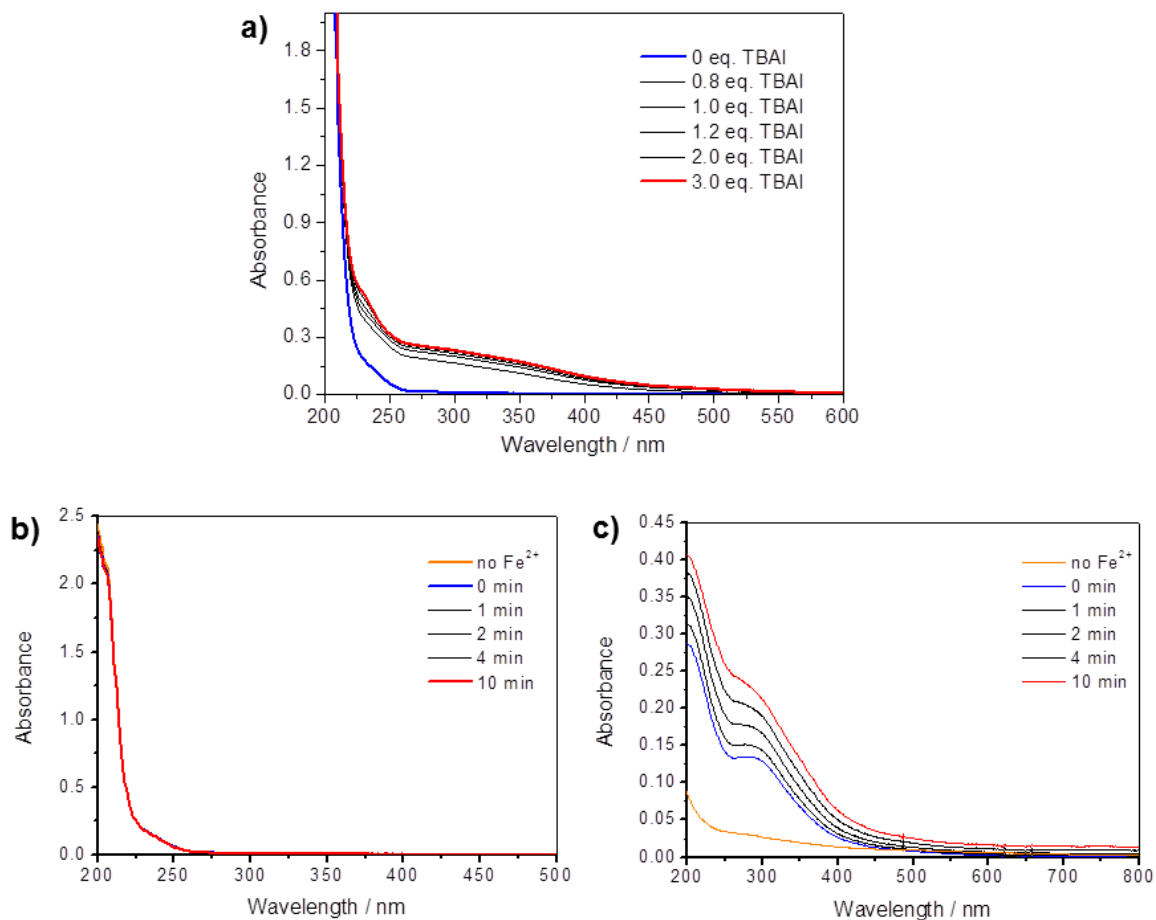
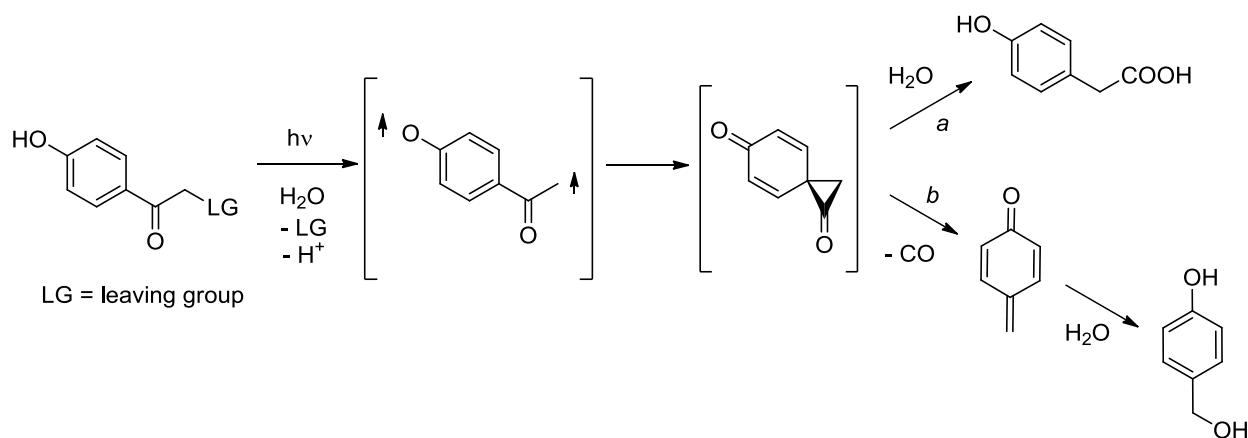


Figure 5.1. a) Spectrophotometric titration of 3.0 mL of a mixture of $\text{Na}_2\text{S}_2\text{O}_8$ ($3.5 \times 10^{-5} \text{ M}$), FeSO_4 ($7.1 \times 10^{-5} \text{ M}$) and **BU** ($5.7 \times 10^{-5} \text{ M}$) in water by TBAI. The equivalents of TBAI are referred to those of **BU**. b) The absorption spectra of a solution of $\text{Na}_2\text{S}_2\text{O}_8$ ($3.6 \times 10^{-5} \text{ M}$) and **BU** ($5.7 \times 10^{-5} \text{ M}$) in water measured before and upon the addition of one equivalent of FeSO_4 (up to 10 min). c) Changes in the absorption spectra of a solution of $\text{Na}_2\text{S}_2\text{O}_8$ and FeSO_4 (both $3.6 \times 10^{-5} \text{ M}$) measured within 10 min.

Moreover the addition of Fe^{2+} ions to a solution of $\text{Na}_2\text{S}_2\text{O}_8$ and **BU** caused instead no evident changes in the absorption spectrum of the solution, sign of the stability of the system (see Figure 5.1b). For a comparison, absorption spectra of a solution of FeSO_4 before and after addition of $\text{Na}_2\text{S}_2\text{O}_8$ (in absence of **BU**) are provided as well (Figure 5.1c). Results shown in Figure 1 can be

explained only by accepting the inactivity of persulfate in the complex with **BU** and the ability of iodide to replace $S_2O_8^{2-}$ inside the macrocycle, liberating it. Thus our initial hypothesis was confirmed.

The next step was to develop proper compounds able to release iodide upon irradiation and *p*-hydroxyphenacyl photoremovable protecting group was thought to be the right moiety. Indeed *p*-hydroxyphenacyl caged compounds are known to be photoreactive and, once irradiated in water (as in the present case), give a photo-Favorskii rearrangement from the triplet excited state to phenylacetic acids (Scheme 5.2, *path a*) or to benzyl alcohols (*path b*).^[91] In this way they are able to release a wide variety of compounds of biological interest (among the others: nucleotides, aminoacids, thiols).^[19,82,91a,92]



Scheme 5.2. Photo-Favorskii rearrangement for the release of caged compounds (LG in the scheme).

Therefore we decided to apply this peculiar photochemical behavior to release iodide (in the form of HI) and we synthesized compounds with the photolabile moiety coupled with iodide (**11a** and **11b**, see Chart 5.1). The synthesis proceeded starting with bromination by CuBr_2 of the corresponding acetophenones,^[93] followed by a Finkelstein reaction.

The photochemical study on these compounds started measuring UV-visible absorption spectra in 99:1 water acetonitrile mixtures. The presence of acetonitrile was mandatory to reach a good solubility for the substrates. As pointed out in the spectra of Figure 5.2, both **11a** and **11b** have an intense absorption bands near 300 nm, thus making UV light the proper radiation for photorelease experiment.

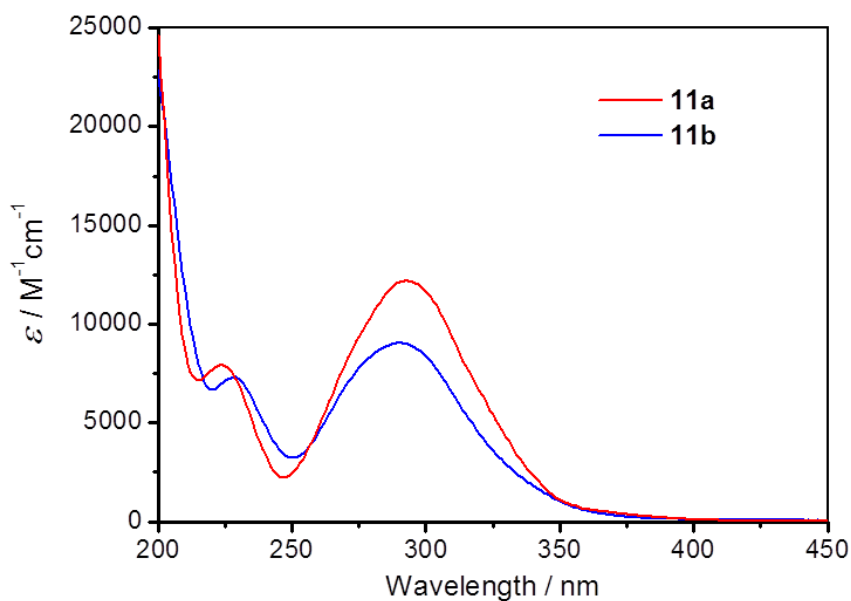


Figure 5.2. UV-visible absorption spectra of **11a** and **11b** (concentration $\sim 5.0 \times 10^{-5}$ M) in water/acetonitrile (99 : 1).

Accordingly **11a** (chosen as model compound) was irradiated by a Xe lamp in a 1:1 mixture of D_2O and CD_3CN for 3 hours in the absence of oxygen, until total consumption of **11a**. 1H -NMR spectra were taken before and after the irradiation to verify **11a** conversion and check the distribution of photoproducts (Figure 5.3). Interestingly, irradiation of **11a** brought not only to photo-Favorskii rearrangement products (**12a** and **13a**, Figure 5.3 and Scheme 5.3), but also to the photosolvolysis derivative (**14a**). Similar products have been already observed in past when

simple phenacyl derivatives ^[94] and 4-hydroxyphenacyl derivatives were irradiated, (the latter in very low chemical yields).^[95]

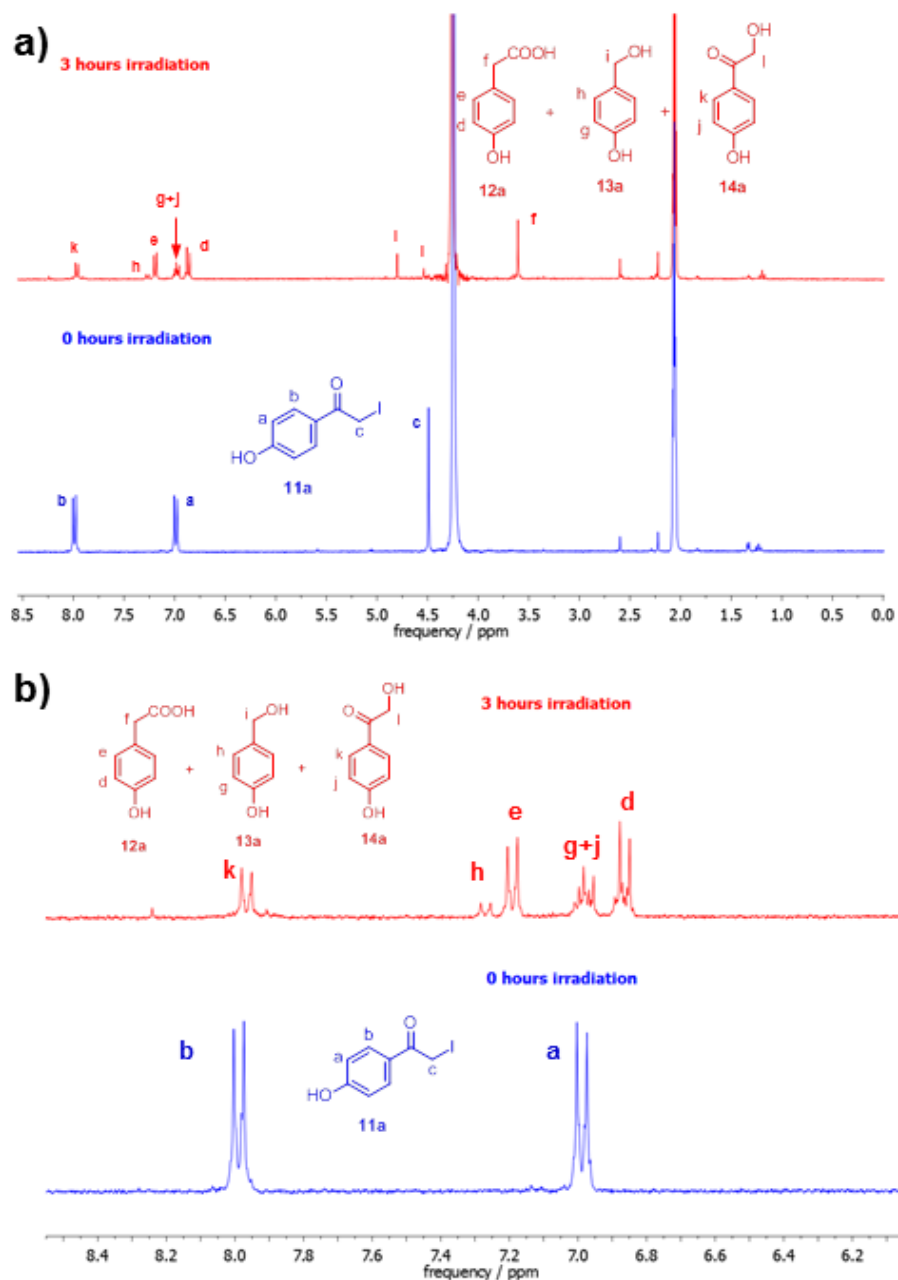
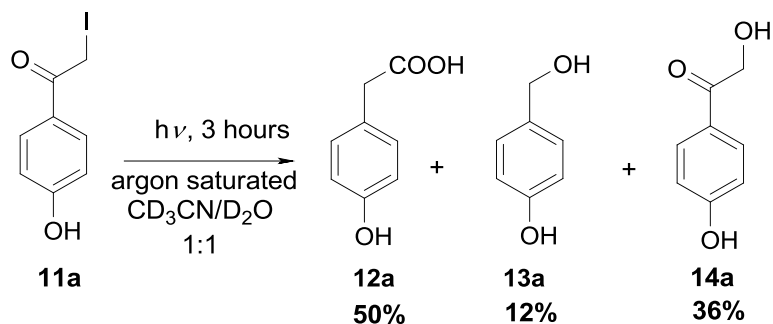


Figure 5.3. a) ¹H-NMR spectra of **11a** (6.8×10^{-3} M, 1.0 mL) in an argon saturated CD₃CN/D₂O (1 : 1) mixture before and after 3 h of irradiation using a 1000-W Xe lamp. b) Enlargement in the 6.1-8.5 ppm region.



Scheme 5.3. Photoproducts distribution from irradiation of **11a** (6.8×10^{-3} M, 1.0 mL) by a 1000 W Xe lamp. Yields determined by $^1\text{H-NMR}$ spectroscopy. The residual signal of CD_3CN was used as an internal standard.

Regarding the release of iodide, both **11a** and **11b** were found to photorelease quantitative amounts ($> 91\%$) of I^- (actually HI) after only 10 minutes of irradiation (see below in the chapter, Table 5.1). The amount of iodide liberated during irradiation was quantified exploiting the affinity of the ion toward **BU**: if the irradiation of **11a** and **11b** brought to iodide formation, this would promptly form a 1:1 complex with **BU**.

Thus two solutions containing the macrocycle and 1.1 equivalents of either **11a** or **11b** were irradiated and the iodide released was determined by monitoring the change in the chemical shifts of signals assigned to **BU**. In particular, the change in the positions of two signals from 5.38 and 4.93 ppm to 5.64 and 5.00 ppm was attributed to the change from the anion-free form of **BU** to its complex with I^- (by comparing with the authentic samples, Figure 5.4).

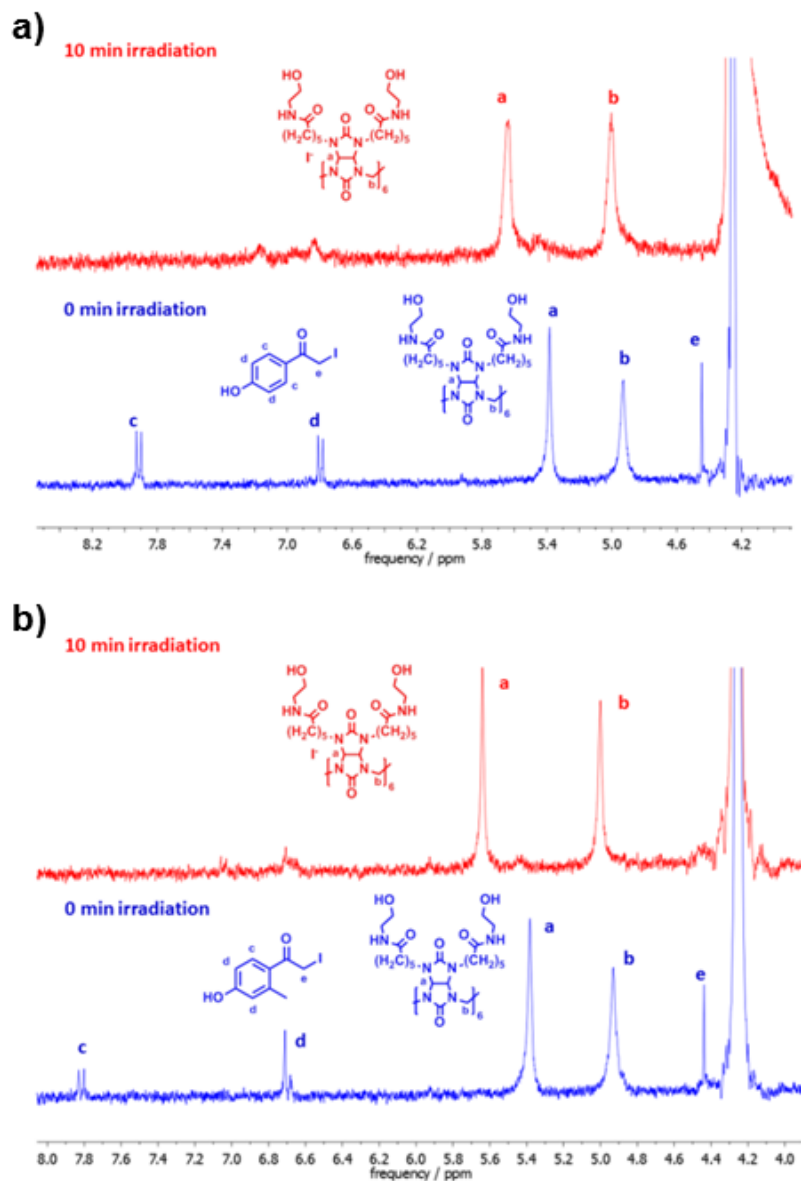


Figure 5.4. ¹H-NMR spectra of the system **11a** + **BU** (or **11b** + **BU**) in an argon saturated CD₃CN/D₂O 1:1 mixture before and after 10 min of irradiation by 1000 W Xe lamp. The molar ratio between **11a** (or **11b**) and **BU** is 1.1. Concentration of **11a** (or **11b**) is 5.63×10^{-4} M. a) Spectrum obtained for **11a**; b) spectrum obtained for **11b**.

Once confirmed the potentiality of **11a** and **11b** to photorelease iodide, the next step was to verify if the iodide generated by this way was likewise able to replace S₂O₈²⁻ inside the macrocycle or

if, instead, the photochemical reaction or the presence of photoproducts could interfere with the process. With this purpose, **11b** (4.76×10^{-4} M, 1.1 equiv.) was irradiated by the Xe lamp in a 1:1 mixture of D₂O and CD₃CN containing dissolved Na₂S₂O₈ (1 equiv.) and **BU** (1 equiv.) and ¹H-NMR spectra were recorded before and after irradiation. Signals at 5.61 and 4.93 ppm (typical of the **BU**-S₂O₈²⁻ complex) present before irradiation shifted completely to 5.64 and 5.00 ppm, typical of the complex with I⁻, after 10 minutes of irradiation (Figure 5.5). Thus a complete exchange between I⁻ and S₂O₈²⁻ complex occurred. Furthermore solutions of **BU**-S₂O₈²⁻ and **BU**-I⁻ complexes (5.61×10^{-4} M) in the same solvents mixture gave no change in their ¹H-NMR spectra when kept in dark or irradiated for 10 minutes. Therefore their (photo)chemistry has no role in the ion exchange and the presence of **11a** or **11b** is necessary to make it to occur.

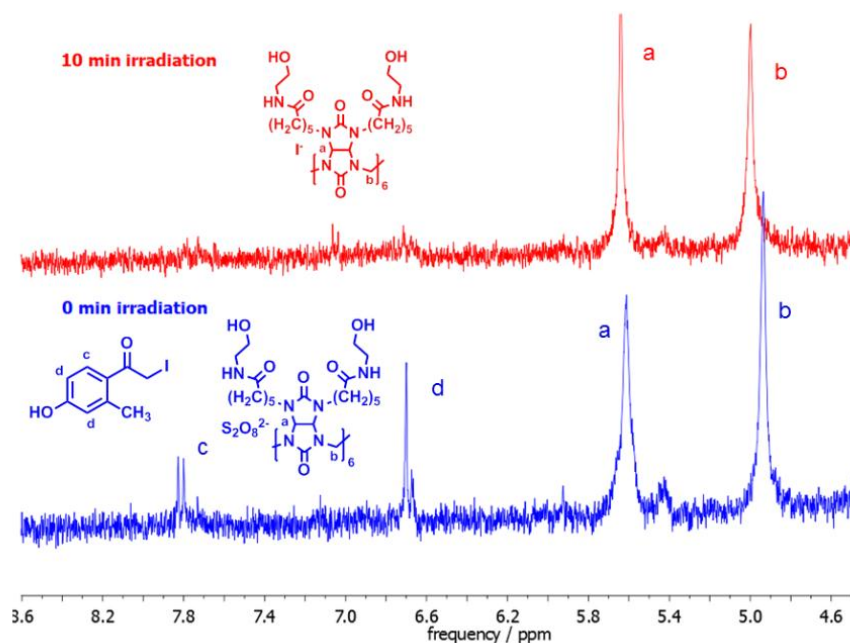


Figure 5.5. ¹H NMR spectra of a solution of **BU** (4.31×10^{-4} M), Na₂S₂O₈ (4.29×10^{-4} M) and **11b** (4.76×10^{-4} M, 1.1 equiv.) in an argon saturated CD₃CN/D₂O 1 : 1 mixture before and after exhaustive irradiation using a 1000-W Xe lamp.

Lastly **11a** and **11b** were tested for the oxidation of Fe (II) to Fe (III). First the stability of these systems was checked looking for any changes in the UV-visible absorption spectrum of solutions containing Fe^{2+} , $\text{S}_2\text{O}_8^{2-}$, **BU** and **11b**. Indeed **11b** could interfere with the complexation of persulfate by **BU**, weakening it. However, no significant changes in the spectra were and the stability of the persulfate and its inactivity toward oxidation (in dark) was confirmed also in the presence of **11b** (Figure 5.6a).

We further proceeded irradiating an argon saturated solution containing Fe^{2+} , $\text{S}_2\text{O}_8^{2-}$, **BU** and **11b** and following the photoreaction by UV-visible absorption spectroscopy, looking for the formation of bands at about 300 nm. Figure 5.6b shows that a big change in that spectral region, attributable not only to the photodecomposition of **11b** (compare with UV spectra in Figure 5.6c), but also to the formation of Fe (III) species, occurred after 10 minutes of irradiation, similarly to what already seen in Figure 5.1a for the titration with TBAI.

A blank test was done as well irradiating a solution containing Fe^{2+} , $\text{S}_2\text{O}_8^{2-}$ and **BU** for 10 minutes. Since no change in the absorption spectrum occurred (Figure 5.6d), it confirmed that the photochemical behaviors of Fe^{2+} [96] and $\text{S}_2\text{O}_8^{2-}$ [97] had no role in the oxidation process and that the latter was due only to the ability of the photoreleased iodide to replace persulfate and make it free to react.

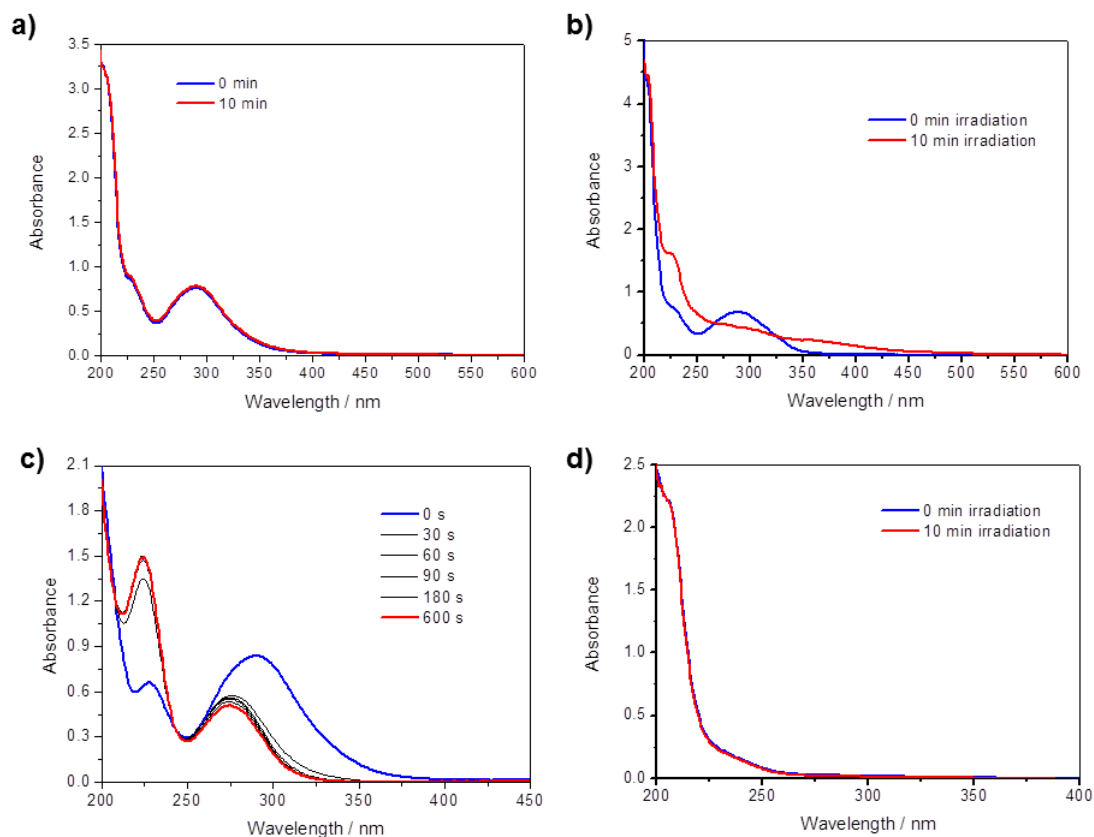


Figure 5.6. a) Absorption spectra of a solution containing FeSO_4 (7.2×10^{-5} M), $\text{Na}_2\text{S}_2\text{O}_8$ (3.6×10^{-5} M), **11b** (8.0×10^{-5} M) and **BU** (5.8×10^{-5} M) in a water/MeCN (99 : 1) mixture measured immediately after the preparation and after 10 min in dark. b) Absorption spectra of a solution of FeSO_4 (7.1×10^{-5} M), $\text{Na}_2\text{S}_2\text{O}_8$ (3.6×10^{-5} M), **BU** (5.7×10^{-5} M) and **11b** (7.8×10^{-5} M) in a water/MeCN (99 : 1) mixture recorded before and after 10 min of irradiation. c) Absorption spectra of **11b** (7.98×10^{-5} m) in an argon saturated water/acetonitrile (99 : 1) mixture during irradiation. d) Absorption spectra of a solution of FeSO_4 (7.3×10^{-5} M), $\text{Na}_2\text{S}_2\text{O}_8$ (3.7×10^{-5} M) and **BU** (5.9×10^{-5} M) in a water/MeCN (99 : 1) mixture recorded before and after 10 min of irradiation. A 1000 W Xe lamp was used for all the irradiations.

However, even if the spectral changes observed in Figure 5.6b were attributed to the oxidation of Fe^{2+} to Fe^{3+} , the shape and the broadening of the absorption shoulder prevent to make this attribution really safe. Thus another method to evaluate the redox reaction was needed and an analytical procedure which relies on the use of 1,10-phenanthroline (phen) was chosen. Indeed phen is able to form with Fe^{2+} the complex $\text{Fe}(\text{phen})_3^{2+}$ (the so-called “ferroin”) which has a very high association constant ($K_a = 2.5 \times 10^6$ in acidic water).^[98] Moreover the resulting complex exhibits a strong visible absorption band centered at 508 nm ($\epsilon = 11100 \text{ M}^{-1}\text{cm}^{-1}$ in water) and the formation of the complex is actually a colorimetric method to determine the amount of Fe (II) species present in real samples.^[99] In the present study the method was applied to determine the amount of Fe^{2+} still present after the phototriggered oxidation.

In detail argon saturated solutions containing Fe^{2+} , $\text{S}_2\text{O}_8^{2-}$, **BU** and either **11a** or **11b** were irradiated for 10 minutes by the 1000 W Xe lamp and then treated with an excess of 1,10-phenanthroline. Then a UV-visible absorption spectrum was taken and compared with the one obtained from another solution of the four reagents, treated similarly with 1,10-phenanthroline but not irradiated. Confronting the absorbance measured at 508 nm, it was possible to have a safe evidence for the phototriggered redox process and to estimate the yield of the oxidation of Fe^{2+} (see Figure 5.7 for the spectra).

Noteworthy the yields obtained, for both the compounds, are comparable to the yields of iodide released (compare data in the Table 5.1). Hence almost all the HI produced from the irradiation of **11a** and **11b** was really effective to induce the oxidative process.

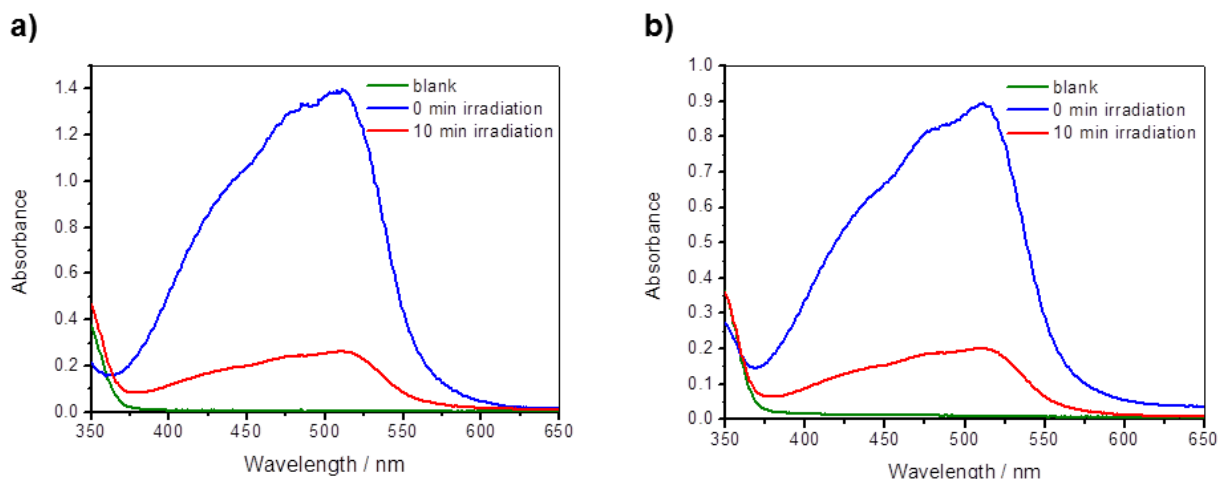


Figure 5.7. a) Absorption bands of $\text{Fe}(\text{phen})_3^{2+}$ complexes obtained by addition of 1,10-phenanthroline (phen) to the irradiated and not irradiated solutions of FeSO_4 (1.7×10^{-4} M), $\text{Na}_2\text{S}_2\text{O}_8$ (8.6×10^{-5} M), **BU** (8.6×10^{-5} M) and **11a** (9.5×10^{-5} M) in an argon saturated water/MeCN 99:1 mixture. b) Absorption bands of $\text{Fe}(\text{phen})_3^{2+}$ complexes obtained by addition of phen to irradiated and not irradiated solutions of FeSO_4 (1.1×10^{-4} M), $\text{Na}_2\text{S}_2\text{O}_8$ (5.5×10^{-5} M), **BU** (5.5×10^{-5} M) and **11b** (6.1×10^{-5} M) in an argon saturated water/MeCN (99 : 1) mixture. The absorption spectra of blank solutions (without FeSO_4) are reported for comparison for both **11a** and **11b**.

Table 5.1. Yields of HI released and Fe²⁺ oxidized upon irradiation of argon-saturated solutions of **11a** and **11b**.

	Conversion % ^[a]	HI released, yield % ^[a]	Fe ²⁺ oxidized, yield % ^[b]
11a	100	>91	82
11b	100	>91	79

^[a] Solutions of **BU** (5.1×10^{-4} M) and **11a** or **11b** (5.6×10^{-4} M, 1.1 equiv.) in a D₂O/CD₃CN (1 : 1) mixture irradiated for 10 minutes using a 1000-W Xe lamp. The reaction conversion (the consumption of *pHP* derivatives) and the yields of iodide released as a complex with **BU** were estimated by ¹H-NMR. ^[b] The concentrations of Fe²⁺ ions was determined in the presence of 1,10-phenanthroline using absorption spectroscopy. Solutions of either **11a** (9.5×10^{-5} M) or **11b** (6.1×10^{-5} M) in a water/CH₃CN (99 : 1) mixture irradiated for 10 minutes in the presence of **BU**, Na₂S₂O₈ and FeSO₄ (molar ratios: 1.1 : 1 : 1 : 2).

5.3 Conclusion.

Summing up, although the data reported in this chapter are only preliminary, the particular reactivity of **BU** with persulfate and iodide was exploited to develop phototriggers for the oxidation of Fe²⁺ by S₂O₈²⁻. Indeed, the UV irradiation of **11a** and **11b** (compounds able to photorelease iodide) in the presence of **BU** and persulfate brought to the quantitative replacement of S₂O₈²⁻ by I⁻ in the complex with **BU**, thus enabling the otherwise prevented redox reaction. This elegant phototrigger could find application, for example, in polymer chemistry, as initiator for radical photopolymerization.

6 Photoinduced trifluoromethylation of aromatics

by an *N*-arylsulfonimide

6.1 Introduction.

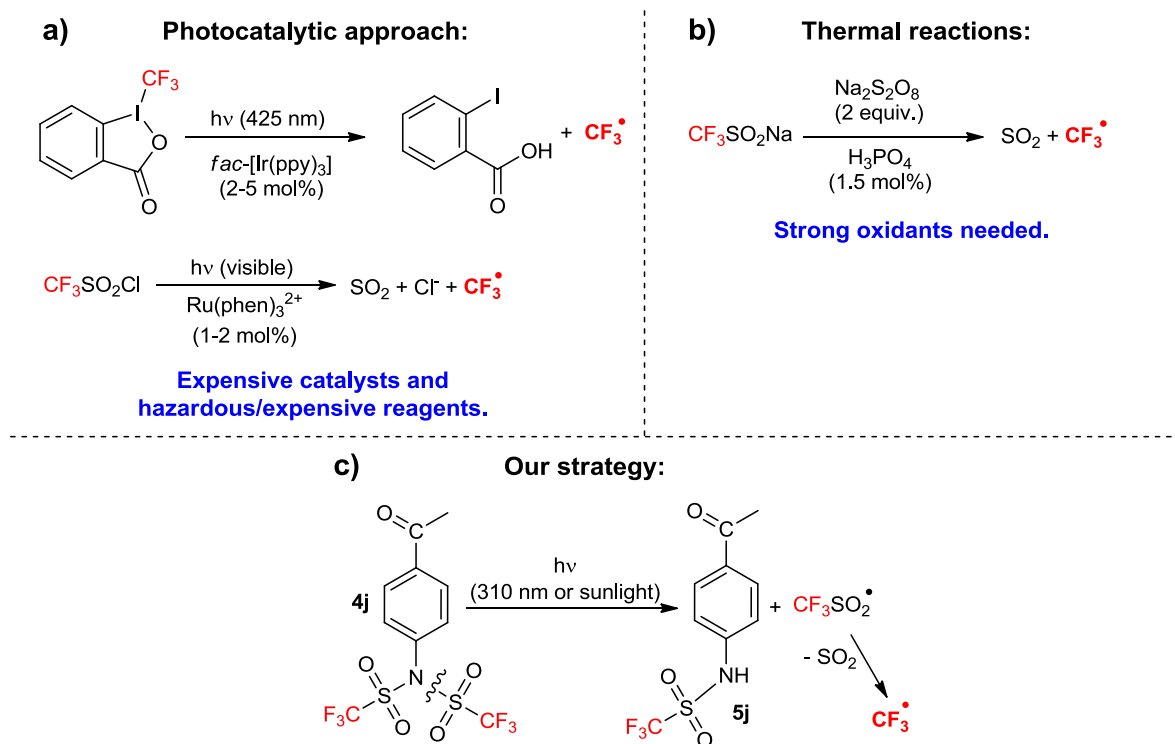
This chapter will not be concerned on photoacid generators and proton release and photorelease. Indeed it represent a sort of appendix where it is described how a particular compound, tested as non-ionic PAG and seen ineffective in this role, was re-invented as a reagent to perform important organic syntheses.

In particular, we described in the chapter 3 that the irradiation of trifluoromethanesulfonimide **4j** leads to the homolysis of the *N*-S bond, giving trifluoromethanesulfonyl radicals. However these intermediates give F_3C^\bullet radicals by SO_2 loss from $CF_3SO_2^\bullet$.^[48] Thus, unfortunately, no strong sulfonic acid is liberated and only species such as HF, CHF_3 and hexafluoroethane are produced from the F_3C^\bullet radical (Scheme 3.2), preventing the possibility to use **4j** as PAG or photoinitiator for cationic polymerization (see Figure 3.6b).^[53]

Nonetheless F_3C^\bullet radical is a very useful intermediate in organic synthesis. Indeed the trifluoromethyl (CF_3) group is a key substituent in medicinal chemistry, since it often enhances the lipophilicity, bioavailability and metabolic stability of bioactive molecules.^[100] Hence trifluoromethylated aromatics are the core building blocks in both pharmaceuticals (including, among others, nilutamide, fluoxetine and leflunomide) and in drug candidates. For this aim, the incorporation of a $-CF_3$ moiety into aromatic rings is a crucial challenge in organic synthesis and impressive efforts have been carried out to develop new trifluoromethylating protocols.^[101]

Most of the recent strategies developed rely on the (photo)generation of trifluoromethyl radicals (Scheme 6.1). Photoredox catalysis is an elegant approach for the formation of these species from

a suitable redox active precursor.^[102] However, the widespread use of expensive catalysts such as iridium and ruthenium complexes and harmful reactants like CF₃I, CF₃SO₂Cl or the Umemoto's and the Togni's reagents (Scheme 6.1a) prompts for the development of cheaper and safer synthetic alternatives.



Scheme 6.1. Typical approaches for the generation of the trifluoromethyl radical making use of a) expensive photocatalysts and hazardous reagents or b) strong oxidants. c) Our proposed (photo)catalyst free formation of the trifluoromethyl radical via photoinduced cleavage of the N-S bond in *N*-aryltrifluoromethanesulfonimide **4j**.

Accordingly, both thermal^[103] and photochemical^[104] catalyst-free strategies have been reported, but in most cases the use of strong oxidants (e.g. persulfate ion, Scheme 6.1b),^[103a,b,d,e] gaseous CF₃I^[104a,c-f,h-j] and moisture sensitive trifluoroacetic anhydride^[103b,d] were mandatory for the process. Furthermore, the developed photochemical methodologies usually made use of

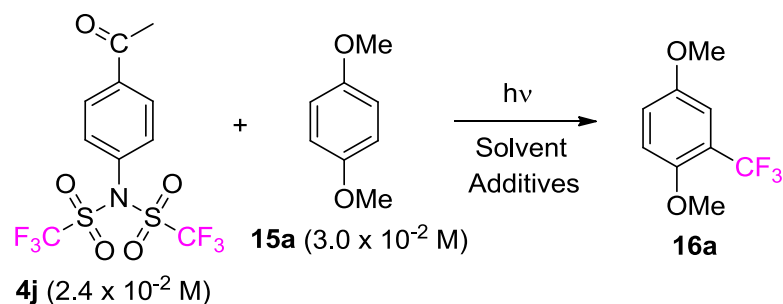
undesirable UVC radiation ($\lambda = 254$ nm) to take place.^[104d-f,h-j] In this scenario, we reasoned that *N*-aryltrifluoromethanesulfonimides such as **4j** could be successfully applied as simple, cheap and easy to handle reagents for photochemical trifluoromethylations (Scheme 6.1c). Moreover, since also the photogenerated sulfonamide **5j** is photoreactive,^[48] both the N-S bonds of **4j** can be cleaved and up to two equivalents of F_3C^\bullet radicals can be photogenerated. This gives an added value to the proposed trifluoromethylating strategy.

6.2 Results and discussion.

The functionalization of 1,4-dimethoxybenzene (**15a**) in the presence of **4j** as trifluoromethylating agent was investigated as the model reaction. Deaerated solutions of the two reagents in different solvents were irradiated in a multi-lamp reactor equipped with 10 phosphor coated lamps (15 W) emitting at 310 nm until no reagent **4j** or photogenerated sulfonamide **5j** were present. A molar ratio of **4j/15a** = 0.8 was used to have a reasonable excess of the F_3C^\bullet radical that could be released. The consumption of **15a** and the yield of trifluoromethylated compound **16a** are listed in Table 6.1.

As depicted in Table 6.1, the reaction took place efficiently in acetonitrile and dichloromethane (ca. 70-80% yields of **16a**, according to the GC analyses), with a slight preference for the latter. In contrast, the conversion of **15a** to **16a** was unsatisfactory in ethyl acetate, methanol and almost negligible in diethyl ether. Notably, omitting water was beneficial for the overall yield (see for instance entries 6 and 7). We then proceeded in the optimization of the reaction protocol by tuning the amount of **4j**. Lowering the concentration of **4j** down to 0.015 M (entry 8) caused the formation of **16a** in only 58% yield, whereas when adopting a large excess of the trifluoromethylating agent (0.03 M), the desired product was obtained in 84% yield (entry 9) but a higher irradiation time (18 h) was required.

Table 6.1. Optimization of the reaction conditions for the trifluoromethylation of 1,4-dimethoxybenzene **15a**.^[a]



Entry	Solvent	Additives	Irradiation conditions	15a Conv., % ^[b]	16a , yield % ^[b]
1	CH ₂ Cl ₂	-	310 nm, 12h	90	81
2	AcOEt	-	310 nm, 12h	62	55
3	CH ₃ OH	-	310 nm, 12h	23	16
4	CH ₃ CN	-	310 nm, 12h	83	74
5	Et ₂ O	-	310 nm, 12h	7	0
6	dry CH ₃ CN	-	310 nm, 12h	88	81
7	dry CH₂Cl₂	-	310 nm, 12h	100	87
8 ^[c]	dry CH ₂ Cl ₂	-	310 nm, 6h	65	58
9 ^[d]	dry CH ₂ Cl ₂	-	310 nm, 18h	100	84
10 ^[e]	dry CH ₂ Cl ₂	Cs ₂ CO ₃ , 0.12 M	310 nm, 16h	84	76
11 ^[e]	dry CH ₂ Cl ₂	K ₂ S ₂ O ₈ , 0.048 M	310 nm, 12h	86	79
12 ^[f]	dry CH ₂ Cl ₂	-	310 nm, 12h	91	83
13 ^[g]	dry CH ₂ Cl ₂	-	Sunlight, 18h	100	86
14 ^[h]	dry CH ₂ Cl ₂	-	dark, 12h	0	0
15 ^[i]	dry CH ₂ Cl ₂	-	310 nm, 72h	80	69

^[a] **15a** (3.0×10^{-2} M), **4j** (2.4×10^{-2} M). Reagents and additives were dissolved in 3.0 mL of the chosen medium and irradiated in quartz tubes under deaerated conditions. The best reaction conditions are given in bold. ^[b] Gas Chromatography (GC) yields referred to the initial amount of **15a**. α, α, α -Trifluorotoluene was used as internal standard. ^[c] **4j** (1.5×10^{-2} M). ^[d] **4j** (3.0×10^{-2} M). ^[e] Irradiation performed under stirring. ^[f] Under air equilibrated conditions. ^[g] Irradiation performed in a Pyrex vessel exposed to sunlight (3 days, 6 h/day) in July 2017, Pavia (Italy). ^[h] Blank experiment performed in the absence of light by covering the reaction tube with an aluminum foil and placing the sample in the 310 nm reactor, as done for entries 1-12. ^[i] **5j** (4.8×10^{-2} M) used as the trifluoromethylating agent.

Since compound **4j** photoreleases huge amounts of HF and H₂SO₃,^[48] we found convenient to perform the irradiation in the presence of a buffering agent. The presence of Cs₂CO₃ in the reaction mixture (entry 10) was however detrimental as it was the use of persulfate anion (entry 11), often employed as auxiliary oxidant in the radical functionalization of (hetero)aromatics.^[105] The presence of molecular oxygen in the samples had a marginal effect on the photoreaction (entry 12). Noteworthy, **16a** was formed roughly in the same yield when using sunlight as the radiation source (entry 13). As pointed out in entry 14, no reaction was observed when keeping the starting reaction mixture in the dark. Lastly, **5j** (4.8×10⁻² M) was tested as the trifluoromethylating reagent (entry 15) but **16a** was obtained in only 69% yield after 72 h irradiation, showing that **4j** performed better, although the double amount of triflamide **5j** employed could in principle release the same amount of F₃C[•] radicals.

With these results in our hands, we extended the scope of the reaction by applying the trifluoromethylation to a range of aromatic and heteroaromatic derivatives (Table 6.2). The adopted experimental conditions were those described in Table 6.1, entry 7. The irradiation of **4j** in the presence of arenes **15a-f** led to the formation of **16a-f** in satisfactory yields (60-85%). In the case of mesitylene **15e** a minor amount of 1,3-bis(trifluoromethyl) derivative (**16e-bis**, 12% yield) was formed along with the desired **16e**. Despite the electrophilic nature of the trifluoromethyl radical,^[106] the present methodology appears to be suitable also for electron-poor aromatics, as pointed out by the functionalization of 2',4',6'-trimethylacetophenone **15g**, which gave **16g** in 74% yield, (3.2 equiv. of **4j** used).

The scope was further extended to heterocycles. Irradiation of 3,4-ethylenedioxythiophene **15h** resulted in the formation of bis-trifluoromethylated **16h-bis** (59% yield). However, when

decreasing the concentration of **4j** (down to 0.015 M), mono-trifluoromethylated compound **16h** became the major product.^[102g,107]

Moving to nitrogen based heterocycles, pyridines **15i,j** gave **16i,j** in satisfactory amounts, whereas derivative **16k** was the only product isolated starting from 2-methylimidazole **15k**, via N-C bond formation. This result is striking since radical trifluoromethylation of imidazoles usually brings to the formation of C-CF₃ bonds^[104b,e,f,h,i,108] and *N*-CF₃ imidazoles are otherwise difficult to prepare.^[109] Bioactive methylxanthines such as caffeine and theophylline^[110] were selectively functionalized and **16l,m** were obtained in 58% and 67% yield, respectively. As shown in Table 6.1, (entry 13) solar light may be adopted to promote the reaction. Accordingly, Pyrex vessels containing selected reaction mixtures were exposed to natural sunlight for three days (6 h for day) and compounds **16a**, **16d**, **16j**, **16l** were isolated in yields comparable to those observed when using phosphor coated lamps as the light sources (Scheme 6.2).

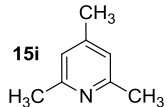
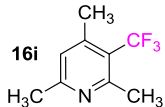
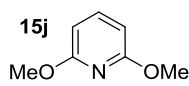
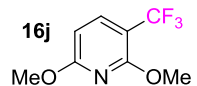
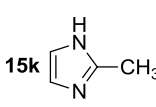
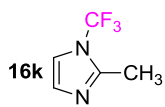
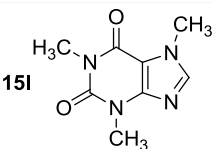
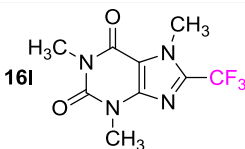
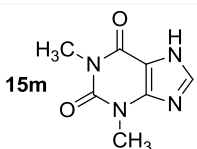
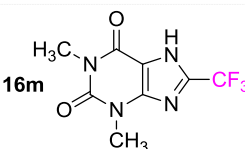
Continuous-flow conditions were likewise explored in order to develop an experimental scalable setup.^[111] The reactions were carried out in a photoreactor consisting in coils of UV-transparent FEP tubing wrapped around a traditional water cooled 500 W medium pressure mercury lamp.^[112] Dry acetonitrile, however, was the best reaction medium in this case. The photolyzing solutions were circulated at a rate of 10 mL hour⁻¹. As depicted in Scheme 6.2, for all the reactions tested, products **16** were obtained in higher yields (up to 30%) than those performed under batch experiments. Moreover, the reaction was completed after only 5 h irradiation, whereas 12 h were required when using a multilamp reactor (compare data reported in Table 6.2 and Scheme 6.2).

Table 6.2. Trifluoromethylation of aromatics and heteroaromatics.

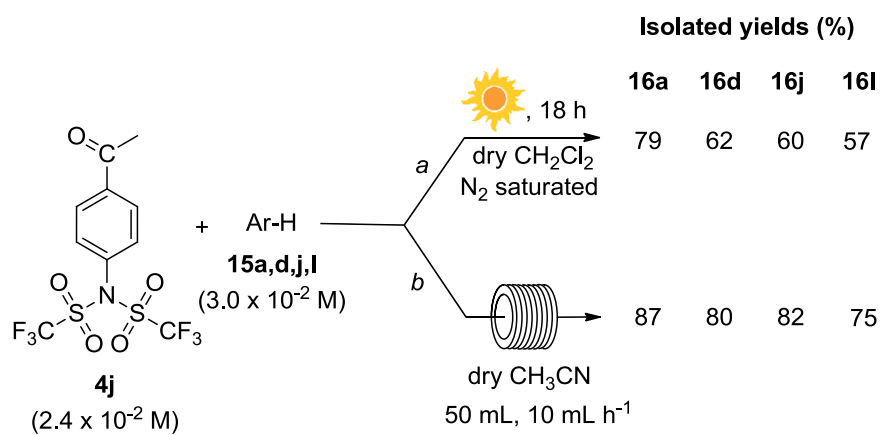
$$\begin{array}{c}
 \text{O} \\
 \parallel \\
 \text{C} \\
 | \\
 \text{C}_6\text{H}_4 \\
 | \\
 \text{N} \\
 / \quad \backslash \\
 \text{S} \quad \text{S} \\
 \backslash \quad / \\
 \text{O} \quad \text{O} \\
 | \quad | \\
 \text{F}_3\text{C} \quad \text{CF}_3
 \end{array}
 + \text{Ar-H} \xrightarrow[\text{dry CH}_2\text{Cl}_2, \text{N}_2 \text{ saturated}]{h\nu (310 \text{ nm}), 12 \text{ h}} \text{Ar-CF}_3$$

4j ($2.4 \times 10^{-2} \text{ M}$) **15a-m** ($3.0 \times 10^{-2} \text{ M}$) **16a-m**

Substrate	Products	16a-m , yields % ^[a]	
<p>15a</p>	<p>16a</p>	81	
<p>15b</p>	<p>16b</p>	85	
<p>15c</p>	<p>16c</p>	79	
<p>15d</p>	<p>16d</p>	61	
<p>15e</p>	<p>16e</p>	<p>16e-bis</p>	16e , 60; 16e-bis , 12
<p>15f</p>	<p>16f</p>	73 ^[b]	
<p>15g</p>	<p>16g</p>	74 ^[c]	
<p>15h</p>	<p>16h</p>	<p>16h-bis</p>	16h-bis , 59 16h , ^[d] 26; 16h-bis , ^[d] 18

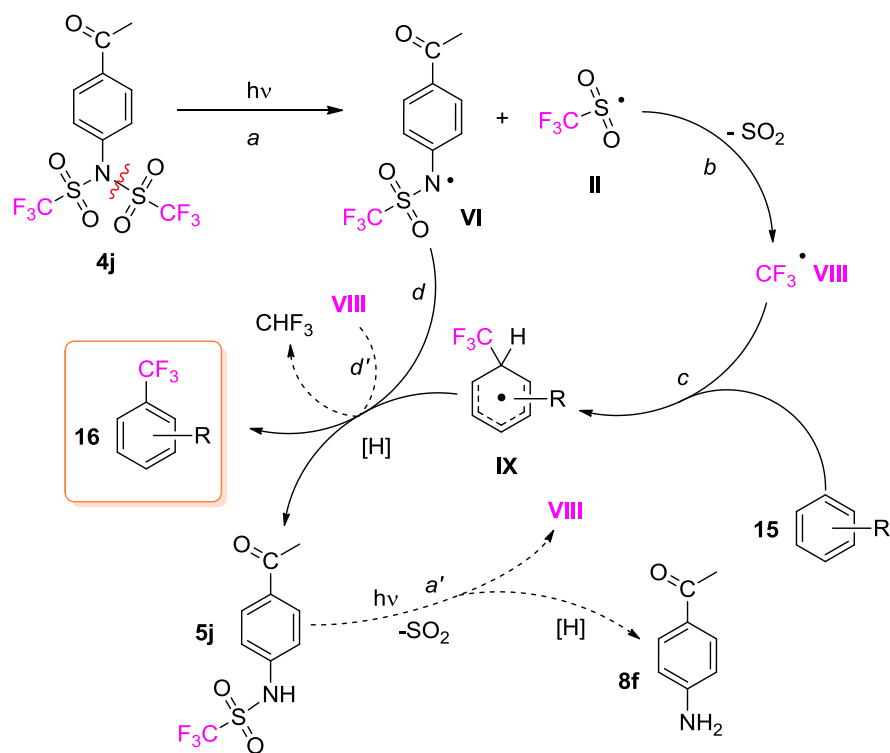
Substrate	Products	16a-m, yields % ^[a]
		59
		64
		69
		58
		67 ^[c]

^[a] Yields of products isolated by distillation or by column chromatography. ^[b] Yield obtained by means of a GC calibration curves by using *n*-dodecane as internal standard. ^[c] [4j] = 4.8×10^{-2} M (irradiation time: 42 h). ^[d] [4j] = 1.5×10^{-2} M (irradiation time: 6 h). ^[e] Irradiation performed in CH₃CN/H₂O 5:1.



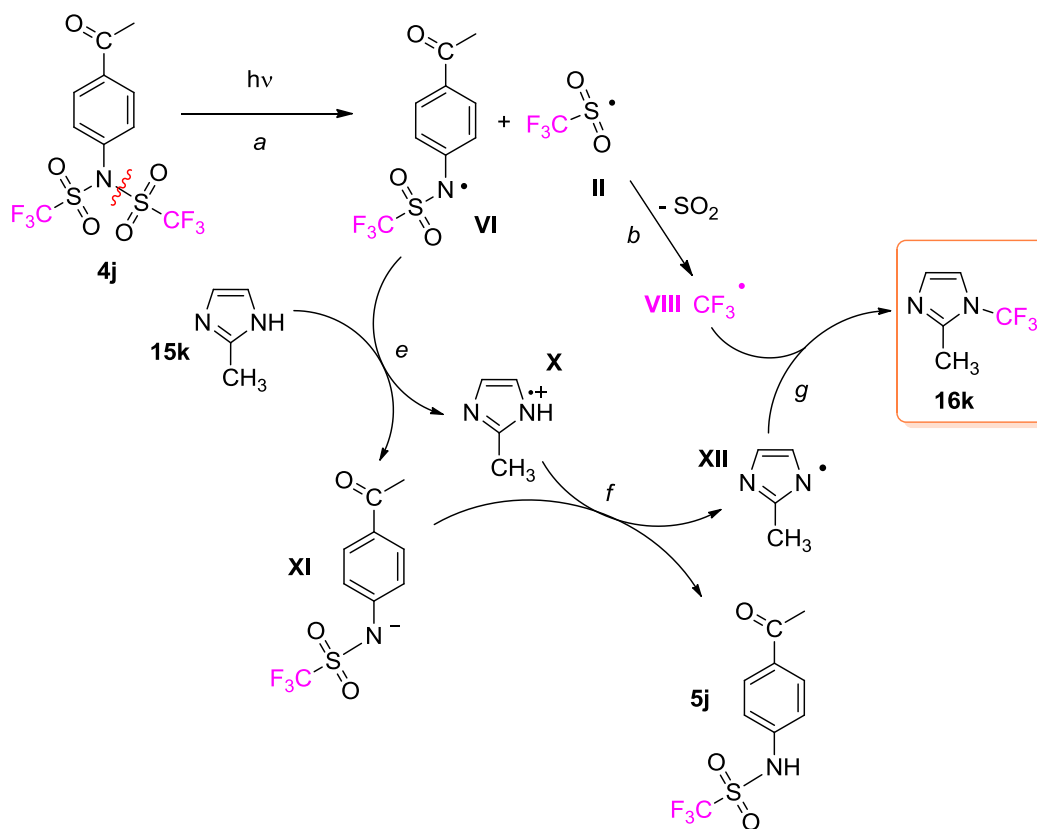
Scheme 6.2. Photochemical trifluoromethylation of **15a,d,j,l** under a) solar irradiation and b) flow conditions.

The proposed mechanism for the examined process is described in Scheme 6.3. Compound **4j** undergoes photoinduced homolysis of one of the N-S bonds (*path a*)^[48] to afford radicals **II** and **VI**. Loss of SO₂ from **II** gives F₃C• radical (**VIII**, *path b*) that is in turn trapped by the (hetero)aromatic **15**, to give intermediate **IX** (*path c*). Compound **16** is then formed via hydrogen atom transfer by the reactive sulfonamido radical **VI** (*path d*). Hydrogen abstraction by the F₃C• radical from **IX** (*path d'*)^[102f,113] or from the reaction medium^[27,48,54] had a role since CHF₃ was detected by headspace FT-IR analysis of the photolyzed solution of **4j** in the presence (or in the absence)^[27,48,114] of **15f** in CH₂Cl₂. Nonetheless, even if some CHF₃ is formed, the overall efficiency of the process is satisfactory thanks also to the photoinduced release of another equivalent of F₃C• radical from sulfonamide **5j** (*path a'*), to give 4'-aminoacetophenone **8f** as a side-product.^[48]



Scheme 6.3. Proposed pathways involved in the photochemical trifluoromethylation of (hetero)arenes by **4j**.

The proposed mechanism is however not applicable to the trifluoromethylation of **15k**. In this case we propose that **16k** could be formed by the mechanism depicted in Scheme 6.4. In detail we suggest that, after the photoinduced homolysis of a C-S bond and formation of radicals **VI** and **VIII**, the former oxidizes imidazole **15k** (*path e*). Then radical cation **X** and sulfonamide anion **XI** give a proton exchange (*path f*). Eventually, $\text{F}_3\text{C}^\bullet$ radical **VIII** and the obtained **XII** recombine to give **16k** (*path g*). Related radical couplings had some precedents in the literature^[115] and, however, further experiments have been planned to confirm the proposed mechanisms, which is currently still under investigation.



Scheme 6.4. Proposed mechanism for the photochemical trifluoromethylation **15k**.

6.3 Conclusion.

In this chapter we demonstrated that *N*-aryltrifluoromethanesulfonimide **4j** is a simple and cost-effective reagent for the photoinduced, catalyst-free trifluoromethylation of differently substituted (hetero)aromatics, including bioactive molecules. The reaction is characterized by a satisfactory efficiency and versatility, being suitable for both electron-rich and electron-poor substrates and needing no other external additive than the photolabile trifluoromethylating reagent. Moreover it can be successfully adapted to sustainable strategies, including the use of solar radiation as a totally free, green and natural light source ^[116] as well as continuous flow conditions.^[111a] This makes the proposed methodology potentially useful for the synthesis of drugs candidates and bulk chemicals.

7 Conclusion

This thesis described many different ways to develop simple, cheap and efficient non-ionic photoacid generators. Accordingly, the photochemistry of aryl tosylates was studied^[33] and we found that, in the presence of oxygen, photoinduced homolysis of the O-S bond from the singlet excited state, followed by trapping of the photogenerated tosyl radical by oxygen, brings to high yields of *p*-toluenesulfonic acid. The studied compounds acted also as good photoinitiators for cationic polymerization of a hybrid organic-inorganic epoxy-based material, thus confirming their potentiality as PAGs.

Then our attention moved on systems able to release more than one equivalent of acid from one equivalent of PAG, namely *N*-arylsulfonimides.^[48] In this case the homolysis of the N-S bonds give up to two equivalents of strong sulfonic acids. These compounds were successfully employed as photoinitiators for both cationic polymerization (behaving similarly to commercial sulfonium PAGs) and photolithography, allowing to obtain well resolved microstructures.^[53] A peculiar case relied on the photochemistry of *N*-aryltrifluoromethanesulfonimides. Despite being not able to release trifluoromethanesulfonic acid, they were nonetheless successfully exploited in organic synthesis to perform a catalyst-free, photochemical, radical trifluoromethylation of aromatic compounds.

At this point, our research moved to the development of initiators for next generation EUV lithography. Specifically designed fluorinated aryl sulfonates, coupled with hybrid organic-inorganic photoresists, were found to be more efficient than commercially available ionic PAGs and EUV irradiation of these systems brought to patterns with sub-micrometric resolution (~ 100 nm).

Lastly, in collaboration with Prof. Klán (Masaryk University, Brno), we focused on the release of HI from simple non-ionic photoactivable compounds. The iodide released was used to trigger the oxidation of Fe^{2+} ion by persulfate, in the presence of a macrocyclic cage. Thus the system was designed to have a phototriggered oxidation and an on-demand Fenton's like reagent to be used, potentially, as photoinitiator in radical polymerization.^[83]

Summing up, the light-driven release of acids from many different non-ionic compounds by different radiation sources was successfully achieved and was tested for several technological applications of relevant importance. Hence we have found systems that, in the future, could be applied, for example, as PAGs for photolithography, as well as for photoinitiators for both cationic and radical polymerization.

8 Experimental Section

8.1 *Experimental details regarding chapter 2.*

8.1.1 General Information.

NMR spectra were recorded on a 300 MHz spectrometer. The attributions were made on the basis of ^1H and ^{13}C NMR, as well as DEPT-135 experiments; chemical shifts are reported in ppm downfield from TMS. The photochemical reactions were performed using nitrogen- or oxygen-saturated solutions in quartz tubes in a multilamp reactor fitted with 4×15 W Hg lamps (emission centered at 254 nm) for the irradiation. The reaction course was followed by GC analyses and the products formed were identified and quantified by comparison with authentic samples. Workup of the photolytes involved concentration in vacuo and chromatographic separation using silica gel. Solvents of HPLC purity were employed in the photochemical reactions. Quantum yields were measured at 254 nm (1 Hg lamp, 15W).

GC analyses were carried out using a chromatograph equipped with a FID detector. A 30 m × 0.25 mm × 0.25 μm capillary column was used for analytes separation with nitrogen as carrier gas at 1 mL min⁻¹. The injection in the GC system was performed in split mode and the injector temperature was 250 °C. The GC oven temperature was held at 120 °C for 2 min, increased to 250 °C by a temperature ramp of 10 °C min⁻¹ and held for ten min.

The acidity released was determined on 5 mL of the photolysed solutions by dilution with water (25 mL) and titration with aqueous 0.1 M NaOH by means of a potentiometer equipped with a pH glass combined electrode. *p*-toluenesulfonic (PTSA), and *p*-toluenesulfonic were determined via HPLC ion chromatography and quantified by means of calibration curves obtained with authentic samples of commercially available sodium *p*-toluenesulfinate and *p*-toluenesulfonic

acid monohydrate (PTSA). Ion chromatography analyses were performed by means of an instrument equipped with a conductimetric detector, an electrochemical suppressor, a chromatographic column (4 mm x 250 mm), and a guard column (4 mm × 50 mm). Eluant: NaHCO₃ 0.8 mM + Na₂CO₃ 4.5 mM; flux: 1 mL min⁻¹; current imposed at detector: 50 mA.

Microsecond transient absorption experiments were performed using a nanosecond laser flash photolysis apparatus equipped with a 20-Hz Nd:YAG laser (20 ns, 1 mJ at 266 nm) and a 150 W Xe flash lamp as probe light. Samples were placed in a quartz cell (10×10 mm² section) at a concentration adjusted to obtain an OD value of 1.0 at 266 nm.

Phenols **2b-f**, 3-glycidoxypropyltrimethoxysilane (GPTMS) and germanium tetraethoxide (TEOG) were commercially available and used as received. 4-*N,N*-dimethylaminophenol **2a** [30b] and 4-methoxy-3-trimethylsilylphenol **2g** [34b] were prepared by known procedures.

8.1.2 Synthesis of aryl tosylates 1a-g.

Compounds **1a-g** were synthesized by adapting a known procedure.^[35] To a solution of the chosen phenol (20 mmol) in dichloromethane (80 mL) and triethylamine (15 mL) at room temperature, *p*-toluenesulfonyl chloride (24 mmol) was added portion wise, and the resulting mixture was stirred overnight. Water (25 mL) was then added and the resulting mixture was stirred for an additional 3 h. The mixture was then extracted with ethyl acetate (4×50 mL) and the organic layers were reunited and washed with water (3×50 mL), 10% aqueous HCl (3×150 mL, except in the case of **1a**), water (2×150 mL), saturated aqueous NaHCO₃ (2×150 mL) and brine (2×100 mL) and dried over Na₂SO₄. The solvent was evaporated under vacuum. The resulting residue was purified by column chromatography or recrystallization.

4-N,N-dimethylaminophenyl *p*-toluenesulfonate (**1a**). Obtained in 72% yield from *N,N*-dimethylaminophenol (**2a**),^[30b] purification by column chromatography (eluant:

cyclohexane/ethyl acetate 9:1). White solid, m.p. = 123-125 °C, lit. 117-120 °C.^[30b] Spectroscopic data for **1a** were in accordance with the literature.^[35] Anal. Calcd for C₁₅H₁₇NO₃S: C, 61.83; H, 5.88; N, 4.81. Found: C, 61.8; H, 5.9, N, 4.8.

4-methoxyphenyl p-toluenesulfonate (1b). Obtained in 89% yield from 4-methoxyphenol **2b**. Purification by column chromatography (eluant: cyclohexane/ethyl acetate 9:1). White solid, m.p. = 67-70 °C, lit. 69-70 °C.^[35] Spectroscopic data for **1b** were in accordance with the literature.^[35] Anal. Calcd for C₁₄H₁₄O₄S: C, 60.42; H, 5.07. Found: C, 60.4; H, 5.1.

4-tertbutylphenyl p-toluenesulfonate (1c). Obtained in 85% yield from 4-tertbutylphenol **2c**. Purification by recrystallization from MeOH/H₂O. White solid m.p. = 112-114 °C, lit. 113-115 °C.^[117] Spectroscopic data for **1c** are in accordance with the literature.^[117] Anal. Calcd for C₁₇H₂₀O₃S: C, 67.08; H, 6.62. Found: C, 67.1; H, 6.6.

4-acetylphenyl p-toluenesulfonate (1d). Obtained in 71% yield from 4-hydroxyacetophenone **2d**. Purification by recrystallization from MeOH/H₂O. White solid, m.p. = 71-73 °C, lit. 69-70 °C.^[118] Spectroscopic data for **1d** are in accordance with the literature.^[35] Anal. Calcd for C₁₅H₁₄O₄S: C, 62.05; H, 4.86. Found: C, 62.0; H, 4.8.

4-nitrophenyl p-toluenesulfonate (1e). Obtained in 62% yield from 4-nitrophenol **2e**. Purification by recrystallization from MeOH/H₂O. Pale yellow solid, m.p. = 102-104 °C, lit. 98 °C.^[119] Spectroscopic data for **1e** are in accordance with the literature.^[119] Anal. Calcd for C₁₃H₁₁NO₅S: C, 53.24; H, 3.78; N, 4.78. Found: C, 53.2; H, 3.8, N, 4.9.

3-methoxyphenyl p-toluenesulfonate (1f). Obtained in 68% yield from 3-methoxyphenol **2f**. Purification by recrystallization from MeOH/H₂O. Colorless solid, m.p. = 49-51 °C, lit. 59-60 °C.^[120] Spectroscopic data are in accordance with literature.^[120] Anal. Calcd for C₁₄H₁₄O₄S: C, 60.42; H, 5.07. Found: C, 60.6; H, 5.2.

4-methoxy-2-trimethylsilylphenyl-p-toluenesulfonate (1g). Obtained in 55% yield from 4-methoxy-3-trimethylsilylphenol (**2g**).^[34b] Purification by column chromatography (eluant: cyclohexane/ethyl acetate 9:1). Colorless solid, m.p. = 60-62 °C. ¹H NMR (CDCl₃) δ: 7.85-7.35 (AA'BB' system, 4 H), 6.95 (m, 2 H), 6.75 (dd, 1 H, *J* = 3 Hz and 9 Hz), 3.80 (s, 3H), 2.45 (s, 3H), 0.30 (s, 9H). ¹³C NMR (CDCl₃) δ: 157.0, 148.4, 145.0, 134.2, 134.0, 129.7 (CH), 128.2 (CH), 121.0 (CH), 120.5 (CH), 114.5 (CH), 55.4 (CH₃), 21.6 (CH₃), -0.7 (CH₃). IR (KBr, v/cm⁻¹): 2956, 1467, 1370, 1194, 1179, 1157, 1093, 1037. Anal. Calcd for C₁₇H₂₂O₄SSi: C, 58.25; H, 6.33. Found: C, 58.2; H, 6.2.

8.1.3 Preparative irradiations.

Irradiation of 4-N,N-dimethylaminophenyl p-toluenesulfonate (1a) in MeOH. A nitrogen-saturated solution of **1a** (440 mg, 1.5 mmol, 0.03 M) in MeOH was irradiated for 4 h at 254 nm. The photolysed solution was then evaporated and the resulting residue was purified by column chromatography (eluant: cyclohexane/ethyl acetate 9:1) to afford 330 mg of 4-(*N,N*-dimethylamino)-2-(*p*-toluenesulfonyl)phenol (**3a**, colorless solid, 75% yield, m.p. = 133-135 °C). **3a**: ¹H NMR (CDCl₃) δ: 8.55 (s, 1H), 7.80-7.30 (AA'BB' system, 4H), 6.90-6.80 (m, 3H), 2.80 (s, 6H), 2.40 (s, 3H); ¹³C NMR (CDCl₃) δ: 146.0, 145.0, 144.4, 138.9, 129.9 (CH), 126.7 (CH), 123.5, 121.8 (CH), 119.6 (CH), 110.9 (CH), 41.0 (CH₃), 21.5 (CH₃). IR (KBr, v/cm⁻¹): 3377, 2924, 1503, 1139, 1090, 963. Anal. Calcd for C₁₅H₁₇NO₃S: C, 61.83; H, 5.88; N, 4.81. Found: C, 61.9; H, 6.1, N, 4.9.

Irradiation of 4-methoxyphenyl p-toluenesulfonate (1b) in MeOH. A nitrogen-saturated solution of **1b** (150 mg, 0.01 M) in MeOH (55 mL) was irradiated at 254 nm for 12 h (90% consumption of **1b**). The photolysed solution was then evaporated and the resulting residue was purified by column chromatography (eluant: cyclohexane/ethyl acetate 9:1) to give a mixture of 4-methoxy-

2-(*p*-toluenesulfonyl)phenol (**3b**, 44 mg, 32% yield based on consumed **1b**) and of unreacted **1b** (3 mg). **3b**: ^1H NMR (from the mixture, CDCl_3) δ : 7.85-7.30 (AA'BB', 4H), 7.15 (d, 1H, $J = 3$ Hz), 7.05 (dd, 1H, $J = 3$ and 9 Hz), 6.95 (d, 1H, $J = 9$ Hz), 6.80 (s, 1H), 3.70 (s, 3H), 2.40 (s, 3H). ^{13}C NMR (from the mixture, CDCl_3) δ : 153.0, 149.7, 144.8, 138.4, 130.0 (CH), 126.8 (CH), 123.7 (CH), 123.4, 120.1 (CH), 111.2 (CH), 55.7 (CH_3), 21.5 (CH_3).

Irradiation of 4-tert-butylphenyl p-toluenesulfonate (1c) in MeOH. A nitrogen saturated solution of **1c** (340 mg, 0.022 M) in methanol (50 mL) was irradiated for 6 h. The photolysed solution was then evaporated and the resulting residue was purified by column chromatography (eluant: cyclohexane/ethyl acetate 8:2) to afford 143 mg of a mixture of 4-*tert*-butylphenol (**2c**, 79 mg, 23%) and 4-*tert*-butyl-2-(*p*-toluenesulfonyl)phenol (**3c**, 64 mg, 19% yield). **3c**: ^1H NMR (from the mixture, CDCl_3) δ : 7.80-7.35 (AA'BB', 4H), 7.65 (d, 1H, $J = 3$ Hz), 7.48 (dd, 1H, $J = 3$ and 9 Hz), 7.35 (s, 1H), 6.90 (d, 1H, $J = 9$ Hz), 3.80 (s, 3H), 2.45 (s, 3H). ^{13}C NMR (from the mixture, CDCl_3) δ : 153.4, 143.9, 138.4, 133.5 (CH), 130.0 (CH), 129.7, 126.7 (CH), 125.0 (CH), 123.4, 118.6 (CH), 34.2, 31.1 (CH_3). IR (of the mixture, KBr, v/cm^{-1}): 3392, 2963, 1516, 1227, 1141, 831.

Irradiation of 4-methoxy-3-trimethylsilylphenyl p-toluenesulfonate (1g) in MeOH. A nitrogen saturated solution of **1g** (180 mg, 0.01 M) in methanol (50 mL) was irradiated at 254 nm for 5 hours (90% consumption of **1g**). The photolysed solution was then evaporated and the resulting residue was purified by column chromatography (eluant: cyclohexane/ethyl acetate 9:1), to afford a mixture of 22 mg of 4-methoxy-2-(*p*-toluenesulfonyl)-5-trimethylsilyl-phenol (**3g**, 14% yield based on consumed **1g**) along with 6 mg of unreacted **1g**. **3g**: ^1H NMR (from the mixture, CDCl_3) δ : 9.05 (s, 1H), 7.85-7.30 (AA'BB', 4H), 7.15 (d, 1H, $J = 3$ Hz), 7.10 (d, 1H, $J = 3$ Hz), 3.80 (s, 3H), 2.40 (s, 3H), 0.30 (s, 9H). ^{13}C NMR (from the mixture, CDCl_3) δ : 153.9, 152.6, 144.6,

136.4, 132.3, 129.9 (CH), 126.7 (CH), 126.4 (CH), 122.1, 111.6 (CH), 55.8 (CH₃), 21.5 (CH₃), 1.3 (CH₃).

8.1.4 Use of aryl tosylates in polymerization processes.

Experiments described in this section were performed at the Department of Industrial Engineering of the University of Padova (Italy), under the supervision of Dr. Gioia Della Giustina.

Sol-gel matrix synthesis. The detailed protocol for the synthesis of G8Ge2 system has already been described.^[31c] The epoxy based sol-gel system was synthesized by a sol-gel method based on hydrolysis and condensation reaction of silicon and germanium alkoxides. In detail 3-glycidyloxypropyltrimethoxysilane (GPTMS), the organically modified precursor, was hydrolyzed at room temperature in bidistilled water for 1 hour, with molar ratio H₂O:GPTMS = 3:1. Aqueous HCl 1 N was used as a catalyst (molar ratio HCl:GPTMS = 0.005:1). Then 2-methoxyethanol, germanium tetraethoxide (TEOG) and bidistilled water (molar ratios: GPTMS:TEOG = 80:20; TEOG:H₂O:2-methoxyethanol = 1:2:6) were added to the previous mixture and the obtained solution was left to react at 80 °C for 1 h 30 min. The resulting system was then diluted in 2-methoxyethanol to achieve the desired concentration (2 M respect to the epoxy groups). The resulting solution was eventually filtered through a microporous membrane (0.2 μm Millipore) to obtain a better film quality.

Photopolymerization experiments. Sol-gel films of the synthesized epoxy based matrix were deposited by spin coating on Si (100) substrates, with different thicknesses, by tailoring the sol concentration and the spin rate. No adhesion problems were observed for these substrates. After these preliminary tests films containing the different tosylates (**1a-d,1f-g**) were prepared: the selected PAG was dissolved in the previously synthesized sol-gel system (1% molar

concentration with respect to the epoxy groups) and the obtained mixture was spin coated on Si (100), obtaining a film with a thickness of 1 μm which was then irradiated with increasing UV exposure doses (1-18 min). Photopolymerization experiments were performed by means of a Hamamatsu LC5 Hg-Xe UV spot light source, enhanced in the deep UV (250 nm band), with a power density of 150 mW/cm^2 on the sample surface. The evolution of organic-inorganic network, with particular regard to epoxy rings,^[36] was monitored by FT-IR spectroscopy. Analyses were performed within the 400-4000 cm^{-1} range, with a 4 cm^{-1} resolution for a total of 32 scans.

8.2 *Experimental details regarding chapter 3.*

8.2.1 General Information.

^1H NMR spectra were recorded with a 300 MHz spectrometer, while ^{13}C NMR spectra were recorded with a 75 MHz spectrometer. Attributions were made on the basis of ^1H and ^{13}C NMR, as well as DEPT-135 experiments; chemical shifts are reported in ppm downfield from TMS.

The photochemical reactions were performed using nitrogen- or oxygen-saturated solutions in quartz tubes in a multi-lamp reactor equipped with 4 \times 15 W Hg lamps (emission centered at 254 nm) for irradiation. Quantum yields were measured at 254 nm (1 Hg lamp, 15 W). Solvents of HPLC grade purity were employed for all the photochemical reactions. The reaction course was followed either by GC (compounds **4c**, **4d** and **4h**) or HPLC analyses (all the other compounds) and the products formed were identified and quantified by comparison with calibration curves of authentic samples.

GC analyses were carried out using the same equipment and the same conditions described in the section 8.1.1 for aryl tosylates. HPLC analyses were carried out on a HPLC apparatus equipped

with two pumps and a UV detector (C-18 column: 300 × 3.9 mm; eluant: MeCN/water 30:70, flux 0.5 mL min⁻¹).

The acidity liberated was determined on 5 mL of the photolysed solutions by dilution with water (25 mL) and titration with aqueous 0.1 M NaOH: titrations were followed using a potentiometer equipped with a pH glass combined electrode. Ion chromatography analyses were performed by using the same apparatus and conditions described for aryl tosylates in the section 8.1.1. Commercially available sodium methanesulfinate, sodium *p*-toluenesulfinate, methanesulfonic acid, acetic acid and *p*-toluenesulfonic acid monohydrate (PTSA) were used as standards.

The presence of fluoroform and hexafluoroethane when irradiating **4j** was detected by IR ^[27,54] and GC-MS analyses.

Microsecond transient absorption experiments were performed using a nanosecond laser flash photolysis apparatus equipped with a 20 Hz Nd:YAG laser (25 ns, 25 mJ at 266 nm) and a 150 W Xe flash lamp as the probe light. Samples were placed in a quartz cell (10×10 mm section) at a concentration adjusted to obtain an OD value of 1.0 at 266 nm.

EPR Experiments were performed on 0.01 M solution of the chosen compounds in freshly distilled benzonitrile. It was employed a spectrometer equipped with high pressure 500 W Hg lamp focused on the window of the cavity by means of a crown glass lens (spot diameter about 4 cm). When spin trap agents (*N*-tert-butyl- α -phenylnitrone, PBN, and 2-methyl-2-nitrosopropane, MNP) were present, a concentration of 10⁻¹ M was used. These EPR experiments were performed under the supervision of Dr. Simone Lazzaroni and Prof. Daniele Dondi (University of Pavia).

All the other reagents, solvents and materials employed were purchased by commercial suppliers and used with no further purification.

8.2.2 Synthesis of *N*-arylsulfonamides 5a-j.

Methanesulfonamides **5a-h** were prepared following a known procedure described just below.^[121] Sulfonamides **5i** and **5j** were instead synthesized by a different methodology (see further below in this section). Regarding **5a-h**, a solution of the chosen aniline **8a-h** (10 mmol), pyridine (0.90 mL, 11 mmol) in dry dichloromethane (25 mL) was cooled to 0 °C under nitrogen atmosphere. Methanesulfonyl chloride (0.85 mL, 11 mmol) was added dropwise while stirring, then the mixture was allowed to warm to room temperature and stirred overnight. The reaction was quenched with 6 N aqueous NaOH (50 mL) and water was added to the resulting mixture in order to dissolve the resultant salts. The layers were then separated, the aqueous phase washed with CH₂Cl₂ (3×40 mL) and cooled to 0 °C. Upon subsequent acidification to pH 2.0 (by adding aqueous HCl 18%) a white solid precipitated. The obtained product was collected on a sintered glass funnel, washed repeatedly with cold water and then dried in vacuum, affording the desired compounds without need of further purification.

N-[4-(dimethylamino)phenyl]methanesulfonamide (**5a**). Obtained in a 66% yield. White solid, m.p. = 165-168 °C, lit. 174-175 °C.^[122] Spectroscopic data were in accordance with the literature.^[122] Anal. Calcd for C₉H₁₄N₂O₂S: C, 50.45; H, 6.59; N, 13.07. Found: C, 50.3; H, 6.7; N, 13.0.

N-(4-methoxyphenyl)methanesulfonamide (**5b**). Obtained in a 76% yield. White solid, m.p. = 122-125 °C, lit. 117-118 °C.^[122] Spectroscopic data were in accordance with the literature.^[122] Anal. Calcd for C₈H₁₁NO₃S: C, 47.75; H, 5.51; N, 6.96. Found: C, 47.8; H, 5.5; N, 7.0.

N-(4-*tert*-butylphenyl)methanesulfonamide (**5c**). Obtained in a 80% yield. White solid, m.p. = 84-87 °C, lit. 80-81 °C.^[123] Spectroscopic data are in accordance with the literature.^[123] Anal. Calcd for C₁₁H₁₇NO₂S: C, 58.12; H, 7.54; N, 6.16. Found: C, 58.2; H, 7.5; N, 6.1.

N-phenylmethanesulfonamide (**5d**). Obtained in a 71% yield. White solid, m.p. = 98-100 °C, lit. 101-103 °C.^[122] Spectroscopic data are in accordance with the literature.^[122] Anal. Calcd for C₇H₉NO₂S: C, 49.10; H, 5.30; N, 8.18. Found: C, 49.2; H, 5.3; N, 8.1.

N-(4-cyanophenyl)methanesulfonamide (**5e**). Obtained in a 94% yield. White solid, m.p. = 192-194 °C, lit. 192-194 °C.^[124] **5e**: ¹H NMR (acetone-*d*₆) δ: 9.22 (brs, 1H), 7.80-7.45 (AA'BB' system, 4H), 3.16 (s, 3H). ¹³C NMR (acetone-*d*₆) δ: 144.1, 134.8 (CH), 119.8 (CH), 119.6, 107.7, 40.6 (CH₃). IR (KBr, v/cm⁻¹): 3301, 2226, 1608, 1506, 1332, 1153, 978, 916, 835. Anal. Calcd for C₈H₈N₂O₂S: C, 48.97; H, 4.11; N, 14.28. Found: C, 49.0; H, 4.2; N, 14.3.

N-(4-acetylphenyl)methanesulfonamide (**5f**). Obtained in a 74% yield. White solid, m.p. = 150-153 °C, lit. 155-157 °C.^[124] Spectroscopic data are in accordance with the literature.^[125] Anal. Calcd for C₉H₁₁NO₃S: C, 50.69; H, 5.20; N, 6.57. Found: C, 50.6; H, 5.1; N, 6.6.

N-(4-nitrophenyl)methanesulfonamide (**5g**). Obtained in a 75% yield. White solid, m.p. = 181-183 °C, lit. 180-182 °C.^[126] Spectroscopic data are in accordance with the literature.^[127] Anal. Calcd for C₇H₈N₂O₄S: C, 38.88; H, 3.73; N, 12.96. Found: C, 39.0; H, 3.5; N, 13.0.

N-(2,4,6-trimethylphenyl)methanesulfonamide (**5h**). Obtained in a 96% yield. White solid, m.p. = 151-153 °C. ¹H NMR (CD₃OD) δ: 6.92 (s, 2H), 3.05 (s, 3H), 2.36 (s, 6H), 2.26 (s, 3H), 1.31 (s, 1H). ¹³C NMR (CD₃OD) δ: 139.0, 138.7, 132.4, 130.5 (CH), 42.5 (CH₃), 21.2 (CH₃), 19.6 (CH₃). IR (KBr, v/cm⁻¹): 3283, 2910, 1643, 1394, 1318, 1141, 968. Anal. Calcd for C₁₀H₁₅NO₂S: C, 56.31; H, 7.09; N, 6.57. Found: C, 56.3; H, 7.0; N, 6.4.

N-(4-acetylphenyl)-*p*-toluenesulfonamide (**5i**). Compound **5i** was synthesized adapting the procedure employed for the synthesis of *N*-arylmethanesulfonamides **5a-h**.^[121] A solution of aniline **8f** (1.35 g, 10 mmol) and pyridine (1.50 mL, 19 mmol) in CH₂Cl₂ (35 mL) was cooled to 0 °C. *p*-Toluenesulfonyl chloride (2.28 g, 12 mmol) was added portionwise under stirring. The resulting mixture was then allowed to warm to room temperature and stirred overnight. The

reaction was quenched with 6 N aqueous NaOH (50 mL), and water was added to resulting mixture in order to dissolve the resultant salts. The layers were separated, the aqueous phase was washed with CH₂Cl₂ (3×40 mL), cooled to 0 °C and upon subsequent acidification to pH 2.0 (by adding aqueous HCl 18%) a white solid precipitated. This solid was separated by filtration on a sintered glass funnel and washed with cold water affording **5i** as a white solid in 87% yield without any further purification (m.p. = 199-202 °C, lit. 196-198 °C)^[128]. ¹H NMR (acetone-*d*₆) δ: 9.47 (brs, 1H), 7.95-7.30 (AA'BB' system, 4H), 7.85-7.30 (AA'BB' system, 4H), 2.50 (s, 3H), 2.38 (s, 3H). ¹³C NMR (acetone-*d*₆) δ: 196.9, 145.3, 143.6, 138.2, 134.0, 131.0 (CH), 130.9 (CH), 128.4 (CH), 119.6 (CH), 26.8 (CH₃), 21.7 (CH₃). IR (KBr, v/cm⁻¹): 3214, 1670, 1654, 1560, 1276, 1159, 1090, 912, 661. Anal. Calcd for C₁₅H₁₅NO₃S: C, 62.26; H, 5.23; N, 4.84. Found: C, 62.4; H, 5.2; N, 4.7.

N-(4-acetylphenyl)-1,1,1-trifluoromethanesulfonamide (**5j**). Compound **5j** was synthesized adapting the procedure employed for the synthesis of *N*-alkyltrifluoromethanesulfonamides.^[129] To a cooled solution (-78 °C) of **8f** (1.35 g, 10 mmol) and triethylamine (1.6 mL, 11 mmol) in dry CH₂Cl₂ (35 mL) under nitrogen atmosphere, trifluoromethanesulfonic anhydride (1.8 mL, 11 mmol) was added dropwise while stirring. The mixture was stirred at -78 °C for 2 h, allowed to warm to room temperature, transferred in a separatory funnel and quenched with 60 mL of water. The aqueous layer was extracted with CH₂Cl₂ (2×25 mL), the organic phases reunited, treated with 6 N aqueous NaOH (50 mL) and water to dissolve the resultant salts. The layers were separated, the aqueous phase washed with CH₂Cl₂ (3×40 mL) and cooled to 0 °C. Upon acidification to pH 2.0 (by adding aqueous HCl 18%) a white solid precipitated. This solid was separated by filtration on a sintered glass funnel and washed with cold water. **5j** was thus obtained as a white solid in a 70% yield without any further purification (m.p. = 139-142 °C). ¹H NMR (DMSO-*d*₆) δ: 10.66 (brs, 1H), 8.05-7.35 (AA'BB' system, 4H), 2.56 (s, 3H). ¹³C NMR

(DMSO-*d*₆) δ : 196.6, 139.6, 134.1, 129.9 (CH), 120.9 (CH), 119.6 (q, CF₃, *J* = 322 Hz), 26.6 (CH₃). IR (KBr, ν/cm^{-1}): 3109, 2935, 1663, 1608, 1585, 1375, 1205, 1182, 958. Anal. Calcd for C₉H₈F₃NO₃S: C, 40.45; H, 3.02; N, 5.24. Found: C, 40.4; H, 3.0; N, 5.4.

8.2.3 Synthesis of *N*-arylsulfonimides 4a-j.

Methanesulfonimides **4a-h** were prepared following a known procedure described just below.^[130] Sulfonimides **4i** and **4j** were instead synthesized by different methodologies (see further below in this section).

As for compounds **4a-h**, they were obtained from **5a-h**. Methanesulfonyl chloride (0.57 mL, 7.4 mmol) was rapidly added to a solution of the chosen **5a-h** (5.0 mmol) and NaOH (5.2 mmol) in water (15 mL) under vigorous stirring. A white precipitate appeared instantaneously, the resulting mixture was further stirred for 30 min and then extracted with CH₂Cl₂ (3×20 mL). The organic phases were reunited, washed with aqueous NaOH 10% (2×20 mL), dried over Na₂SO₄, and the solvent was evaporated, to give **4a-h** as white solids without any further purification.

N-[4-(dimethylamino)phenyl]-*N*-(methylsulfonyl)methanesulfonamide (**4a**). Obtained in a 70% yield. White solid, m.p. = 215-217 °C, lit. 220 °C.^[131] ¹H NMR (acetone-*d*₆) δ : 7.30-6.70 (AA'BB' system, 4H), 3.42 (s, 6H), 3.01 (s, 6H). ¹³C NMR (acetone-*d*₆) δ : 152.7, 132.6 (CH), 123.0, 113.2 (CH), 43.3 (CH₃), 40.7 (CH₃). IR (KBr, ν/cm^{-1}): 1604, 1528, 1356, 1138, 1161, 882. Anal. Calcd for C₁₀H₁₆N₂O₄S₂: C, 41.08; H, 5.52; N, 9.58. Found: C, 41.0; H, 5.6; N, 9.5.

N-(4-methoxyphenyl)-*N*-(methylsulfonyl)methanesulfonamide (**4b**). Obtained in a 90% yield. White solid, m.p. = 174-176 °C, lit. 174-176 °C.^[132] ¹H NMR (CDCl₃) δ : 7.35-6.95 (AA'BB' system, 4H), 3.85 (s, 3H), 3.41 (s, 6H). ¹³C NMR (CDCl₃) δ : 160.9, 131.7 (CH), 125.6, 114.8 (CH), 55.5 (CH₃), 42.4 (CH₃). IR (KBr, ν/cm^{-1}): 1654, 1560, 1508, 1364, 1346, 1158. Anal. Calcd for C₉H₁₃NO₅S₂: C, 38.70; H, 4.69; N, 5.01. Found: C, 38.5; H, 4.8; N, 5.0.

N-(4-*tert*-butylphenyl)-*N*-(methylsulfonyl)methanesulfonamide (**4c**). Obtained in a 59% yield. White solid, m.p. = 235-238 °C. ¹H NMR (CDCl₃) δ: 7.55-7.25 (AA'BB' system, 4H), 3.42 (s, 6H), 1.35 (s, 9H). ¹³C NMR (CDCl₃) δ: 153.7, 130.5, 130.0 (CH), 126.7 (CH), 42.5 (CH₃), 34.7, 31.1 (CH₃). IR (KBr, v/cm⁻¹): 2954, 1654, 1560, 1348, 1158, 910. Anal. Calcd for C₁₂H₁₉NO₄S₂: C, 47.19; H, 6.27; N, 4.59. Found: C, 47.1; H, 6.1; N, 4.8.

N-phenyl-*N*-(methylsulfonyl)methanesulfonamide (**4d**). Obtained in a 82% yield. White solid, m.p. = 194-196 °C, lit. 201-202 °C.^[133] ¹H NMR (CDCl₃) δ: 7.55-7.45 (m, 3H), 7.40-7.30 (m, 2H), 3.40 (s, 6H). ¹³C NMR (CDCl₃) δ: 133.4, 130.6 (CH), 130.5 (CH), 129.6 (CH), 42.6 (CH₃). IR (KBr, v/cm⁻¹): 1348, 1159, 943, 887, 764, 694. Anal. Calcd for C₈H₁₁NO₄S₂: C, 38.54; H, 4.45; N, 5.62. Found: C, 38.5; H, 4.6; N, 5.7.

N-(4-cyanophenyl)-*N*-(methylsulfonyl)methanesulfonamide (**4e**). Obtained in a 62% yield. White solid, m.p. = 183-185 °C. ¹H NMR (CDCl₃) δ: 7.85-7.45 (AA'BB' system, 4H), 3.42 (s, 6H). ¹³C NMR (CDCl₃) δ: 137.2, 133.4 (CH), 131.6 (CH), 117.2, 114.5, 42.7 (CH₃). IR (KBr, v/cm⁻¹): 2236, 1506, 1368, 1158, 982, 925, 762. Anal. Calcd for C₉H₁₀N₂O₄S₂: C, 39.41; H, 3.67; N, 10.21. Found: C, 39.5; H, 3.5; N, 10.4.

N-(4-acetylphenyl)-*N*-(methylsulfonyl)methanesulfonamide (**4f**). Obtained in a 59% yield. White solid, m.p. = 146-149 °C. ¹H NMR (DMSO-*d*₆) δ: 8.10-7.60 (AA'BB' system, 4H), 3.58 (s, 6H), 2.64 (s, 3H). ¹³C NMR (DMSO-*d*₆) δ: 197.4, 137.8 (2C), 131.1 (CH), 129.2 (CH), 42.9 (CH₃), 26.8 (CH₃). IR (KBr, v/cm⁻¹): 3032, 1682, 1598, 1376, 1347, 1157, 912, 760. Anal. Calcd for C₁₀H₁₃NO₅S₂: C, 41.23; H, 4.50; N, 4.81. Found: C, 41.0; H, 4.6; N, 4.9.

N-(4-nitrophenyl)-*N*-(methylsulfonyl)methanesulfonamide (**4g**). Obtained in a 59% yield. White solid, m.p. = 224-227 °C, lit. 230-231 °C.^[133] ¹H NMR (acetone-*d*₆) δ: 8.40-7.80 (AA'BB' system, 4H), 3.59 (s, 6H). ¹³C NMR (acetone-*d*₆) δ: 149.9, 141.1, 133.7 (CH), 125.7 (CH), 43.8

(CH₃). IR (KBr, v/cm⁻¹): 3113, 1591, 1526, 1369, 1348, 1156, 927, 763. Anal. Calcd for C₈H₁₀N₂O₆S₂: C, 32.65; H, 3.42; N, 9.52. Found: C, 32.7; H, 3.5; N, 9.6.

N-(methylsulfonyl)-*N*-(2,4,6-trimethylphenyl)methanesulfonamide (**4h**). Obtained in a 47% yield. White solid, m.p. = 187-190 °C. ¹H NMR (CDCl₃) δ: 6.97 (s, 2H), 3.46 (s, 6H), 2.42 (s, 6H), 2.29 (s, 3H). ¹³C NMR (CDCl₃) δ: 140.0, 139.1, 130.1 (CH), 129.6, 43.9 (CH₃), 20.9 (CH₃), 19.6 (CH₃). IR (KBr, v/cm⁻¹): 2921, 1480, 1359, 1317, 1160, 975, 890, 758. Anal. Calcd for C₁₁H₁₇NO₄S₂: C, 45.34; H, 5.88; N, 4.81. Found: C, 45.5; H, 5.9; N, 4.9.

N-(4-acetylphenyl)-*N*-(*p*-tolylsulfonyl)-*p*-toluenesulfonamide (**4i**). Compound **4i** was synthesized adapting a known procedure for the synthesis of *N*-aryl-*p*-toluenesulfonimides.^[132] To a solution of aniline **8f** (1.35 g, 10 mmol), triethylamine (4.2 mL, 30 mmol) in CH₂Cl₂ (30 mL), *p*-toluenesulfonyl chloride (4.0 g, 21 mmol) was added portionwise under stirring at room temperature. After 24 hours of stirring the mixture was quenched with water (30 mL) and then extracted with CH₂Cl₂ (3×30 mL). The organic layer was washed sequentially with water (75 mL), 10% aqueous HCl (3×30 mL), water (2×50 mL), 10% aqueous NaOH (2×30 mL) and brine (2×30 mL) and eventually dried on dry Na₂SO₄. The solvent was then evaporated, affording the crude product. After purification by column chromatography (eluant: cyclohexane/ethyl acetate, 9:1) **4i** was obtained as a white solid in a 77% yield (m.p. = 177-179 °C, lit. 182 °C).^[134] ¹H NMR (CDCl₃) δ: 8.00-7.10 (AA'BB' system, 4H), 7.90-7.30 (AA'BB' system, 8H), 2.63 (s, 3H), 2.50 (s, 6H). ¹³C NMR (CDCl₃) δ: 196.9, 145.2, 138.3, 137.9, 136.2, 131.8 (CH), 129.6 (CH), 129.0 (CH), 128.4 (CH), 26.6 (CH₃), 21.6 (CH₃). IR (KBr, v/cm⁻¹): 3072, 1687, 1598, 1380, 1168, 915, 661. Anal. Calcd for C₂₂H₂₁NO₅S₂: C, 59.57; H, 4.77; N, 3.16. Found: C, 59.5; H, 4.8; N, 3.2.

N-(4-acetylphenyl)-1,1,1-trifluoro-*N*-[(trifluoromethyl)sulfonyl]methanesulfonamide (**4j**).

Compound **4j** was synthesized using a procedure employed for the synthesis of *N*-(4-

vinylphenyl)-1,1,1-trifluoro-*N*-[(trifluoromethyl)sulfonyl]methanesulfonamide.^[135] To a cooled solution (-78 °C) of **8f** (1.35 g, 10 mmol), triethylamine (4.0 mL, 30 mmol) in dry CH₂Cl₂ (35 mL) under nitrogen atmosphere, trifluoromethanesulfonic anhydride (3.6 mL, 21 mmol), was added dropwise. The mixture was kept under stirring at -78 °C for 1 hour, allowed to warm to room temperature and then further stirred for another hour. The resulting mixture was diluted with 80 mL of dichloromethane and washed with saturated aqueous NaHCO₃ (3×30 mL) and brine (3×30 mL). The organic layer was then dried over Na₂SO₄ and the solvent was evaporated. The crude residue was thus purified by column chromatography (eluant: hexane/ethyl acetate, 95:5), affording **1j** as a white solid (83% yield, m.p. = 87-89 °C). ¹H NMR (CDCl₃) δ: 8.10-7.50 (AA'BB' system, 4H), 2.65 (s, 3H). ¹³C NMR (CDCl₃) δ: 196.0, 139.5, 135.3, 131.2 (CH), 129.6 (CH), 119.2 (q, CF₃, *J* = 323 Hz), 26.6 (CH₃). IR (KBr, ν/cm⁻¹): 1695, 1448, 1416, 1210, 1123, 913. Anal. Calcd for C₁₀H₇F₆NO₅S₂: C, 30.08; H, 1.77; N, 3.51. Found: C, 30.3; H, 1.8; N, 3.5.

8.2.4 Preparative irradiations.

Photochemical reactions were performed using nitrogen saturated solutions (0.012-0.052 M) in quartz tubes for irradiation. Workup of the photolytes involved concentration in vacuo (80-100 Torr) and chromatographic separation.

Irradiation of 4a in MeCN. A nitrogen-saturated solution of **4a** (400 mg, 1.4 mmol, 0.027 M) in MeCN was irradiated for 3 hours. The photolysed solution was then evaporated and the resulting residue purified by column chromatography (eluant: cyclohexane/ethyl acetate 70:30) to afford 240 mg of *N*-[4-(dimethylamino)-2-(methylsulfonyl)phenyl]methanesulfonamide (**6a**, white solid, 60% yield,) along with 100 mg of a mixture of **6a** (80 mg) and 4-(dimethylamino)-2,6-bis(methylsulfonyl)aniline (**9a**, 20 mg, 5% yield).

6a: white solid, m.p. = 126-129 °C. ¹H NMR (CDCl₃) δ: 8.13 (s, 1H), 7.48 (d, 1H, *J* = 9 Hz), 7.17 (d, 1H, *J* = 3 Hz), 6.93 (dd, 1H, *J* = 3 and 9 Hz), 3.16 (s, 3H), 3.13 (s, 3H), 3.00 (s, 6H). ¹³C NMR (CDCl₃) δ: 147.7, 130.2 (2 C), 124.2 (CH), 118.3 (CH), 111.8 (CH), 44.4(CH₃), 41.0 (CH₃), 40.3 (CH₃). IR (KBr, v/cm⁻¹): 3284, 2930, 1610, 1508, 1297, 1151, 969. Anal. Calcd for C₁₀H₁₆N₂O₄S₂: C, 41.08; H, 5.52; N, 9.58. Found: C, 41.3; H, 5.3; N, 9.8.

9a: ¹H NMR (from the mixture, CDCl₃) δ: 7.63 (s, 2H), 5.30 (s, 2H), 3.12 (s, 6H), 2.99 (s, 6H). ¹³C NMR (from the mixture, CDCl₃) δ: 147.2, 125.7, 124.9 (CH), 121.3, 42.3 (CH₃), 41.9 (CH₃). IR of the mixture (KBr, v/cm⁻¹): 3274, 2926, 1653, 1507, 1299, 1150, 1052, 970, 751.

Irradiation of 4b in MeCN. A nitrogen-saturated solution of **4b** (450 mg, 1.6 mmol, 0.032 M) in MeCN was irradiated for 5 hours. The photolysed solution was basified with triethylamine (2 mL), then the solvent evaporated. The resulting residue was then purified by column chromatography (eluant: cyclohexane/ethyl acetate 70:30) to afford 68 mg of **5b** (21% yield), 40 mg of **8b** (20% yield), 55 mg of *N*-[4-methoxy-2-(methylsulfonyl)phenyl]methanesulfonamide (**6b**, white solid, 12% yield, m.p. = 155-158 °C), a mixture of 4-(methoxy)-2,6-bis(methylsulfonyl)aniline (**9b**, 75 mg, 17% yield) and **6b** (27 mg) and a mixture of **5b** (12 mg) and 4-methoxy-2-(methylsulfonyl)aniline (**7b**, 3 mg, yield < 1%).

6b: ¹H NMR (CDCl₃) δ: 8.40, (s, 1H), 7.60 (d, 1H, *J* = 9 Hz), 7.45 (d, 1H, *J* = 3 Hz), 7.20 (dd, 1H, *J* = 3 and 9 Hz), 3.85 (s, 3H), 3.20 (s, 3H), 3.18 (s, 3H). ¹³C NMR (CDCl₃) δ: 156.3, 129.3, 129.1, 123.2 (CH), 121.9 (CH), 113.7 (CH), 55.9 (CH₃), 44.2 (CH₃), 41.2 (CH₃). IR (KBr, v/cm⁻¹): 3315, 1644, 1498, 1326, 1281, 1144, 1132, 1033, 957. Anal. Calcd for C₉H₁₃NO₅S₂: C, 38.70; H, 4.69; N, 5.01. Found: C, 38.9; H, 4.5; N, 4.8.

7b: ¹H NMR (from the mixture, CDCl₃) δ: 7.27 (d, 1H, *J* = 3 Hz), 7.01 (dd, 1H, *J* = 3 and 9 Hz), 6.80 (d, 1H, *J* = 9 Hz), 3.78 (s, 3H), 3.10 (s, 3H). IR of the mixture (KBr, v/cm⁻¹): 3248, 1508, 1319, 1146, 1032, 824, 768.

9b: ^1H NMR (from the mixture, CDCl_3) δ : 7.63 (s, 2H), 6.10 (brs, 2H), 3.82 (s, 3H), 3.11 (s, 6H).

^{13}C NMR (from the mixture, CDCl_3) δ : 150.0, 138.7, 125.0, 121.2 (CH), 55.9(CH_3), 42.0 (CH_3).

IR (of the mixture, KBr, v/cm^{-1}): 3471, 3370, 2927, 1475, 1303, 1131, 961, 810.

Irradiation of 4c in MeCN. A nitrogen-saturated solution of **4c** (300 mg, 1.0 mmol, 0.020 M) in MeCN was irradiated for 16 hours. The photolysed solution was thus basified with triethylamine (2 mL) and then evaporated. The resulting residue was purified by column chromatography (eluant: cyclohexane/ethyl acetate 70:30) to afford 30 mg of **8c** (20% yield) and 140 mg of a mixture of **5c** (60 mg, 27% yield) and 4-*t*-butyl-2-(methylsulfonyl)aniline (**7c**, 80 mg, 36% yield).

7c: ^1H NMR (from the mixture, CDCl_3) δ : 7.72 (d, 1H, $J = 2$ Hz), 7.42 (dd, 1H, $J = 2$ and 9 Hz), 6.81 (brs, 2H), 6.75 (d, 1H, $J = 9$ Hz), 3.07 (s, 3H), 1.29 (s, 9H). ^{13}C NMR (from the mixture, CDCl_3) δ : 143.4, 141.5, 132.5 (CH), 125.3 (CH), 121.7, 117.7 (CH), 42.1(CH_3), 34.1, 31.1 (CH_3).

IR (of the mixture, KBr, v/cm^{-1}): 3466, 3372, 3263, 2963, 1625, 1499, 1330, 1292, 1156, 966.

Irradiation of 4d in MeCN. A nitrogen-saturated solution of **4d** (250 mg, 1.0 mmol, 0.020 M) in MeCN was irradiated for 10 hours. The photolysed solution was basified with triethylamine (2 mL) and then evaporated. The resulting residue was purified by column chromatography (eluant: cyclohexane/ethyl acetate 70:30) to afford 51 mg of **5d** (30% yield), 9 mg of **8d** (10% yield) and 39 mg of 4-(methylsulfonyl)aniline (**10d**, 23% yield, white solid, m.p. = 135-139 °C, lit. 134 °C).^[136]

10d: ^1H NMR ($\text{DMSO}-d_6$) δ : 7.55-6.65 (AA'BB' system, 4H), 6.09 (s, 2H), 3.03 (s, 3H). ^{13}C NMR ($\text{DMSO}-d_6$) δ : 153.4, 128.8 (CH), 125.8, 112.7 (CH), 44.4 (CH_3). IR (KBr, v/cm^{-1}): 3374, 2926, 1595, 1505, 1289, 1139, 1090, 959, 832, 767. Anal. Calcd for $\text{C}_7\text{H}_9\text{NO}_2\text{S}$: C, 49.10; H, 5.30; N, 8.18. Found: C, 49.3; H, 5.2; N, 8.0.

Irradiation of 4e in MeCN. A nitrogen-saturated solution of **4e** (275 mg, 1.0 mmol, 0.020 M) in MeCN was irradiated for 6 hours. The photolysed solution was basified with triethylamine (2

mL) and then evaporated. Purification of the resulting residue by column chromatography (eluant: hexane/ethyl acetate 70:30) afforded 15 mg of **5e** (8% yield), 94 mg of 4-cyano-2-(methylsulfonyl)aniline (**7e**, 48% yield, white solid, m.p. = 145-148 °C) and 49 mg of **8e** (33% yield).

7e: ^1H NMR (CDCl_3) δ : 8.04 (d, 1H, $J = 2$ Hz), 7.57 (dd, 1H, $J = 2$ and 9 Hz), 6.80 (d, 1H, $J = 9$ Hz), 5.63 (brs, 2H), 3.07 (s, 3H). ^{13}C NMR (CDCl_3) δ : 149.2, 137.7 (CH), 134.8 (CH), 121.7, 118.0, 117.9 (CH), 100.6, 42.6 (CH_3). IR (KBr, v/cm^{-1}): 3464, 3364, 2926, 2222, 1626, 1500, 1294, 1134, 960, 832, 746. Anal. Calcd for $\text{C}_8\text{H}_8\text{N}_2\text{O}_2\text{S}$: C, 48.97; H, 4.11; N, 14.28. Found: C, 49.1; H, 4.2; N, 14.1.

Irradiation of 4f in MeCN. A nitrogen-saturated solution of **4f** (380 mg, 1.3 mmol, 0.052 M) in MeCN was irradiated for 24 hours. The photolysed solution was basified with triethylamine (2 mL) and then evaporated. The resulting residue was purified by column chromatography (eluant: cyclohexane/ethyl acetate 70:30) to afford 33 mg of **5f** (12% yield), 53 mg of **8f** (30% yield) and 86 mg of a mixture of 1-[4-amino-3-(methylsulfonyl) phenyl] ethanone (**7f**, 72 mg, 26% yield), **5f** (9 mg) and 4-(methylsulfonyl)aniline (**10d**, 14 mg, 5% yield).

7f: ^1H NMR (from the mixture, $\text{DMSO}-d_6$) δ : 8.14 (d, 1H, $J = 2$ Hz), 7.91 (dd, 1H, $J = 2$ and 9 Hz), 6.93 (d, 1H, $J = 9$ Hz), 4.20 (brs, 2H), 3.17 (s, 3H), 2.46 (s, 3H). ^{13}C NMR (from the mixture, $\text{DMSO}-d_6$) δ : 194.6, 150.7, 134.4 (CH), 130.8 (CH), 124.7, 119.4, 116.7 (CH), 42.1 (CH_3), 26.0 (CH_3). IR of the mixture (KBr, v/cm^{-1}): 3460, 3361, 1636, 1560, 1506, 1292, 1136, 959, 783.

Irradiation of 4i in MeCN. A nitrogen-saturated solution of **4i** (445 mg, 1.0 mmol, 0.040 M) in MeCN was irradiated for 6 hours. The photolysed solution was basified with triethylamine (2 mL) and then evaporated. The resulting residue was purified by column chromatography (eluant: cyclohexane/ethyl acetate 70:30) to afford 15 mg of **5i** (5% yield), 48 mg of **8f** (35% yield) and

148 mg of a mixture of 1-[4-amino-3-(*p*-tolylsulfonyl)phenyl]ethanone (**7i**, 111 mg, 38% yield) and 4-(*p*-tolylsulfonyl)aniline (**10i**, 37 mg, 15% yield).

7i: ^1H NMR (from the mixture, CDCl_3) δ : 8.45 (d, 1H, $J = 2$ Hz), 7.90 (dd, 1H, $J = 2$ and 9 Hz), 7.85-7.25 (AA'BB' system, 4 H), 6.72 (d, 1H, $J = 9$ Hz), 5.80 (brs, 2H), 2.55 (s, 3H), 2.41 (s, 3H). ^{13}C NMR (from the mixture, CDCl_3) δ : 195.2, 149.7, 144.4, 138.2, 134.4 (CH), 131.6 (CH), 130.7, 129.8 (CH), 126.8 (CH), 121.1, 117.3 (CH), 26.0 (CH_3), 21.5 (CH_3).

10i: ^1H NMR^[60a] (from the mixture, CDCl_3) δ : 7.80-7.25 (AA'BB' system, 4H), 7.70-6.65 (AA'BB' system, 4H), 3.93 (brs, 2H), 2.39 (s, 3H). ^{13}C NMR (from the mixture, CDCl_3) δ : 151.0, 143.3, 139.9, 129.6 (CH), 129.5 (CH), 129.4, 126.9 (CH), 114.1 (CH), 21.4 (CH_3). IR of the mixture (KBr, v/cm^{-1}): 3460, 3368, 2925, 1653, 1506, 1289, 1146, 1106, 866.

Irradiation of 5a in MeCN. A nitrogen-saturated solution of **5a** (133 mg, 0.62 mmol, 0.012 M) in MeCN was irradiated for 3 hours. The photolysed solution was then evaporated and the resulting residue purified by column chromatography (eluant: hexane/ethyl acetate 70:30) to afford 92 mg of 4-(dimethylamino)-2-(methylsulfonyl)aniline (**7a**, white solid, 69% yield, m.p. = 168-171 °C).

7a: ^1H NMR (CDCl_3) δ : 7.13 (d, 1H, $J = 3$ Hz), 6.91 (dd, 1H, $J = 3$ and 9 Hz), 6.72 (d, 1H, $J = 9$ Hz), 4.52 (brs, 2H), 3.07 (s, 3H), 2.86 (s, 6H). ^{13}C NMR (CDCl_3) δ : 143.9, 137.1, 123.0, 121.7 (CH), 119.1 (CH), 112.5 (CH), 41.7 (CH_3), 41.4 (CH_3). IR (KBr, v/cm^{-1}): 3443, 3364, 2931, 1724, 1610, 1507, 1290, 1134, 954. Anal. Calcd for $\text{C}_9\text{H}_{14}\text{N}_2\text{O}_2\text{S}_2$: C, 50.45; H, 6.59; N, 13.07. Found: C, 50.7; H, 6.3; N, 13.0.

8.2.5 Photopolymerization and photopatterning experiments with sulfonimides.

Experiments described in this section were performed at the Department of Industrial Engineering of the University of Padova (Italy) by Dr. Gioia Della Giustina.

The synthesis of G8Ge2 matrix was achieved with the same procedure described in the section 8.1.4. Photopolymerization experiments were likewise performed with the same equipment and methodology described in the section 8.1.4 for aryl tosylates (the only difference being the use of **4b,e,f,i,j** and DPST as PAGs to be tested).

Concerning photopatterning tests, microstructures were realised on films containing compound **1** by using the same UV light source used for photopolymerization. Post application-bake (PAB) in a forced air oven at 70 °C for 30 min was adopted to remove residual solvent. In particular, the photosensitive sol-gel films were exposed in air using a quartz chromium mask with different geometries and sizes (features resolution between 2 and 100 µm). The optimal UV dose on silicon varied between 12 and 25 J/cm² (1-3 min), depending on the pattern dimensions and resolution. After exposure, post-exposure bake (PEB) at 80-100 °C for 30 s was performed to increase the film contrast, followed by development in a HCl/ethanol mixture (volume ratio 1:1) for 15-60 s, rinsing in water, and drying in nitrogen.

8.3 *Experimental details regarding chapter 4.*

8.3.1 General Information.

¹H NMR spectra were recorded with a 300 MHz spectrometer, while ¹³C NMR spectra were recorded with a 75 MHz spectrometer. Chemical shifts are reported in ppm downfield from TMS. The electrochemical measurements were carried out by a computer-controlled electrochemical analyzer.

(4-Phenylthiophenyl)diphenylsulfonium trifluoromethanesulfonate (DPST) and all of the other reagents, solvents and materials used for the synthesis of photoacid generators, for the preparation of the sol-gel hybrid organic-inorganic matrices and for the polymerization and

patterning experiments were purchased by commercial suppliers and used with no further purification.

8.3.2 Synthesis of photoacid generators 1d, 1i and 1j.

4-acetylphenyl p-toluenesulfonate (1d). Compound **1d** was synthesized as described in the section 8.1.2.

Pentafluorophenyl p-toluenesulfonate (1h). Compound **1h** was synthesized following the known general procedure described at the beginning of the section 8.1.2,^[35] starting from 2,3,4,5,6-pentafluorophenol (3.68 g, 20 mmol). **1h** was obtained as a white solid (m.p. = 62-65°C, lit. = 66-69°C)^[137] after purification of the crude product by recrystallization from methanol (4.74 g, 75% yield). Spectroscopic NMR and IR data were in accordance with the literature.^[135] Anal. Calcd for C₁₃H₇F₅O₃S: C, 46.16; H, 2.09. Found: C, 46.5; H, 2.4.

Pentafluorophenyl trifluoromethanesulfonate (1j). Compound **1j** was synthesized using a known procedure.^[74] To a cooled solution (-78 °C) of 2,3,4,5,6-pentafluorophenol (3.68 g, 20 mmol) and triethylamine (7.2 mL, 51 mmol) in dry dichloromethane (30 mL) under nitrogen atmosphere, trifluoromethanesulfonic anhydride (3.7 mL, 22 mmol) was added dropwise while stirring. The resulting mixture was stirred for 10 minutes at -78 °C and then for 1 h. at room temperature. The obtained red solution was thus quenched with saturated aqueous NaHCO₃ (100 mL) and then washed sequentially with water (60 mL), 10% aqueous HCl (60 mL), brine (60 mL) and water (60 mL). The organic layer was separated and dried over Na₂SO₄. The solvent was evaporated under reduced pressure and the resulting yellow oil was eventually purified by distillation under reduced pressure (25 torr, 80 °C), affording the desired compound as a colorless liquid (4.30 g, 68% yield). Spectroscopic NMR and IR data were in accordance with the literature.^[74] Anal. Calcd for C₇F₈O₃S: C, 26.60. Found: C, 26.9.

8.3.3 Synthesis of hybrid organic-inorganic matrices.

Experiments described in this section were performed at the Department of Industrial Engineering of the University of Padova (Italy) by Dr. Gioia Della Giustina.

Synthesis of G8Ge2 matrix. G8Ge2 matrix was synthesized as described in the section 8.1.4 for polymerization experiments on aryl tosylates.

Synthesis of GB matrix. GB was synthesized similarly to what described for G8Ge2, following a sol-gel method previously described in literature.^[31c] GPTMS was hydrolyzed in basic conditions (by NaOH) at 80 °C in bidistilled water for 1 hour. The molar ratios employed were GPTMS:H₂O:NaOH = 1:3:0.003. The resulting system was then diluted in 2-methoxyethanol to achieve the desired concentration (2 M respect to the epoxy groups). Filtration through a microporous membrane (0.2 μm Millipore) was performed before deposition for photopolymerization and photopatterning experiments.

8.3.4 Polymerization and patterning experiments.

Experiments described in this section were performed at the ENEA research center of Frascati (Italy) by Dr. Gioia Della Giustina and Dr. Luca Mezi.

EUV radiation source. The utilized EUV source (located at the ENEA Research Center in Frascati, Italy) was a xenon Discharge Produced Plasma (DPP) apparatus.^[138] Its working principles can be schematized as following. First, low pressure (0.5-1.0 mbar) Xe gas, filling an alumina tube of 3 mm in inner diameter and 12 mm in length, was pre-ionized by a first discharge (current = 20-30 A, duration = 10-20 μs). Then, a low-inductance 50 nF glycol cylindrical capacitor, charged up to 25 kV, produced a second (main) discharge (about 12 kA peak current, 240 ns base duration) in the pre-ionized gas. Thus the resulting magnetic field (>1 T at the alumina tube inner wall) pinched the plasma towards the tube axis, making the plasma resistance

to rise and the temperature to increase up to 30-40 eV (about 400000 K). In this way the hot plasma emitted EUV, UV and visible radiation before relaxing and cooling. The ENEA DPP was able to emit more than 35 mJ/sr/shot in the $\lambda = 10\text{-}20$ nm wavelength spectral range at 10 Hz repetition rate. The duration of each EUV pulse was about 100 ns FWHM. The optical EUV source transverse size was less than 300 μm .

The used DPP is suitable for applications in surface treatments, photonic materials processing, nano-structuring, etc.

Debris Mitigation System (DMS). For extremely delicate contact EUV lithography experiments, a Debris Mitigation System (DMS) was needed. Thus the DPP source was equipped with an efficient properly designed DMS composed by a permanent magnet dipole placed at about 3 cm from the source to deflect ions and a 13 cm in diameter rotating structure (RS) having 31 radial vanes. The latter was placed between the source and the sample to be patterned and served to stop particulate debris.

The magnet, having a transverse average field of 0.2 T along the longitudinal ion path, could vertically deflect Xe ions with energies up to 10-20 keV, in such a way to avoid their impact on the exposed samples.

The RS, placed in front of the source at 11 cm from it, with its rotating axis parallel to the optical one, was positioned in such a way that EUV radiation could reach the sample passing between two adjacent vanes thanks to a proper synchronisation between the RS phase and the DPP triggering. The RS had a longitudinal length of 5 cm and rotated up to 100 Hz.

Equipment setup for polymerization and patterning experiments. EUV exposures (both for polymerization tests and lithography) were performed by keeping the samples to be exposed in a vacuum chamber (10^{-5} mbar of air, and 10^{-2} mbar of Xe when the source was operating) connected with the DPP source. In particular, the samples were positioned at 12 cm from the

radiation source for polymerization tests while, in the case of patterning, they were placed in a holder at 17 cm from the source, because of the DMS insertion. In both cases, the EUV radiation in the 10-20 nm wavelength spectral range was selected by a thin (150 nm) Zr filter, supported by a Ni wire mesh and positioned at few millimeters from the samples.

For patterning experiments a specific contact EUVL technique was developed to reach an effective sub-micrometric resolution for photoresist testing. In this technique, special EUV transmitting masks, obtained by depositing 200 nm thick Au patterns on 50 nm thick Si₃N₄ membranes, were placed in the holder together with samples to be patterned, at 3 μm from them (see Figure 4.3). With this setup the total exposed area was about 400 × 400 μm².

The mask membrane, which transmitted less than 30% of the incident EUV radiation, was so fragile and delicate that, without a DMS system, it would have been broken after few shots of the DPP source. Thus the previously described DMS was used in photopatterning experiments, with the sample holder just few mm behind the RS.

Polymerization and patterning experimental procedure. Polymerization experiments were performed similarly to what described in the section 8.1.4. To test the suitability of the synthesized materials, sol-gel films of the epoxy based matrices were deposited by spin coating on Si (100) substrates, with different thicknesses, by tailoring the spin rate. No adhesion problems were observed for these substrates. After these tests, films containing the different PAGs in GB and G8Ge2 were prepared. In each case the selected PAG was dissolved in the previously synthesized sol-gel systems (1% molar concentration with respect to the epoxy groups) and the obtained mixture was spin coated on Si (100) wafers at 4000 rpm for 30 s, obtaining a film with a thickness of about 100-150 nm. This value was the proper one to allow the complete penetration of radiation into the exposed sample.

Polymerization experiments were performed cutting the synthesized films into slices and irradiating then the obtained slices by the DPP source, each one with a different EUV exposure dose (25-400 mJ/cm² on the sample surface). For each experiment, the evolution of organic-inorganic network, with particular regard to epoxy rings, was monitored by FT-IR spectroscopy. Analyses were performed within the 400-4000 cm⁻¹ range, with a 4 cm⁻¹ resolution for a total of 32 scans. Degrees of polymerization were calculated referring to an unexposed resist kept in the same vacuum chamber of the exposed ones.

Microstructured patterns were realised on GB films containing **1h** (1% molar) by using the DPP EUV source with doses between 5 and 100 mJ/cm². Sol-gel films were treated by post-application bake (PAB) in a forced air oven at 70 °C for 30 min to remove residual solvent. After that, they were exposed in vacuum (10⁻⁵ mbar of air, and 10⁻² mbar of Xe when the source was operating) through Au/Si₃N₄ masks with different geometries and sizes. The optimal EUV doses were found to be 6 and 11 mJ/cm², depending on the pattern geometries. After exposure, post-exposure bake (PEB) at 80-100 °C for 30 sec was performed to increase the film contrast. Eventually, development in a NaOH 1 M / DMSO mixture (volume ratio 1:1) for 15-60 s, rinsing in ethanol and drying in nitrogen brought to the final patterned materials.

8.3.5 Determination of PAGs reduction potentials.

Experiments described in this section were carried out under the supervision of Dr. Daniele Merli (University of Pavia). Electrochemical measurements (cyclic voltammetry) were performed on ca. 10⁻³ M solutions of the chosen PAG in a three-electrode cell (volume: 5 mL, tetrabutylammonium perchlorate 0.1 M in *N,N*-dimethylformamide as the supporting electrolyte). A glassy carbon electrode (diameter 2 mm) was chosen as the working electrode, Pt wire as the auxiliary electrode, and Ag/AgCl (3 M NaCl) as the reference electrode. Scan speed was 100 mV

s⁻¹. The potential range investigated was between -0.5 V and -2.5 V (vs. Ag/AgCl, 3 M NaCl). No iR-compensation was performed.

Prior to each experiment the electrodes were washed with *N,N*-dimethylformamide, the working electrode was further cleaned using a polishing alumina slurry and the electrolyte solution was checked by conducting a cyclic voltammetry across the whole potential range. Moreover the electrolyte solutions containing the different PAGs were purged with nitrogen for 5-10 minutes before every measurements.

The potentials measured are cathodic peak potentials and are referred to Ag/AgCl (3 M NaCl). In all cases, a quasi-reversible redox behavior was observed, as peak potential changed little with scan speed and the reverse peak was clearly visible by presenting the voltammograms as semiderivative curves.^[139] For this reason, the $E_{1/2 \text{ CAT}}$ values obtained were approximated with the formal redox potential ($E^{0'}$).^[140]

8.4 *Experimental details regarding chapter 5.*

8.4.1 General Information.

¹H NMR spectra were recorded with a 300 MHz spectrometer, while ¹³C NMR spectra were recorded with a 75 MHz spectrometer. Chemical shifts are reported in ppm downfield from TMS. HRMS spectra were obtained on a triple quadrupole ESI mass spectrometer in a positive and/or negative mode. MALDI-TOF mass spectrum was recorded on a MALDI-TOF spectrometer with the sample ionized with the aid of a nitrogen laser (wavelength 337 nm, maximum power 6 MW), α -cyano-4-hydroxycinnamic acid (HCCA) was used as a matrix. All solvents and chemicals used were used as purchased or purified by standard procedures when necessary.

Irradiations were performed on argon saturated solutions by a 1000 W Xe lamp (through a Pyrex filter), cooling the irradiated samples in a water bath kept at 10-15 °C.

Calorimetric measurements were carried out by researchers belonging to the group of Prof. Vladimír Šindelář (Masaryk University, Brno), which collaborated with us in the project. Even if I have no experience with this technique, I describe the procedure adopted by them. They performed experiments using a VP-ITC microcalorimeter. Experiments were carried out in ultrapure water at 303.15 ± 0.1 K. Anion binding to **BU** was investigated via a classical isothermal titration experiments (either 5 or 10 μL additions of solutions of salts of the chosen anion). Integrated heat effects were analyzed by non-linear regression using a single-site binding. The experimental data fitted to a theoretical titration curve provided the association constant K_a and the enthalpy of binding ΔH° . The first smaller addition (5 μL), which was used to compensate for diffusion of the guest from an injector during equilibration, was discarded prior to data fitting. Control experiments were performed by titration of the guest solution in pure water and the corresponding heat effects were subtracted from the titration data prior to fitting procedure.

8.4.2 Syntheses.

2-Bromo-1-(4-hydroxyphenyl)ethanone. The synthesis was performed using a known procedure.^[93] 4'-Hydroxyacetophenone (500 mg, 3.7 mmol) was dissolved in an ethyl acetate/chloroform mixture (1 : 1, 30 mL) containing CuBr_2 (1878 mg, 8.41 mmol). The mixture was stirred vigorously and refluxed for 2 h. Then it was let to cool down at room temperature and filtered on a silica pad. The solvent was removed under reduced pressure and the crude residue was purified by column chromatography (eluent: hexane/ethyl acetate, 85 : 15) to give pure 2-bromo-1-(4-hydroxyphenyl)ethanone as a white powder. Yield: 358 mg (45%). ^1H NMR ($\text{DMSO}-d_6$) δ : 10.49 (s, 1H), 7.90–6.85 (AA'BB' system, 4H), 4.77 (s, 2H), in accordance with the literature data.^[141]

2-Iodo-1-(4-hydroxyphenyl)ethanone (IIa). The synthesis was performed according to two procedures reported in the literature, starting from 2-bromo-1-(4-hydroxyphenyl)ethanone.^[142] 2-Bromo-1-(4-hydroxyphenyl)ethanone (300 mg, 1.40 mmol) was dissolved in acetone (10 mL), and NaI (418 mg, 2.79 mmol) was added portionwise. The resulting mixture was stirred for 1 h, and then the solvent was removed under reduced pressure (the reaction was performed under exclusion of light). The crude residue was diluted with diethyl ether (15 mL) and washed then with a 1% aqueous sodium thiosulfate solution (40 mL). The layers were separated, and the aqueous layer was extracted with diethyl ether (3 × 20 mL). The organic layers were combined and dried over Na₂SO₄. The solvent was removed and the crude product was obtained. This residue was dissolved in acetone (150 mL) and filtered on a silica pad to give the title compound as an off-white solid. Yield: 312 mg (85%). ¹H NMR (DMSO-*d*₆) δ: 10.47 (s, 1H), 7.90–6.84 (AA'BB' system, 4H), 4.48 (s, 2H). ¹³C NMR (DMSO-*d*₆) δ: 191.8, 162.5, 131.5 (CH), 124.8, 115.4 (CH), 4.5 (CH₂). HRMS (TOF MS ESI⁻) *m/z*: calc. for C₈H₆IO₂⁻ [M – H]⁻ 260.9412; found 260.9415. Spectroscopic NMR data were in accordance with the literature data.^[143]

2-Bromo-1-(4-hydroxy-2-methylphenyl)ethanone. The synthesis was performed using a known procedure.^[93] 4-Hydroxy-2-methylacetophenone (500 mg, 3.3 mmol) was dissolved in an ethyl acetate/chloroform mixture (1 : 1, 30 mL) containing CuBr₂ (1700 mg, 7.61 mmol). The mixture was stirred vigorously and refluxed overnight. Then it was let to cool down to room temperature and filtered through a silica pad. The solvent was removed under reduced pressure and the crude residue was purified by column chromatography (eluent: dichloromethane/hexane, 9 : 1) to give pure 2-bromo-1-(4-hydroxy-2-methylphenyl)ethanone as a white powder. Yield: 137 mg (18%). ¹H NMR (DMSO-*d*₆) δ: 10.28 (s, 1H), 7.85–7.81 (m, 1H), 6.71–6.67 (m, 2H), 4.73 (s, 2H), 2.41 (s, 3H), in accordance with the reported data.^[93]

2-Iodo-1-(4-hydroxy-2-methylphenyl)ethanone (11b). The synthesis was performed using two reported procedures, starting from 2-bromo-1-(4-hydroxy-2-methylphenyl)ethanone.^[142] 2-Bromo-1-(4-hydroxy-2-methylphenyl)ethanone (137 mg, 0.60 mmol) was dissolved in acetone (10 mL), and NaI (179 mg, 1.19 mmol) was added portionwise. The resulting mixture was stirred overnight and then the solvent was removed under reduced pressure (the reaction was performed under exclusion of light). The crude residue was diluted with diethyl ether (15 mL) and then washed with a saturated aqueous sodium thiosulfate solution (40 mL). The layers were separated and the aqueous part was extracted with diethyl ether (3 × 20 mL). The combined organic layers were dried over Na₂SO₄, and the solvent was removed to give the crude product. This residue was dissolved in acetone (150 mL) and filtered on a silica pad to give the desired **11b** as an off-white solid. Yield: 131 mg (80%). ¹H NMR (DMSO-*d*₆) δ: 10.24 (s, 1H), 7.83–7.79 (m, 1H), 6.70–6.65 (m, 2H), 4.45 (s, 2H), 2.38 (s, 3H). ¹³C NMR (DMSO-*d*₆) δ: 194.0, 160.9, 142.4, 133.0 (CH), 124.7, 118.7 (CH), 112.4 (CH), 21.8 (CH₃), 8.0 (CH₂). HRMS (TOF MS ESI⁻) *m/z*: calc. for C₉H₈IO₂⁻ [M – H]⁻ 274.9569; found 274.9570.

Dodecakis(6-[(2-hydroxyethyl)amino]-6-oxohexyl)bambus[6]uril (BU). The synthesis was carried out by researchers of Prof. Šindelář's group. It is however described below. It was performed starting from dodecakis(5-carboxypentyl)-bambus[6]uril (250 mg, 0.109 mmol), synthesized according to a known procedure.^[88a] Thus the reagent and ethanolamine (320 mg, 5.24 mmol) were added to a microwave tube. Toluene (5 ml) was added, and the mixture was subjected to microwave irradiation (150 W, 200 °C) for 1 h. During this time, the solid salt melts into an oily viscous compound that sticks to the bottom of the tube. After cooling to room temperature, toluene was carefully decanted and the residue was dissolved in a small amount of methanol, neutralized with diluted acetic acid and finally diluted with water to an approx. volume of 20 ml. The crude product was purified by a repeated dialysis against deionized water (6 × 1 L

of H₂O, equilibrated for at least for 6 h) using a benzoylated cellulose membrane. After evaporation of the solvent (either water or methanol) and drying in vacuum, the product was obtained as a yellowish viscous oil (264 mg, 71% yield).

¹H NMR (DMSO-*d*₆) δ: 7.83–7.61 (m, 12H), 5.33 (s, 12H), 4.93 (s, 12H), 4.61 (s, 12H), 3.51 (s, 12H), 3.41–3.35 (m, 36H), 3.10 (q, 24H, *J* = 6.0 Hz), 2.04 (t, 24H, *J* = 7.5 Hz), 1.60 (s, 12H), 1.54–1.36 (m, 36H), 1.28–1.09 (m, 24H). ¹³C NMR (DMSO-*d*₆) δ: 172.36, 159.39, 158.57, 68.29, 59.98, 47.26, 43.79, 41.46, 35.34, 28.99, 26.08, 24.99. MALDI-TOF HRMS: *m/z* calcd for [C₁₂₆H₂₁₆N₃₆O₃₆ + I]⁻ 2936.5223, found 2936.5152 ± 0.0095.

8.4.3 Photochemical experiments on 11a and 11b.

Formation of photoproducts from 11a. A solution of **11a** (6.8×10^{-3} M, 1.0 mL) in a D₂O/CD₃CN mixture (1 : 1) was inserted in an NMR tube, purged with argon to remove oxygen and sealed with a septum, and an ¹H NMR spectrum was measured. Then it was for 3 h, until the conversion of **11a** was complete. ¹H NMR was measured again, the photoproducts were identified and their concentrations quantified using a residual signal of CD₃CN as an internal standard. The identification of **12a**, **13a**^[141] and **14a**^[144] was made by comparison of their NMR spectra to those found in the literature.

2-(4-Hydroxyphenyl)acetic acid (**12a**): ¹H NMR (CD₃CN/D₂O 1:1) δ: 7.21–6.85 (AA'BB' system, 4H), 3.61 (s, 2H).

4-(Hydroxymethyl)phenol (**13a**): ¹H NMR (CD₃CN/D₂O 1:1) δ: 7.28–6.95 (AA'BB' system, 4H), 4.54 (s, 2H).

2-Hydroxy-1-(4-hydroxyphenyl)ethanone (**14a**): ¹H NMR (CD₃CN/D₂O 1:1) δ: 7.98–6.95 (AA'BB' system, 4H), 4.80 (s, 2H).

Photochemistry of 11b followed by absorption spectroscopy. A solution of **11b** (7.98×10^{-5} M) in water/acetonitrile (99 : 1), purged with argon, was irradiated for ten minutes. The reaction course was followed by absorption spectroscopy, measuring spectra at different irradiation times (see Figure 5.6c).

Determination of photoreleased iodide. **11a** (or **11b**) (3.94×10^{-4} mmol) was added to 0.7 mL of a mixture of D₂O/CD₃CN 1 : 1 containing **BU** (3.58×10^{-4} mmol, 0.91 equiv.). The solution was inserted to an NMR tube, purged with argon to remove oxygen, sealed with a septum, and ¹H NMR spectrum was obtained. Then it was irradiated until the conversion of either **11a** or **11b** was complete. The amount of iodide released was determined by monitoring the change in the chemical shifts of signals assigned to **BU**. This analysis showed that the photorelease of iodide was quantitative: the 91% value obtained for the yield is due to the little excess of **11a** or **11b** used respect with **BU**. Thus it is the highest yield that could be measured by this method.

Photodriven exchange between S₂O₈²⁻ and I into BU macrocycle. A solution of **BU**, Na₂S₂O₈ and **11b** (concentration of **BU** = 4.31×10^{-4} M, molar ratio between **11b**, S₂O₈²⁻ and **BU** was 1.1:1:1) in a mixture CD₃CN/D₂O 1:1 (0.7 mL) was put in a NMR tube, bubbled with argon to remove oxygen and sealed with a septum. ¹H-NMR was measured on this tube. Then the tube was irradiated for 10 minutes and an ¹H-NMR spectrum was recorded again.

The exchange between the two anions was checked looking at the changes in chemical shifts assigned to **BU**.

Furthermore a blank experiment was performed irradiating a similar solution not containing **11b**. In detail 0.75 mL of a 5.22×10^{-4} M solution of **BU** in CD₃CN/D₂O 1:1 mixture containing an equimolar amount of Na₂S₂O₈ were put in a NMR tube, bubbled with argon to remove oxygen and sealed with a septum. ¹H-NMR was measured on this tube. Then the tube was for 10 minutes.

$^1\text{H-NMR}$ spectrum was recorded again. No difference in the chemical shifts was observed in this case.

8.4.4 Experiments on phototriggered oxidation of Fe^{2+} .

*Oxidation of Fe^{2+} phototriggered by **11b**.* A solution of FeSO_4 (7.12×10^{-5} M) in water was added to a mixture of **BU** (5.73×10^{-5} M), $\text{Na}_2\text{S}_2\text{O}_8$ (3.55×10^{-5} M) and **11b** (7.84×10^{-5} M) in water/acetonitrile (99 : 1). The resulting solution (3.0 mL) was put in a quartz cuvette, purged with argon to remove oxygen, and irradiated for 10 min. Absorption spectra were measured before and after irradiation (see Figure 5.6b).

*Blank thermal experiment: absorption spectra of a system containing Fe^{2+} , $\text{S}_2\text{O}_8^{2-}$, **11b**, **BU**.* A solution containing FeSO_4 (7.25×10^{-5} M), **BU** (5.85×10^{-5} M), $\text{Na}_2\text{S}_2\text{O}_8$ (3.64×10^{-5} M) and **11b** (7.98×10^{-5} M) in a water/acetonitrile (99 : 1) mixture was prepared (3.0 mL). Important: FeSO_4 was the last compound to be added in the preparation of the solution and the solution was deaerated by putting it in a quartz cuvette and purging with argon (to avoid oxidation of Fe^{2+} by molecular oxygen). Absorption spectra of the resulting solution were measured immediately and after 10 minutes, while keeping the cuvette in the dark (Figure 5.6a).

*Blank irradiation experiment not containing **11b**.* A solution of FeSO_4 (7.33×10^{-5} M), **BU** (5.89×10^{-5} M) and $\text{Na}_2\text{S}_2\text{O}_8$ (3.66×10^{-5} M) in a water/acetonitrile (99 : 1) mixture was prepared (2 mL) adding FeSO_4 to a solution of the other three compounds. It was put in a quartz cuvette, purged with argon and irradiated for 10 min. The absorption spectra were recorded before and after irradiation (Figure 5.6d).

8.4.5 Determination of the Fe²⁺ concentration by 1,10-phenanthroline.

Determination of yields of phototriggered oxidation of Fe²⁺ in the presence of 11a. First, an acetate buffer was prepared by dissolving ammonium acetate (2.5 g) in water (2.25 mL) and adding glacial acetic (7.5 mL) acid to the solution (pH~4). Then a solution of 1,10-phenanthroline (phen) was prepared by dissolving of 1,10-phenanthroline monohydrate (50 mg) in 50 mL of water (two drops of 37% aq. HCl were added to improve the phen solubility). The final phen concentration was 5.04×10^{-3} M.

A third solution of FeSO₄ (1.71×10^{-4} M), **BU** (8.64×10^{-5} M), Na₂S₂O₈ (8.59×10^{-5} M), and **11a** (9.50×10^{-5} M) in a water/acetonitrile (99 : 1) mixture was prepared. The solution was prepared adding FeSO₄ to the other reagents. The molar ratio among FeSO₄, **BU**, Na₂S₂O₈ and **11a** was 2 : 1 : 1 : 1.1. Then, 2.0 mL of this solution were put in a quartz cuvette, purged with argon and irradiated for 10 min. Subsequently, acetate buffer (0.5 mL) and a phen solution (0.2 mL) were added to the cuvette. The resulting solution was again purged with argon and kept in the dark for 10 min. after that a absorption spectrum was recorded and absorbance at 508 nm measured. The spectrum of the same solution (not irradiated but kept in dark for ten minutes) was recorded as well after an analogous treatment with phen and the acetate buffer. Lastly the spectrum of a blank solution (not containing FeSO₄ but all the other compounds) was recorded after treating it likewise with phen and the acetate buffer. The yield of oxidation of Fe²⁺ to Fe³⁺ was calculated from the decrease in the absorbance at 508 from the non-irradiated solution to the irradiated one (upon subtraction of the blank absorbance).

Determination of yields of phototriggered oxidation of Fe²⁺ in the presence of 11b. The same procedure to that described for **11a** was followed. The concentrations of the components were: FeSO₄ (1.09×10^{-4} M), **BU** (5.54×10^{-5} M), Na₂S₂O₈ (5.47×10^{-5} M), and **11b** (6.10×10^{-5} M). The molar ratio among FeSO₄, **BU**, Na₂S₂O₈ and **11b** was 2 : 1 : 1 : 1.1.

8.5 *Experimental details regarding chapter 6.*

8.5.1 General Information.

All the chemicals and solvents employed were commercially available and used as received. The only exceptions were diethyl ether, which was passed through alumina and distilled prior to use, and dichloromethane and acetonitrile, which were previously dried on CaCl₂. The solvents used for irradiations were of GC or HPLC grade purity.

¹H NMR spectra were recorded with a 300 MHz spectrometer, while ¹³C NMR spectra were recorded with a 75 MHz spectrometer. Attributions were made on the basis of ¹H and ¹³C NMR, as well as DEPT-135 experiments; chemical shifts are reported in ppm downfield from TMS.

The photochemical batch reactions were performed using nitrogen- or oxygen-saturated solutions in quartz tubes in a multi-lamp reactor equipped with 10 ×15 W phosphor-coated lamps (emission centered at 310 nm) for irradiation. In selected cases irradiations were repeated exposing solutions in a Pyrex vessel (see Figure 8.1a)^[145] to solar light (in July 2017, Pavia, Italy) on a window ledge.

Flow photochemical reactions were performed in a quartz photochemical reactor (see Figure 8.1b) equipped with a water-cooled 500 W medium pressure mercury lamp. All the tubing used in this work are made of Fluorinated Ethylene Propylene (FEP, outer diameter: 3.18 mm; inner diameter: 2.1 mm; reactor volume: 50 mL). Injection of the solutions and flow rate control were achieved by a syringe pump.^[112a]

All the reactions and irradiation were monitored by gas chromatographic (GC) analyses and by thin-layer chromatography (TLC). GC analyses were carried out using a chromatograph equipped with a FID detector. A 30 m × 0.25 mm × 0.25 μm capillary column was used for analytes separation with nitrogen as carrier gas at 1 mL min⁻¹. The injection in the GC system was performed in split mode and the injector temperature was 250 °C. The GC oven temperature was

held at 50 °C for 2 min, increased to 250 °C by a temperature ramp of 10 °C min⁻¹ and held for 20 min.

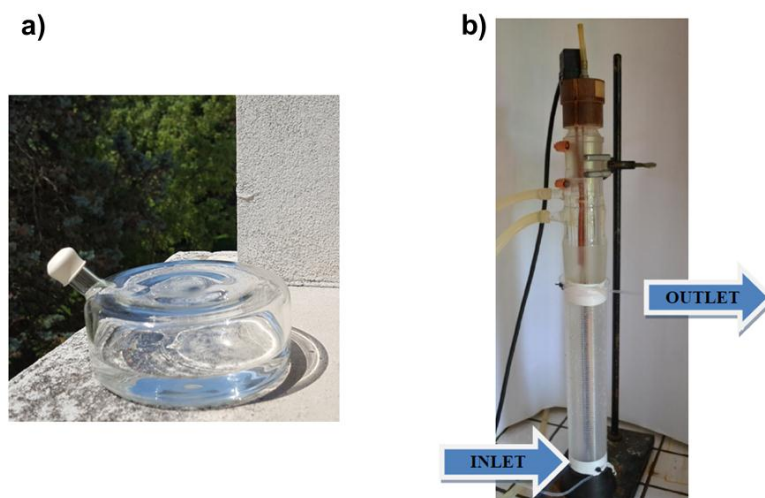


Figure 8.1. a) Pyrex vessel used for solar irradiations. b) flow photoreactions experimental setup.

GC-MS analysis were carried out using a single quadrupole GC/MS system. A 30 m × 0.25 mm × 0.25 μm capillary column was used for analytes separation with helium as carrier gas at 1 mL min⁻¹. The injection in the GC system was performed in split mode and the injector temperature was 250 °C. The GC oven temperature was held at 50 °C for 2 min, increased to 250 °C by a temperature ramp of 10 °C min⁻¹ and held for 20 min. The transfer line temperature was 270 °C and the ion source temperature 250 °C. Mass spectral analysis was carried out in full scan mode. The formation of deuterated fluoroform when irradiating **4j** in the presence of benzene **15f** was detected by FT-IR measurements on the head-space performed in a chamber with NaCl windows.

8.5.2 Synthesis of sulfonimide 4j and sulfonamide 5j.

The two trifluoromethylating agents **4j** and **5j** were synthesized according to what described in the sections 8.2.3 and 8.2.2, respectively.

8.5.3 General procedures for photochemical trifluoromethylations.

Batch photochemical trifluoromethylations. A dry dichloromethane solution (15 mL) of compound **4j** (144 mg, 0.36 mmol, 0.024 M) and the chosen aromatic compound (**15a-m**; 0.45 mmol, 0.03 M) was poured in a previously dried quartz tube capped with a septum and then purged for 10 min with nitrogen. Then the tube was irradiated for 12 h in the multi-lamp reactor (emitting at 310 nm), until none of compounds **4j** and **5j** could be detected by both GC and TLC analysis on the photolyzed solutions. In selected cases the irradiation was performed also exposing solutions in a Pyrex vessel to solar light on a window ledge. In any case, the photolyzed solution was then diluted with 20 mL of dichloromethane and washed sequentially with saturated aqueous NaHCO₃ (3×10 mL), water (10 mL) and brine (2×10 mL). The organic layer was then dried over Na₂SO₄ and the solvent was evaporated under reduced pressure (being careful of volatile products). The crude residue was thus purified by silica-gel column chromatography or by distillation.

Flow photochemical trifluoromethylations. A dry acetonitrile solution (10 mL) of compound **4j** (96 mg, 0.24 mmol, 0.024 M) and the chosen aromatic compound (**15a**, **15d**, **15j**, **15l**; 0.30 mmol, 0.03 M) was charged in a polypropylene syringe and pumped through the flow irradiating apparatus with a flow rate of 10.0 mL/h. The solvent was then removed under reduced pressure from the photolyzed solution. 30 mL of dichloromethane were added to the obtained residue and the resulting solution was washed sequentially with saturated aqueous NaHCO₃ (3×10 mL), water (10 mL) and brine (2×10 mL). The organic layer was then dried over Na₂SO₄ and the

solvent evaporated under reduced pressure (being careful of volatile products). The crude product was thus purified by silica-gel column chromatography.

8.5.4 Compounds synthesized by photochemical trifluoromethylations.

1,4-Dimethoxy-2-(trifluoromethyl)benzene (16a). From 62 mg of 1,4-dimethoxybenzene (**15a**). Purification of the residue by column chromatography (eluant: hexane/ethyl acetate 95:5) afforded 75 mg of **16a** as a colorless liquid in 81% yield (using 310 nm batch radiation source). Solar irradiation (6 hours \times 3 days) gave 73 mg of **16a** (79% yield). Continuous flow irradiation of 41 mg of **15a** afforded 53 mg of **16a** (87% yield). ^1H NMR (CDCl_3)^[107b] δ : 7.12 (d, 1H, $J = 3$ Hz), 7.02 (dd, 1H, $J = 3$ and 9 Hz), 6.93 (d, 1H, $J = 9$ Hz), 3.86 (s, 3H), 3.80 (s, 3H). ^{13}C NMR (CDCl_3)^[107b] δ : 153.1, 151.7, 123.6 (q, CF_3 , $J = 271$ Hz), 119.6 (q, $J = 31$ Hz), 118.3 (CH), 113.8 (CH), 113.0 (q, CH, $J = 5$ Hz), 56.8 (CH_3), 56.1 (CH_3). IR (KBr, v/cm^{-1}): 3008, 2958, 2938, 2842, 1594, 1505, 1467, 1432, 1335, 1306, 1130, 1053, 892, 811, 728. Anal. Calcd for $\text{C}_9\text{H}_9\text{F}_3\text{O}_2$: C, 52.43; H, 4.40. Found: C, 52.5; H, 4.3.

1,3,5-Trimethoxy-2-(trifluoromethyl)benzene (16b). From 76 mg of 1,3,5-trimethoxybenzene (**15b**). Purification of the residue by column chromatography (eluant: hexane/ethyl acetate 9:1) afforded 90 mg of **16b** as a white solid (85% yield, m.p. = 58-60°C, lit. = 51-53°C).^[103a] ^1H NMR (CDCl_3)^[103a] δ : 6.12 (s, 2H), 3.83 (s, 9H). ^{13}C NMR (CDCl_3)^[103a] δ : 163.6, 160.5, 124.5 (q, CF_3 , $J = 272$ Hz), 100.4 (q, $J = 29$ Hz), 91.3 (CH), 56.3 (CH_3), 55.5 (CH_3). IR (KBr, v/cm^{-1}): 2972, 2956, 2849, 1610, 1594, 1469, 1440, 1421, 1285, 1209, 1108, 1026, 953, 926, 871, 792, 746, 642, 625. Anal. Calcd for $\text{C}_{10}\text{H}_{11}\text{F}_3\text{O}_3$: C, 50.85; H, 4.69. Found: C, 50.8; H, 4.7.

1,3,5-Trimethoxy-5-methyl-4-(trifluoromethyl)benzene (16c). From 82 mg of 3,4,5-trimethoxytoluene (**15c**). Purification of the residue by column chromatography (eluant: hexane/ethyl acetate 9:1) afforded 89 mg of **16c** as a colorless liquid in 85% yield. ^1H NMR

(CDCl₃)^[104b] δ: 6.49 (s, 1H), 3.89 (s, 3H), 3.87 (s, 3H), 3.84 (s, 3H), 2.40 (q, 3H, *J* = 3 Hz). ¹³C NMR CDCl₃^[104b] δ: 156.3, 153.5 (q, *J* = 2 Hz), 141.0, 133.2 (q, *J* = 2 Hz), 125.0 (q, CF₃, *J* = 272 Hz), 115.5 (q, *J* = 29 Hz), 110.8 (CH), 61.8 (CH₃), 60.8 (CH₃), 56.0 (CH₃), 125.0 (q, CH₃, *J* = 4 Hz). IR (KBr, v/cm⁻¹):^[104b] 2978, 2944, 2840, 1598, 1576, 1503, 1468, 1405, 1337, 1305, 1247, 1203, 1139, 1110, 1056, 1014, 974, 927, 840, 737. Anal. Calcd for C₁₁H₁₃F₃O₃: C, 52.80; H, 5.24. Found: C, 52.7; H, 5.2.

1,2,4,5-Tetramethyl-3-(trifluoromethyl)benzene (16d). From 60 mg of durene (**15d**). Purification of the residue by column chromatography (eluant: hexane) afforded 55 mg of **16d** as a white solid, using 310 nm batch radiation source (61% yield, m.p. = 37-40°C, lit. = 35-36°C).^[146] Solar irradiation (6 hours × 3 days) gave 56 mg of **16d** (62% yield). Continuous flow irradiation of 40 mg of **15d** afforded 48 mg of **16d** (80% yield). ¹H NMR (CDCl₃)^[146] δ: 7.09 (s, 1H), 2.32 (q, 6H, *J* = 3 Hz), 2.26 (s, 6H). ¹³C NMR CDCl₃ δ: 135.2, 134.7 (CH), 133.6 (q, *J* = 2 Hz), 128.2 (q, *J* = 27 Hz), 126.5 (q, CF₃, *J* = 274 Hz), 20.7 (CH₃), 16.8 (q, CH₃, *J* = 5 Hz). IR (KBr, v/cm⁻¹): 2924, 1472, 1374, 1317, 1246, 1147, 1104, 1072, 1016, 888, 720. Anal. Calcd for C₁₁H₁₃F₃: C, 65.33; H, 6.48. Found: C, 65.5; H, 6.6.

1,3,5-Trimethyl-2-(trifluoromethyl)benzene (16e) and *1,3,5-trimethyl-2,4-bis(trifluoromethyl)benzene (16e-bis)*. From 63 μL (54 mg) of mesitylene (**15e**). Purification of the residue by reduced pressure distillation (25 torr, 80 °C) afforded 65 mg of a colorless liquid mixture containing 1,3,5-Trimethyl-2-(trifluoromethyl)benzene (**16e**, 51 mg, 60% yield) and 2,4-bis(trifluoromethyl)-1,3,5-trimethylbenzene (**16e-bis**, 14 mg, 12% yield). **16e**: ¹H NMR (from the mixture, CDCl₃)^[147] δ: 6.90 (s, 2H), 2.44 (q, 6H, *J* = 3 Hz), 2.30 (s, 3H). ¹³C NMR (from the mixture, CDCl₃)^[147] δ: 141.0, 137.4 (q, *J* = 2 Hz), 131.0 (CH), 126.4 (q, CF₃, *J* = 274 Hz), 124.9 (q, *J* = 28 Hz), 21.4 (q, CH₃, *J* = 4 Hz), 21.0 (CH₃). **16e-bis**: ¹H NMR (from the mixture, CDCl₃)^[148] δ: 6.99 (s, 1H), 2.55-2.45 (m, 9H). ¹³C NMR (from the mixture, CDCl₃)^[148] δ: 140.3,

138.9-138.8 (m), 134.6 (CH), 127.9 (q, $J = 28$ Hz), 125.6 (q, CF₃, $J = 274$ Hz), 22.2 (q, CH₃, $J = 5$ Hz), 17.58-17.36 (m, CH₃). IR (of the mixture, KBr, v/cm⁻¹): 2982, 2948, 1612, 1459, 1434, 1295, 1150, 1111, 1040, 853.

(*Trifluoromethyl*)benzene (**16f**). From 40 μ L (35 mg) of benzene (**15f**). After the basic work-up the dichloromethane solution containing **16f** was directly analyzed by gas chromatography and **3f** was quantified by comparison with an authentic commercial sample (dodecane was added to this solution as an internal standard). GC yield: 73% (48 mg estimated).

1-[2,4,6-trimethyl-3-(trifluoromethyl)phenyl]ethanone (**16g**). From 287 mg (0.72 mmol, 0.048 M) of **4j** and 75 μ L (73 mg) of 2',4',6'-trimethylacetophenone (**15g**). Irradiation lasted 42 hours until total consumption of **4j**, **5j** and **15g**. Column chromatography of the obtained crude residue (eluant: hexane/ethyl acetate 95:5) afforded 77 mg of **16g** as a colorless liquid in 74% yield. ¹H NMR (CDCl₃)^[104b] δ : 6.94 (s, 1H), 2.46 (s, 3H), 2.44 (q, 3H, $J = 3$ Hz), 2.32 (q, 3H, $J = 3$ Hz), 2.21 (s, 3H). ¹³C NMR (CDCl₃)^[104b] δ : 207.8, 142.7, 137.7 (q, $J = 2$ Hz), 135.4, 132.4 (CH), 132.1 (q, $J = 2$ Hz), 126.0 (q, $J = 28$ Hz), 125.9 (q, CF₃, $J = 274$ Hz), 32.6 (CH₃), 21.8 (q, CH₃, $J = 5$ Hz), 19.1 (CH₃), 17.5 (q, CH₃, $J = 4$ Hz). IR (KBr, v/cm⁻¹):^[104b] 2929, 2856, 1702, 1599, 1427, 1356, 1301, 1254, 1203, 1151, 1113, 1070, 958, 871. Anal. Calcd for C₁₂H₁₃F₃O: C, 62.60; H, 5.69. Found: C, 62.8; H, 5.5.

3,4-Ethylenedioxy-2,5-bis(trifluoromethyl)thiophene (**16h-bis**). From 48 μ L (64 mg) of 3,4-ethylenedioxythiophene (**15h**). Purification of the residue (eluant: hexane/ethyl acetate 95:5) afforded 74 mg of **16h-bis** as a colorless liquid in 59% yield. ¹H NMR (CDCl₃) δ : 4.36 (s, 4H). ¹³C NMR CDCl₃ δ : 141.6-141.4 (m), 121.6 (q, CF₃, $J = 268$ Hz), 106.9 (q, $J = 40$ Hz), 64.8 (CH₂). IR (KBr, v/cm⁻¹): 2952, 2891, 1607, 1536, 1462, 1378, 1314, 1246, 1142, 1088, 1053, 1016, 950, 924, 856. Anal. Calcd for C₈H₄F₆O₂S: C, 34.54; H, 1.45. Found: C, 34.5; H, 1.6.

3,4-Ethylenedioxy-2-(trifluoromethyl)thiophene (16h) and *3,4-ethylenedioxy-2,5-bis(trifluoromethyl)thiophene (16h-bis)*. From 90 mg (0.22 mmol, 0.015 M) of **4j** and 48 μ L (64 mg) of 3,4-ethylenedioxythiophene (**15h**). Irradiation lasted 6 hours until total consumption of **4j** and **5j**. Purification of the crude residue (eluant: hexane/ethyl acetate 95:5) afforded 47 mg of a colorless liquid mixture of 3,4-ethylenedioxy-2-(trifluoromethyl)thiophene (**16h**, 25 mg, 26% yield) and 3,4-ethylenedioxy-2,5-bis(trifluoromethyl)thiophene (**16h-bis**, 22 mg, 18% yield). **16h**: ^1H NMR (from the mixture, CDCl_3)^[149] δ : 6.49 (s, 1H), 4.31-4.29 (m, 2H), 4.24-4.21 (m, 2H). ^{13}C NMR (from the mixture, CDCl_3)^[149] δ : 142.1 (q, $J = 4$ Hz), 141.5, 122.4 (q, CF_3 , $J = 266$ Hz), 104.5 (q, $J = 39$ Hz), 102.2 (CH), 65.1 (CH_2), 64.4 (CH_2). IR (of the mixture, KBr, v/cm^{-1}): 2995, 2941, 2885, 1598, 1536, 1506, 1458, 1445, 1375, 1314, 1177, 1151, 1119, 1088, 1073, 1010, 940, 910, 857. GC-MS of the mixture revealed two peaks, one belonging to **16h** and one to **16h-bis**. **16h** (m/z): 210 (M^+ , 88), 195 (20), 181 (7), 164 (45), 113 (17), 85 (12), 69 (27), 45 (36), 28 (100). **16h-bis** (m/z): 278 (M^+ , 100), 259 (26), 232 (49), 212 (16), 184 (22), 137 (31), 122 (28), 113 (73), 94 (33), 69 (20).

2,4,6-Trimethyl-3-(trifluoromethyl)pyridine (16i). From 59 μ L (54 mg) of 2,4,6-trimethylpyridine (**15i**). In the present case the photolyzed solution was washed using saturated aqueous Na_2CO_3 (3×10 mL) instead of NaHCO_3 . Purification of the residue by column chromatography (eluant: hexane/ethyl acetate 9:1) afforded 50 mg of **16i** as a colorless liquid in 59% yield. ^1H NMR (CDCl_3) δ : 6.88 (s, 1H), 2.87 (q, 3H, $J = 3$ Hz), 2.50 (s, 3H), 2.44 (q, 3H, $J = 3$ Hz). ^{13}C NMR (CDCl_3) δ : 159.8, 156.4, 146.7, 125.5 (q, CF_3 , $J = 273$ Hz), 124.1 (CH), 120.7 (q, $J = 30$ Hz), 24.3 (q, CH_3 , $J = 4$ Hz), 24.0 (CH_3), 20.8 (q, CH_3 , $J = 4$ Hz). IR (KBr, v/cm^{-1}): 2928, 2856, 1598, 1558, 1424, 1390, 1296, 1152, 1116, 1038, 862, 755. Anal. Calcd for $\text{C}_9\text{H}_{10}\text{F}_3\text{N}$: C, 57.14; H, 5.33; N, 7.40. Found: C, 57.0; H, 5.4; N, 7.3.

2,6-Dimethoxy-3-(trifluoromethyl)pyridine (16j). From 59 μL (62 mg) of 2,6-dimethoxypyridine (**15j**). In the present case the photolyzed solution was washed using saturated aqueous Na_2CO_3 (3×10 mL) instead of NaHCO_3 . Purification of the residue by column chromatography (eluant: hexane/ethyl acetate 95:5) afforded 59 mg of **16j** as a colorless liquid in 64% yield (using 310 nm batch radiation source). Solar irradiation (6 hours \times 3 days) gave 56 mg of **16j** (60% yield). Continuous flow irradiation of 40 μL (42 mg) of **15j** afforded 51 mg of **16j** (82% yield). ^1H NMR (CDCl_3)^[104b] δ : 7.72 (d, 1H, $J = 9$ Hz), 6.32 (d, 1H, $J = 9$ Hz), 4.02 (s, 3H), 3.96 (s, 3H). ^{13}C NMR (CDCl_3)^[104b] δ : 165.3, 160.6, 138.9 (q, CH, $J = 4$ Hz), 123.9 (q, CF_3 , $J = 268$ Hz), 104.5 (q, $J = 34$ Hz), 100.9 (CH), 54.0 (CH_3), 53.9 (CH_3). IR (KBr, v/cm^{-1}): 2991, 2956, 1606, 1590, 1492, 1473, 1396, 1314, 1247, 1127, 1112, 1059, 1027, 817, 781, 678. Anal. Calcd for $\text{C}_8\text{H}_8\text{F}_3\text{NO}_2$: C, 46.38; H, 3.89; N, 6.76. Found: C, 46.3; H, 3.7; N, 6.8.

2-Methyl-1-(trifluoromethyl)-1H-imidazole (16k). From 37 mg of 2-methylimidazole (**15k**). In the present case the photolyzed solution was washed using saturated aqueous Na_2CO_3 (3×10 mL) instead of NaHCO_3 . Purification of the residue by reduced pressure distillation (25 torr, 85 $^\circ\text{C}$) afforded 47 mg of **16k** as a colorless liquid in 69% yield. ^1H NMR (CDCl_3) δ : 7.28 (d, 1H, $J = 3$ Hz), 7.04 (d, 1H, $J = 3$ Hz), 2.64 (s, 3H). ^{13}C NMR CDCl_3) δ : 146.1, 129.7 (CH), 120.4 (CH), 119.3 (q, CF_3 , $J = 321$ Hz), 15.2 (CH_3). IR (KBr, v/cm^{-1}): 3165, 3132, 1565, 1517, 1442, 1425, 1393, 1346, 1233, 1185, 1147, 1129, 1041, 982, 912, 736, 696, 652, 629. Anal. Calcd for $\text{C}_5\text{H}_5\text{F}_3\text{N}_2$: C, 40.01; H, 3.36; N, 18.66. Found: C, 40.0; H, 3.3; N, 18.8.

1,3,7-Trimethyl-8-(trifluoromethyl)-3,7-dihydro-1H-purine-2,6-dione (16l). From 87 mg of caffeine (**15l**). In the present case the photolyzed solution was washed using 10% aqueous NaOH (3×10 mL) instead of NaHCO_3 . Purification of the residue by column chromatography (eluant: hexane/ethyl acetate 9:1) afforded 68 mg of **16l** as a white solid, using 310 nm batch radiation source (58% yield, m.p. = 126-128 $^\circ\text{C}$, lit. = 131-133 $^\circ\text{C}$).^[150] Solar irradiation (6 hours \times 4 days)

gave 67 mg of **16l** (57% yield). Continuous flow irradiation of 58 mg of **15l** afforded 59 mg of **16l** (75% yield). ^1H NMR (CDCl_3)^[102c] δ : 4.16 (q, 3H, $J = 1$ Hz), 3.59 (s, 3H), 3.42 (s, 3H). ^{13}C NMR (CDCl_3)^[102c] δ : 155.6, 151.5, 146.7, 139.1 (q, $J = 40$ Hz), 118.3 (q, CF_3 , $J = 269$ Hz), 109.8, 33.3 (q, CH_3 , $J = 2$ Hz), 30.0 (CH_3), 28.3 (CH_3). IR (KBr, v/cm^{-1}): 1710, 1667, 1550, 1337, 1290, 1247, 1179, 1147, 1098, 973, 745, 606. Anal. Calcd for $\text{C}_9\text{H}_9\text{F}_3\text{N}_4\text{O}_2$: C, 41.23; H, 3.46; N, 21.37. Found: C, 41.1; H, 3.3; N, 21.4.

1,3-Dimethyl-8-(trifluoromethyl)-3,7-dihydro-1H-purine-2,6-dione (16m). From 81 mg of theophylline (**15m**). In the present case the irradiation was performed in an acetonitrile/water 5:1 mixture and the solvent was removed from the photolyzed solution by reduced pressure directly, without work-up. Purification of the residue by column chromatography (eluant: hexane/ethyl acetate 8:2) afforded 75 mg of **16m** as a white solid (67% yield, m.p. = 270-273°C, lit. = 266-268°C).^[151] ^1H NMR ($\text{DMSO}-d_6$)^[152] δ : 3.43 (s, 3H), 3.24 (s, 3H), 2.92 (brs, 1H). ^{13}C NMR ($\text{DMSO}-d_6$)^[152] δ : 154.6, 151.0, 146.8, 137.3 (q, $J = 40$ Hz), 118.2 (q, CF_3 , $J = 268$ Hz), 109.2, 29.9 (CH_3), 27.9 (CH_3). IR (KBr, v/cm^{-1}).^[151] 3094, 1729, 1713, 1642, 1605, 1559, 1417, 1385, 1362, 1268, 1191, 1152, 1058, 984, 745. Anal. Calcd for $\text{C}_8\text{H}_7\text{F}_3\text{N}_4\text{O}_2$: C, 38.72; H, 2.84; N, 22.58. Found: C, 38.7; H, 2.9; N, 22.

9 Acknowledgements

First of all I would like to thank Fondazione Cariplo for financial support of this research project and Prof. Maurizio Fagnoni for his careful supervision during my whole PhD internship. I would like to give special thanks also to the people who acted as co-supervisors in my PhD: Prof. Petr Klán, Dr. Stefano Protti and Dr. Peter Štacko.

Grateful acknowledgments goes as well to the people which actively collaborated in various ways in the project: Dr. Gioia Della Giustina, Prof. Giovanna Brusatin, Dr. Daniele Merli, Prof. Daniele Dondi, Dr. Luca Mezi, Dr. Sarah Bollanti, Dr. Francesco Flora, Dr. Amalia Torre, Dr. Annamaria Gerardino, Dr. Luca Businaro, Dr. Václav Havel, Dr. Mirza Arfan Yawer, Lucie Ludvíková, Michal Babiak and Prof. Vladimír Šindelář.

Lastly I would like to thank all the people whose help was precious to complete my PhD: Prof. Mariella Mella, Dr. Lukáš Maier, Luboš Jílek, Dr. Simone Lazzaroni, Dr. Andrea Gandini, Dr. Francesco Chiesa, Dr. Mattia Fredditori, Dr. Barbara Mannucci, Prof. Angelo Albini, Prof. Elisa Fasani, Dr. Davide Ravelli and Prof. Patrick Hoggard.

In conclusion I would like to heartily say “thanks” to all the people which believed in my idea to pursue this challenge and sincerely supported me in this long journey. Thank you.

10 References

- [1] a) H. Yu, J. Li, D. Wu, Z. Qiu, Y. Zhang, *Chem. Soc. Rev.* **2010**, *39*, 464-473; b) H.-M. Lee, D. R. Larson, D. S. Lawrence, *ACS Chem. Biol.* **2009**, *4*, 409-427; c) G. C. R. Ellis-Davies, *Nat. Methods* **2007**, *4*, 619-628; d) G. Mayer, A. Heckel, *Angew. Chem. Int. Ed.* **2006**, *45*, 4900-4921.
- [2] a) H. Ito, *Adv. Polym. Sci.* **2005**, *172*, 37-245; b) M. Shirai, M. Tsunooka, *Prog. Polym. Sci.* **1996**, *21*, 1-45; c) J.M. Freché, *Pure Appl. Chem.* **1992**, *64*, 1239-1248; d) E. Reichmanis, F. M. Houlihan, O. Nalamasu, T. X. Neenan, *Chem. Mater.* **1991**, *3*, 394-407.
- [3] For a recent example see: a) M. Jin, H. Honq, J. Xie, J.-P. Malval, A. Spangenberg, O. Soppera, D. Wan, H. Pu, D.-L. Versace, T. Leclerc, P. Baldeck, O. Poizat, S. Knopf, *Polym. Chem.* **2014**, *5*, 4747-4755. For an exhaustive review see: b) J. V. Crivello, *J. Polym. Sci. Part A: Polym. Chem.* **1999**, *37*, 4241-4254.
- [4] a) J. L. Dektar, N. P. Hacker, *J. Org. Chem.* **1990**, *55*, 639-647; b) R. J. Devoe, M. R. V. Sahyun, N. Serpone, D. K. Sharma, *Can. J. Chem.* **1987**, *65*, 2342-2349.
- [5] J. L. Dektar, N. P. Hacker, *J. Chem. Soc. Chem. Commun.* **1987**, 1591-1592.
- [6] a) G. Yilmaz, Y. Yagci, *J. Photopolym. Sci. Technol.* **2016**, *29*, 91-98; b) M. Sangermano, N. Razza, J. V. Crivello, *Macromol. Mater. Eng.* **2014**, *299*, 775-793; c) M. Sangermano, *Pure Appl. Chem.* **2012**, *84*, 2089-2101;
- [7] For two recent reviews see: a) T.-Y. Kwon, R. Bagheri, Y. K. Kim, K.-H. Kim, M. F. Burrow, *J. Investig. Clin. Dent.* **2012**, *3*, 3-16; b) K. Ikemura, T. Endo, *Dent. Mater. J.* **2010**, *29*, 481-501.

- [8] J. Zhang, P. Xiao, C. Dietlin, D. Campolo, F. Dumur, D. Gigmes, F. Morlet-Savary, J.-P. Fouassier, J. Lalevée, *Macromol. Chem. Phys.* **2016**, *217*, 1214-1227.
- [9] A. Vitale, M. Sangermano, R. Bongiovanni, P. Burtscher, N. Moszner, *Materials* **2014**, *7*, 554-562.
- [10] a) K. Yamanishi, E. Sato, A. Matsumoto, *J. Photopolym. Sci. Technol.* **2013**, *26*, 239-244; b) J. V. Crivello, *J. Polym. Sci. Pol. Chem.* **2009**, *47*, 866-875.
- [11] a) A. Al Mousawi, C. Poriel, F. Dumur, J. Toufaily, T. Hamieh, J. P. Fouassier, J. Lalevée, *Macromolecules* **2017**, *50*, 746-753; b) A. Al Mousawi, F. Dumur, P. Garra, J. Toufaily, T. Hamieh, F. Goubard, T.-T. Bui, B. Graff, D. Gigmes, J. P. Fouassier, J. Lalevée, *J. Polym. Sci. Part A: Polym. Chem.* **2017**, *55*, 1189-1199; c) J. Zhang, F. Dumur, P. Xiao, B. Graff, D. Bardelang, D. Gigmes, J. P. Fouassier, J. Lalevée, *Macromolecules* **2015**, *48*, 2054-2063.
- [12] a) W. Li, P. Feng, Y. Zou, B. Hai, *J. Appl. Polym. Sci.* **2014**, 41019; b) M. Ikbāl, R. Banerjee, S. Atta, D. Dhara, A. Anoop, N. D. P. Singh, *J. Org. Chem.* **2012**, *77*, 10557-10567; c) E. Stratakis, A. Mateescu, M. Barberoglou, M. Vamvakaki, C. Fotakis, S. H. Anastasiadis, *Chem. Commun.* **2010**, *46*, 4136-4138.
- [13] a) J. Raeburn, T. O. McDonald, D. J. Adams, *Chem. Commun.* **2012**, *48*, 9355-9357; b) V. Javvaji, A. G. Baradwaj, G. F. Payne, S. R. Raghavan, *Langmuir* **2011**, *27*, 12591-12596.
- [14] a) C. Acikgoz, M. A. Hempenius, J. Huskens, G. J. Vancso, *Eur. Polym. J.* **2011**, *47*, 2033-2052; b) M. G. Ivan, J. C. Scaiano, in *Photochemistry and Photophysics of Polymer Materials*, ed. N. S. Allen, John Wiley & Sons, Inc., Hoboken, NJ, USA, **2010**, 479-507; c) S.-Y. Moon, J.-M. Kim, *J. Photochem. Photobiol. C* **2007**, *8*, 157-173.
- [15] H. Ito, *J. Polym. Sci. Part A: Polym. Chem.* **2003**, *41*, 3863-3870.

- [16] K. L. Covert, D. J. Russell, *J. Appl. Polym. Sci.* **1993**, *49*, 657–671.
- [17] a) K. Sander, T. Gendron, E. Yiannaki, K. Cybulska, T. L. Kalber, M. F. Lythgoe, E. Årstad, *Sci. Rep.* **2015**, *5*, 9941; b) S. K. Sundalam, D. R. Stuart, *J. Org. Chem.* **2015**, *80*, 6456-6466; c) M. Bielawski, D. Aili, B. Olofsson, *J. Org. Chem.* **2008**, *73*, 4602-4607; d) M. Zhu, N. Jalalian, B. Olofsson, *Synlett* **2008**, 592-596; e) S. R. Akhtar, J. V. Crivello, J. L. Lee, M. L. Schmitt, *Chem. Mater.* **1990**, *2*, 732-737.
- [18] For two interesting examples see: a) K. C. Nicolaou, C. W. Hummel, M. Nakada, K. Shibayama, E. N. Pitsinos, H. Saimoto, Y. Mizuno, K. U. Baldenius, A. L. Smith, *J. Am. Chem. Soc.* **1993**, *115*, 7625-7635; b) Y. Gareau, R. Zamboni, A. W. Wong, *J. Org. Chem.* **1993**, *58*, 1582-1585.
- [19] For reviews treating 2-nitrobenzyl photoremovable protecting group see: a) P. Klán, T. Šolomek, C. G. Bochet, A. Blanc, R. Givens, M. Rubina, V. Popik, A. Kostikov, J. Wirz, *Chem. Rev.* **2013**, *113*, 119-191; b) A. P. Pelliccioli, J. Wirz, *Photochem. Photobiol. Sci.* **2002**, *1*, 441-458.
- [20] a) F. M. Houlihan, O. Nalamasu, J. M. Kometani, E. Reichmanis, *J. Imaging Sci. Technol.* **1997**, *41*, 35-40; b) K. E. Uhrich, E. Reichmanis, F. A. Baiocchi, *Chem. Mater.* **1994**, *6*, 295-301; c) F. M. Houlihan, T. X. Neenan, E. Reichmanis, J. M. Kometani, T. Chin, *Chem. Mater.* **1991**, *3*, 462-471; d) T. X. Neenan, F. M. Houlihan, T. Chin, E. Reichmanis, J. M. Kometani, *J. Photopolym. Sci. Technol.* **1991**, *4*, 341-355; e) T. X. Neenan, F. M. Houlihan, E. Reichmanis, J. M. Kometani, B. J. Bachman, L. F. Thompson, *Macromolecules* **1990**, *23*, 145-150; f) F. M. Houlihan, T. X. Neenan, E. Reichmanis, J. M. Kometani, L. F. Thompson, T. Chin, O. Nalamasu, *J. Photopolym. Sci. Technol.* **1990**, *3*, 259-273; g) F. M. Houlihan, A. Shugard, R. Gooden, E. Reichmanis, *Macromolecules* **1988**, *21*, 2001-2006.

- [21] For the mechanism of photorelease from 2-nitrobenzyl protecting group see: Y. V. Il'ichev, J. Wirz, *J. Phys. Chem. A* **2000**, *104*, 7856-7870.
- [22] M. Shirai, M. Tsunooka, *Bull. Chem. Soc. Jpn.* **1998**, *71*, 2483-2507.
- [23] For recent examples see: a) H. Okamura, T. Ashida, S. Kodama, M. Shirai, *Macromol. Symp.* **2015**, *349*, 29-33; b) M. Iqbal, R. Banerjee, S. Barman, S. Atta, D. Dhara, N. D. P. Singh, *J. Mater. Chem. C* **2014**, *2*, 4622-4630; c) S. Kodama, H. Okamura, M. Shirai, *Chem. Lett.* **2012**, *41*, 625-627.
- [24] For some smart examples see: c) Y. Zhang, R. B. Sharma, R. Stuck, D. Greene, R. Gupta, J. D. Fogle, *US Pat.* **2014**, 9383644 B2; b) L. Steidl, S. J. Jhaveri, R. Ayothi, J. Sha, J. D. McMullen, S. Y. C. Ng, W. R. Zipfel, R. Zentel, C. K. Ober, *J. Mater. Chem.* **2009**, *19*, 505-513; c) M. Shirai, H. Okamura, *Prog. Org. Coat.* **2009**, *64*, 175-181.
- [25] For the mechanisms of acids photogeneration from iminosulfonates see: a) P. A. Arnold, L. E. Fratesi, E. Bejan, J. Cameron, G. Pohlers, H. Liu, J. C. Scaiano, *Photochem. Photobiol. Sci.* **2004**, *3*, 864-869; b) M. Shirai, H. Kinoshita, M. Tsunooka, *Eur. Polym. J.* **1992**, *28*, 379-385.
- [26] For the mechanisms of acids photogeneration from imidosulfonates see: a) J.-P. Malval, S. Suzuki, F. Morlet-Savary, X. Allonas, J.-P. Fouassier, S. Takahara, T. Yamaoka, *J. Phys. Chem. A* **2008**, *112*, 3879-3885; b) J.-P. Malval, F. Morlet-Savary, X. Allonas, J.-P. Fouassier, S. Suzuki, S. Takahara, T. Yamaoka, *Chem. Phys. Lett.* **2007**, *443*, 323-327; c) F. Ortica, J. C. Scaiano, G. Pohlers, J. F. Cameron, A. Zampini, *Chem. Mater.* **2000**, *12*, 414-420.
- [27] M. Terpolilli, D. Merli, S. Protti, V. Dichiarante, M. Fagnoni, A. Albin, *Photochem. Photobiol. Sci.* **2011**, *10*, 123-127.

- [28] a) F. Ortica, C. Coenjarts, J. C. Scaiano, H. Liu, G. Pohlers, J. F. Cameron, *Chem. Mater.* **2001**, *13*, 2297-2304; b) C. Coenjarts, F. Ortica, J. Cameron, G. Pohlers, A. Zampini, D. Desilets, H. Liu, J. C. Scaiano, *Chem. Mater.* **2001**, *13*, 2305-2312; c) R. Flyunt, O. Makogon, M. N. Schuchmann, K.-D. Asmus, C. von Sonntag, *J. Chem. Soc., Perkin Trans. 2* **2001**, 787-792.
- [29] G. G. Barclay, D. R. Medeiros, R. F. Sinta, *Chem. Mater.* **1995**, *7*, 1315-1324.
- [30] a) M. Ikbal, A. Jana, N. D. P. Singh, R. Banerjee, D. Dhara, *Tetrahedron* **2011**, *67*, 3733-3742; b) M. De Carolis, S. Protti, M. Fagnoni, A. Albini, *Angew. Chem. Int. Ed.* **2005**, *44*, 1232-1236.
- [31] a) G. Brusatin, G. Della Giustina, *J Sol-Gel Sci. Technol.* **2011**, *60*, 299-314; b) G. Della Giustina, G. Brusatin, M. Guglielmi, C. Palazzesi, E. Orsini, P. Proposito, *Solid State Sci.* **2010**, *12*, 1890-1893; c) G. Della Giustina, G. Brusatin, M. Guglielmi, F. Romanato, *Mater. Sci. Eng. C* **2007**, *27*, 1382-1385.
- [32] a) L. L. Hench, J. K. West, *Chem. Rev.* **1990**, *90*, 33-72; b) C. Sanchez, B. Lebeau, F. Ribot, M. In, *J. Sol-Gel Sci. Techn.* **2000**, *19*, 31-38.
- [33] E. Torti, G. Della Giustina, S. Protti, D. Merli, G. Brusatin, M. Fagnoni, *RSC Adv.* **2015**, *5*, 33239-33248.
- [34] a) S. Crespi, D. Ravelli, S. Protti, A. Albini, M. Fagnoni, *Chem. Eur. J.* **2014**, *20*, 17572-17578; b) E. Abitelli, S. Protti, M. Fagnoni, A. Albini, *J. Org. Chem.* **2012**, *77*, 3501-3507.
- [35] Z.-Y. Tang, Q.-S. Hu, *J. Am. Chem. Soc.* **2004**, *126*, 3058-3059.
- [36] B. Alonso, D. Massiot, F. Babonneau, G. Brusatin, G. Della Giustina, P. Innocenzi, T. Kidchob, *Chem. Mater.* **2005**, *17*, 3172-3180.
- [37] J. L. Stratenus, E. Havinga, *Recl. Trav. Chim. Pays-Bas* **1966**, *85*, 434-436.

- [38] a) D. Shukla, N. P. Schepp, N. Mathivan, L. J. Johnston, *Can J. Chem.* **1997**, *75*, 1820-1829; b) L. J. Johnston, N. Mathivan, F. Negri, W. Siebrand, *Can. J. Chem.* **1993**, *71*, 1655-1662.
- [39] See for example: a) Y. Kageyama, R. Ohshima, K. Sakurama, Y. Fujiwara, Y. Tanimoto, Y. Yamada, S. Aoki, *Chem. Pharm. Bull.* **2009**, *57*, 1257-1266; A. K. Zarkadis, V. Georgakilas, G. P. Perdikomatis, A. Trifonov, G. G. Gurzadyan, S. Skoulika, M. G. Siskosa, *Photochem. Photobiol. Sci.* **2005**, *4*, 469-480; c) I. F. Molokov, Y. P. Tsentalovich, A. V. Yurkovskaya, R. Z. Sagdeev, *J. Photochem. Photobiol. A* **1997**, *110*, 159-165.
- [40] M. Takezaki, N. Hirota, M. Terazima, *J. Phys. Chem. A* **1997**, *101*, 3443-3448.
- [41] See for instance: a) M. M. Miranda, F. Galindo in *Photochemistry of Organic Molecules in Isotropic and Anisotropic Media*, ed. V. Ramamurthy, K. S. Schanze, Marcel Dekker Inc., New York-Basel, **2003**, 43-132; b) G. M. Coppinger, E. R. Bell, *J. Phys. Chem.* **1966**, *70*, 3479-3489.
- [42] M. Gohdo, T. Takamasu, M. Wakasa, *Phys. Chem. Chem. Phys.* **2011**, *13*, 755-761.
- [43] a) M. C. Jiménez, M. A. Miranda, J. C. Scaiano, R. Tormosa, *Chem. Commun.* **1997**, 1487-1488; b) C. E. Kalmus, D. M. Hercules, *J. Am. Chem. Soc.* **1974**, *96*, 449-456.
- [44] C. X. Xue, R. S. Zhang, H. X. Liu, X. J. Yao, M. C. Liu, Z. D. Hu, B. T. Fan, *J. Chem. Inf. Comput. Sci.* **2004**, *44*, 669-677.
- [45] L. Brigo, E. Zanchetta, G. Della Giustina, G. Brusatin, *Proc. SPIE* **2014**, *9161*, 91610B.
- [46] L. Schlegel, T. Ueno, H. Shiraishi, N. Hayashi, T. Iwayanagi, *Chem. Mater.* **1990**, *2*, 299-305.
- [47] K. Tanaka, W. Ohashi, T. Okada, Y. Chujo, *Tetrahedron Lett.* **2014**, *55*, 1635-1639.
- [48] E. Torti, S. Protti, D. Merli, D. Dondi, M. Fagnoni, *Chem. Eur. J.* **2016**, *22*, 16998-17005.

- [49] P. Cowley, A. Wise, *PCT Int. Appl.* **2016**, WO 2016071283 A1 20160512.
- [50] N. Liu, S. Zhu, X. Zhang, X. Yin, G. Dong, J. Yao, Z. Miao, W. Zhang, X. Zhang, C. Sheng, *Chem. Commun.* **2016**, 52, 3340-3343.
- [51] K. Ohno, T. Okita, S. Komori, T. Horitani, K. Izakura, *PCT Int. Appl.* **2016**, WO 2016056565 A1 20160414.
- [52] K. Kawamura, F. Sasaki *J. Photopolym. Sci. Technol.* **2001**, 14, 265–272.
- [53] E. Torti, S. Protti, M. Fagnoni, G. Della Giustina, *ChemistrySelect* **2017**, 2, 3633-3636.
- [54] R. A. Levine, W. B. Person, *J. Phys. Chem.* **1977**, 81, 1118-1119.
- [55] Transient absorption spectra of methanesulfonyl and *para*-toluenesulfonyl radical have been described and compared in C. Chatgililoglu, D. Griller, M. Guerra, *J. Phys. Chem.* **1987**, 91, 3747-3750. For *para*-toluenesulfonyl radical see also Ref. 29a,b.
- [56] a) R. Flyunt, O. Makogon, M. N. Schuchmann, K. D. Asmus, C.von Sonntag, *J. Chem. Soc., Perkin Trans. 2*, **2001**, 787-792; b) J. E. Bennett, G. Brunton, B. C. Gilbert, P. E. Whittall, *J. Chem. Soc., Perkin Trans. 2*, **1988**, 1359-1364.
- [57] F. Saito S. Tobita, H. Shizuka *J. Photoch. Photobiol. A* **1997**, 106, 119-126.
- [58] Assignments were carried out by comparison with the triplet states of acetophenone derivatives, see: H. Lutz, E. Breheret, L. Lindqvist, *J. Phys. Chem.* **1973**, 77, 1758-1762.
- [59] See for reviews: a) D. Bellus, *Adv. Photochem.* **1971**, 8, 109-159; b) Y. Kanaoka, T. Tsuji, K. Itoh, , K. Koyamai, *Chem. Pharm. Bull.* **1973**, 21, 453-454.
- [60] a) K. K. Park, J. J. Lee, J. Ryu *Tetrahedron* **2003**, 59, 7651-7659; b) H. G. Henning, M. Amin, P. J. Wessig, *Prakt. Chem.* **1993**, 335, 42-46; c) K. Pitchumani, M. C. D. Manickam, C. Srinivasan, *Tetrahedron Lett.* **1991**, 32, 2975-2978; d) D. Hellwinkel, R. Lenz, *Chem. Ber.* **1985**, 118, 66-85; e) M. Z. A. Badr, M. M. Aly, A. M. Fahmy, *J. Org. Chem.* **1981**, 46, 4784-4787; f) B. Weiss, H. Durr, H. J. Haas, *Angew. Chem. Int. Ed.*

- Engl.* **1980**, *19*, 648-650; g) H. Nozaki, T. Okada, R. Noyori, M. Kawanisi, *Tetrahedron* **1966**, *22*, 2177-2180.
- [61] M. Fiorentino, L. Testaferri, M. Tiecco, L. Troisi, *J. Chem. Soc. Perkin Trans. 2*, **1977**, 1679-1683.
- [62] M. Fiorentino, L. Testaferri, M. Tiecco, L. Troisi, *J. Chem. Soc. Chem. Commun.* **1976**, 329-330.
- [63] a) F. Bertrand, F. Leguyader, L. Liguori, G. Ouvry, B. Quiclet-Sire, S. Seguin, S. Z. Zard, *C. R. Acad. Sci. II C* **2001**, *4*, 547-555; b) D. Gonbeau, M. F. Guimon, S. Duplantier, J. Ollivier, G. Pfister-Guillouzo, *Chem. Phys.* **1989**, *135*, 85-89.
- [64] E. Rosa, A. Guerrero, M. P. Bosch, L. Julia, *L. Magn. Reson. Chem.* **2010**, *48*, 198–204.
- [65] G. Moore, *Electronics* **1965**, *38*, 114–117.
- [66] a) C. Wagner, N. Harned, *Nat. Photon.* **2010**, *4*, 24-26; b) G. Tallents, E. Wagenaars, G. Pert, *Nat. Photon.* **2010**, *4*, 809-811; c) J. Roberts, T. Bacuita, R. L. Bristol, H. Cao, M. Chandhok, S. H. Lee, M. Leeson, T. Liang, E. Panning, B. J. Rice, U. Shah, M. Shell, W. Yueh, G. Zhang, *Microelectron. Eng.* **2006**, *83*, 672-675; d) K. Kemp, S. Wurm, *C. R. Phys.* **2006**, *7*, 875-886; e) P. J. Silverman, *J. Microlith. Microfab. Microsyst.* **2005**, *4*, 011006.
- [67] a) N. Mojarad, J. Gobrecht, Y. Ekinici, *Sci. Rep.* **2015**, *5*, 9235; b) P. D. Ashby, D. L. Olynick, D. F. Ogletree, P. P. Naulleau, *Adv. Mater.* **2015**, *27*, 5813–5819; c) P.P. Naulleau, C. N. Anderson, L.-M. Baclea-an, P. Denham, S. George, K. A. Goldberg, G. Jones, B. McClinton, R. Miyakawa, S. Rekawa, N. Smith, *Proc. SPIE* **2011**, 7972, 797202; d) I. Aratani, S. Matsunaga, T. Kajiyashiki, T. Watanabe, H. Kinoshita, *Proc. SPIE* **2009**, 7273, 7273-1Z; e) D. Bratton, D. Yang, J. Dai, C. K. Ober, *Polym. Adv.*

- Technol.* **2006**, *17*, 94–103; f) S. Irie, S. Shirayone, S. Mori, E. Yano, S. Okazaki, T. Watanabe, H. Kinoshita, *J. Photopolym. Sci. Technol.* **2000**, *13*, 385-389.
- [68] Few examples: a) J. Passarelli, M. Sortland, R. Del Re, B. Cardineau, C. Sarma, D. A. Freedman, R. L. Brainard, *J. Photopolym. Sci. Technol.* **2014**, *27*, 655-661; b) M. Azam Ali, K. E. Gonsalves, V. Golovkina, F. Cerrina, *Microelectron. Eng.* **2003**, *65*, 454-462.
- [69] R. Sulc, J. M. Blackwell, T. R. Younkin, E. S. Putna, K. Esswein, A. G. Di Pasquale, R. Callahan, H. Tsubaki, T. Tsuchihashi, *Proc. SPIE* **2009**, *7273*, 72733R.
- [70] a) R. Fallica, J. K. Stowers, A. Grenville, A. Frommhold, A. P. G. Robinson, Y. Ekinici, *J. Micro/Nanolith. MEMS MOEMS* **2016**, *15*, 033506; b) B. L. Henke, E. M. Gullikson, J. C. Davis, *Atom. Data Nucl. Data* **1993**, *54*, 181-342.
- [71] J. Torok, R. Del Re, H. Herbol, S. Das, I. Bocharova, A. Paolucci, L. E. Ocola, C. Ventrice Jr., E. Lifshin, G. Denbeaux, R. L. Brainard, *J. Photopolym. Sci. Tec.* **2013**, *26*, 625-634.
- [72] Q.-Y. Chen, Z.-T. Li, *J. Org. Chem.* **1993**, *58*, 2599-2604.
- [73] a) T. Watanabe, T. Harada, *J. Photopolym. Sci. Technol.* **2016**, *29*, 737-744; b) T. Asakura, H. Yamato, Y. Nishimae, K. Okada, M. Ohwa, *J. Photopolym. Sci. Technol.* **2009**, *22*, 89-95.
- [74] A. L. Casado, P. Espinet, A. M. Gallego, *J. Am. Chem. Soc.* **2000**, *122*, 11771-11782.
- [75] J. Thackeray, J. Cameron, V. Jain, P. LaBeaume, S. Coley, O. Ongayi, M. Wagner, A. Rachford, J. Biafore, *J. Photopolym. Sci. Technol.* **2013**, *26*, 605-610.
- [76] J. Macan, H. Ivankovic, M. Ivankovic, H. J. Mencer, *J. Appl. Polym. Sci.* **2004**, *92*, 498-505.
- [77] D. Attwood, in *Soft X-Rays and Extreme Ultraviolet Radiation*, Cambridge University Press, Cambridge, UK, **1999**, 395-416.

- [78] L. Mezi, S. Bollanti, L. Businaro, P. Di Lazzaro, A. Gerardino, F. Flora, D. Murra, A. Torre, "The ENEA discharge produced plasma EUV source: Description and applications" in *18th Italian National Conference on Photonic Technologies (Fotonica 2016)*, Rome, **2016**, doi: 10.1049/cp.2016.0894.
- [79] F. R. Powell, T. A. Johnson, *Proc. SPIE* **2001**, 4343, 585-589.
- [80] P. Di Lazzaro, S. Bollanti, F. Flora, L. Mezi, D. Murra, A. Torre, *Appl. Surf. Sci* **2013**, 272, 13-18.
- [81] G. Baldacchini, F. Bonfigli, F. Flora, R.M. Montereali, D. Murra, E. Nichelatti, A. Faenov, T. Pikuz, *Appl. Phys. Lett.* **2002**, 80, 4810-4812.
- [82] R. S. Givens, M. Rubina, J. Wirz, *Photochem. Photobiol. Sci.* **2012**, 11, 472-488.
- [83] E. Torti, V. Havel, M. A. Yawer, L. Ludvíková, M. Babiak, P. Klán, V. Sindelar, *Chem. Eur. J.* **2017**, 23, 16768-16772.
- [84] D. A. House, *Chem. Rev.* **1962**, 62, 185-203.
- [85] For recent examples see: a) Y.-T. Lin, C. Liang, C.-W. Yu, *Ind. Eng. Chem. Res.* **2016**, 55, 2302-2308; b) S. Hernández, J. K. Papp, D. Bhattacharyya, *Ind. Eng. Chem. Res.* **2014**, 53, 1130-1142.
- [86] For a recent example see: F. Pan, X. Zhong, D. Xia, X. Yin, F. Li, D. Zhao, H. Ji, W. Liu, *Sci. Rep.* **2017**, 7, 44626.
- [87] W. V. Smith, *J. Am. Chem. Soc.*, 1948, **70**, 3695-3702.
- [88] a) V. Havel, M. Babiak, V. Sindelar, *Chem. Eur. J.* **2017**, 23, 8963-8968; b) M. Singh, E. Solel, E. Keinan, O. Reany, *Chem. Eur. J.* **2016**, 22, 8848-8854; c) M. A. Yawer, V. Havel, V. Sindelar, *Angew. Chem. Int. Ed.* **2015**, 54, 276-279; d) M. Singh, E. Solel, E. Keinan, O. Reany, *Chem. Eur. J.* **2015**, 21, 536-540; e) V. Havel, J. Svec, M.

- Wimmerova, M. Dusek, M. Pojarova, V. Sindelar, *Org. Lett.* **2011**, *13*, 4000-4003; f) J. Svec, M. Necas, V. Sindelar, *Angew. Chem. Int. Ed.* **2010**, *49*, 2378-2381.
- [89] M. Dinç, Ö. Metin, S. Özkar, *Catalysis Today* **2012**, *183*, 10-16.
- [90] L. Huang, X. Weng, Z. Chen, M. Megharaj, R. Naidu, *Spectrochim. Acta A* **2014**, *117*, 801-804.
- [91] a) K. Stensrud, J. Noh, K. Kandler, J. Wirz, D. Heger, R. S. Givens, *J. Org. Chem.* **2009**, *74*, 5219-5227; b) R. S. Givens, D. Heger, B. Hellrung, Y. Kamdzhilov, M. Mac, P. G. Conrad II, E. Cope, J. I. Lee, J. F. Mata-Segreda, R. L. Schowen, J. Wirz, *J. Am. Chem. Soc.* **2008**, *130*, 3307-3309.
- [92] a) R. S. Givens, K. Stensrud, P. G. Conrad, A. L. Yousef, C. Perera, S. N. Senadheera, D. Heger, J. Wirz, *Can. J. Chem.* **2011**, *89*, 364-384; b) R. S. Givens, J. F. W. Weber, P. G. Conrad, G. Orosz, S. L. Donahue, S. A. Thayer, *J. Am. Chem. Soc.* **2000**, *122*, 2687-2697; c) R. S. Givens, A. Jung, C.-H. Park, J. Weber, W. Bartlett, *J. Am. Chem. Soc.* **1997**, *119*, 8369-8370; c) R. S. Givens, C.-H. Park, *Tetrahedron Lett.* **1996**, *37*, 6259-6262.
- [93] P. Šebej, B. H. Lim, B. S. Park, R. S. Givens, P. Klán, *Org. Lett.* **2011**, *13*, 644-647.
- [94] W. Chai, A. Takeda, M. Hara, S.-J. Ji, C. A. Horiuchi, *Tetrahedron* **2005**, *61*, 2453-2463.
- [95] R. S. Givens, M. Rubina, K. F. Stensrud, *J. Org. Chem.* **2013**, *78*, 1709-1717.
- [96] N. S. Hush, J. Zeng, J. R. Reimers, J. S. Craw, in *Photochemistry and Radiation Chemistry*, ed. J. F. Wishart, D. G. Nocera, American Chemical Society, Washington DC, USA, **1998**, 263-277.
- [97] H. Herrmann, *Phys. Chem. Chem. Phys.*, **2007**, *9*, 3935-3964.
- [98] I. M. Kolthuff, T. S. Lee, D. S. Leussing, *Anal. Chem.*, **1948**, *20*, 985-985.
- [99] E. B. Sandell, in *Colorimetric Determination of Trace Metals*, Interscience Publishers, New York, USA, **1950**, 375-378.

- [100] a) Y. Zhou, J. Wang, Z. Gu, S. Wang, W. Zhu, J. L. Aceña, V. A. Soloshonok, K. Izawa, H. Liu, *Chem. Rev.* **2016**, *116*, 422-518; b) *Fluorine in Pharmaceutical and Medicinal Chemistry. From Biophysical Aspects to Clinical Applications*, ed. V. Gouverneur and K. Müller, ICP: Oxford, **2012**; c) W. K. Hagmann, *J. Med. Chem.* **2008**, *51*, 4359-4369; d) K. Müller, C. Faeh, F. Diederich, *Science* **2007**, *317*, 1881-1886.
- [101] C. Alonso, E. Martínez de Marigorta, G. Rubiales, F. Palacios, *Chem. Rev.* **2015**, *115*, 1847-1935.
- [102] See for exhaustive reviews: a) T. Koike, M. Akita, *Acc. Chem. Res.* **2016**, *49*, 1937-1945; b) S. Barata-Vallejo, S. M. Bonesi, A. Postigo, *Org. Biomol. Chem.* **2015**, *13*, 11153-11183. For recent examples see: c) J. Lin, Z. Li, J. Kan, S. Huang, W. Su, Y. Li, *Nat. Commun.* **2017**, *8*, 14353; d) M. Daniel, G. Dagousset, P. Diter, P.-A. Klein, B. Tuccio, A.-M. Goncalves, G. Masson, E. Magnier, *Angew. Chem. Int. Ed.* **2017**, *56*, 3997-4001; e) J. W. Beatty, J. J. Douglas, K. P. Cole, C. R. J. Stephenson, *Nat. Commun.* **2015**, *6*, 7919; f) L. Cui, Y. Matusaki, N. Tada, T. Miura, B. Uno, A. Itoh, *Adv. Synth. Catal.* **2013**, *355*, 2203-2207; g) D. A. Nagib, D. W. C. MacMillan, *Nature* **2011**, *480*, 224-228.
- [103] a) D. Wang, G.-J. Deng, S. Chen, H. Gong, *Green Chem.* **2016**, *18*, 5967-5970; b) S. Zhong, A. Hafner, C. Hussal, M. Nieger, S. Bräse, *RSC Adv.* **2015**, *5*, 6255-6258; c) A. Sato, J. Han, T. Ono, A. Wzorek, J. L. Aceña, V. A. Soloshonok, *Chem. Commun.* **2015**, *51*, 5967-5970; d) A. Studer, *Angew. Chem. Int. Ed.* **2012**, *51*, 8950-8958; e) Y. Ji, T. Brueckl, R. D. Baxter, Y. Fujiwara, I. B. Seiple, S. Su, D. G. Blackmond, P. S. Baran, *Proc. Natl. Acad. Sci. U. S. A.* **2011**, *108*, 14411-14415.
- [104] a) Y. Wang, J. Wang, G.-X. Li, G. He, G. Chen, *Org. Lett.* **2017**, *19*, 1442-1445; b) L. Li, X. Mu, W. Liu, Y. Wang, Z. Mi, C.-J. Li, *J. Am. Chem. Soc.* **2016**, *138*, 5809-5812; c) G. Filippini, M. Nappi, P. Melchiorre, *Tetrahedron* **2015**, *71*, 4535-4542; d) K. L. Kirk, M.

- Nishida, S. Fujii, H. Kimoto, *J. Fluorine Chem.* **1992**, *59*, 197-202; e) M. Nishida, H. Kimoto, S. Fujii, Y. Hayakawa, L. A. Cohen, *Bull. Chem. Soc. Jpn.* **1991**, *64*, 2255-2259; f) V. M. Labroo, R. B. Labroo, L. A. Cohen, *Tetrahedron Lett.* **1990**, *40*, 5705-5708; g) T. Akiyama, K. Kato, M. Kajitani, Y. Sakaguchi, J. Nakamura, H. Hayashi, A. Sugimori, *Bull. Chem. Soc. Jpn.* **1988**, *61*, 3531-3537; h) H. Kimoto, S. Fujii, L. A. Cohen, *J. Org. Chem.* **1984**, *49*, 1060-1064; i) H. Kimoto, S. Fujii, L. A. Cohen, *J. Org. Chem.* **1982**, *47*, 2867-2872; j) Y. Kobayashi, I. Kumadaki, A. Ohsawa, S.-I. Murakami, T. Nakano, *Chem. Pharm. Bull.* **1978**, *26*, 1247-1249.
- [105] M. C. Quattrini, S. Fujii, K. Yamada, T. Fukuyama, D. Ravelli, M. Fagnoni, I. Ryu, *Chem. Commun.* **2017**, *53*, 2335-2338.
- [106] a) W. R. Dolbier Jr., *Chem. Rev.* **1996**, *96*, 1557-1584; b) X.-K. Jiang, G.-Z. Ji, J. R.-Y. Xie, *J. Fluorine Chem.* **1996**, *79*, 133-138; c) D. V. Avila, K. U. Ingold, J. Lustyk, W. R. Dolbier Jr., H. Q. Pan, *J. Am. Chem. Soc.* **1994**, *116*, 99-104.
- [107] a) S. P. Pitre, C. D. McTiernan, H. Ismaili, J. C. Scaiano, *ACS Catal.* **2014**, *4*, 2530-2535; b) Y. Ye, S. H. Lee, M. S. Sanford, *Org. Lett.* **2011**, *13*, 5464-5467.
- [108] M. S. Wiehn, E. V. Vinogradova, A. Togni, *J. Fluorine Chem.* **2010**, *131*, 951-957.
- [109] a) T. M. Sokolenko, K. I. Petko, L. M. Yagupolskii, *Chem Heterocycl. Compd.* **2009**, *45*, 430-435; b) G. Bissky, G.-V. Rösenthaller, E. Lork, J. Barten, M. Médebielle, V. Staninets, A. A. Kolomeitsev, *J. Fluorine Chem.* **2001**, *109*, 173-181.
- [110] For a recent review see: J. P. Monteiro, M. G. Alves, P. F. Oliveira, B. M. Silva, *Molecules* **2016**, *21*, 974.
- [111] For a review on flow photochemistry, see: a) D. Cambié, C. Bottecchia, N. J. W. Straathof, V. Hessel, T. Noël, *Chem. Rev.* **2016**, *116*, 10276-10341; for recent applications, see: b) D. Cambié, F. Zhao, V. Hessel, M. G. Debije, T. Noël, *Angew. Chem.*

- Int. Ed.* **2017**, *56*, 1050- 1054; c) L. Capaldo, M. Fagnoni, D. Ravelli, *Chem. Eur. J.* **2017**, *23*, 6527-6530.
- [112] a) M. Bergami, S. Protti, D. Ravelli, M. Fagnoni, *Adv. Synth. Catal.* **2016**, *358*, 1164-1172; b) F. Bonassi, D. Ravelli, S. Protti, M. Fagnoni, *Adv. Synth. Catal.* **2015**, *357*, 3687-3695.
- [113] C. Lai, T. E. Mallouk, *J. Chem. Soc. Chem. Commun.* **1993**, 1359-1361.
- [114] E. R. Morris, J. C. J. Thynne, *Trans. Faraday Soc.* **1968**, *64*, 414-421.
- [115] For recent examples on oxidation of azoles followed by radical coupling see: a) L. Zhang, H. Yi, J. Wang, A. Lei, *J. Org. Chem.* **2017**, *82*, 10704-10709; b) H. Aruri, U. Singh, M. Kumar, S. Sharma; S. K. Aithagani, V. K. Gupta, S. Mignani, R. A. Vishwakarma, P. P. Singh, *J. Org. Chem.* **2017**, *82*, 1000-1012; c) J. Zhao, P. Li, C. Xia, F. Li, *Chem. Commun.* **2014**, *50*, 4751-4754.
- [116] M. Oelgemöller, *Chem. Rev.* **2016**, *116*, 9664-9682.
- [117] R. H. Munday, J. R. Martinelli, S. L. Buchwald, *J. Am. Chem. Soc.* **2008**, *130*, 2754-2755.
- [118] J.-i. Kuroda, K. Inamoto, K. Hiroya, T. Doi, *Eur. J. Org. Chem.* **2009**, 2251-2261.
- [119] J. H. Choi, B. C. Lee, H. W. Lee, I. Lee, *J. Org. Chem.* **2002**, *67*, 1277-1281.
- [120] H.-D. Choi, P.-J. Seo, B.-W. Son, *Arch. Pharm. Res.* **2002**, *25*, 786-789.
- [121] R. Lis, A. J. Marisca, *J. Org. Chem.* **1987**, *52*, 4377-4379.
- [122] M. Yamagishi, K. Nishigai, A. Ishii, T. Hata, H. Urabe, *Angew. Chem., Int. Ed.* **2012**, *51*, 6471-6474.
- [123] F. Buckingham, S. Calderwood, B. Checa, T. Keller, M. Tredwell, T. L. Collier, I. M. Newington, R. Bhalla, M. Glaser, V. Gouverneur, *J. Fluorine Chem.* **2015**, *180*, 33-39.
- [124] B. R. Rosen, J. C. Ruble, T. J. Beauchamp, A. Navarro, *Org. Lett.* **2011**, *13*, 2564-2567.
- [125] N. A. Isley, S. Dobarco, B. H. Lipshutz, *Green Chem.* **2014**, *16*, 1480-1488.

- [126] P. S. Dragovich, D. E. Murphy, C. V. Tran, F. Ruebsam, *Synth. Commun.* **2008**, *38*, 1909-1916.
- [127] a) U. Kloeckner, B. J. Nachtsheim, *Chem. Commun.* **2014**, *50*, 10485-10487; b) C. Laurence, M. Berthelot, M. Lucon, Y. Tsuno, *Spectrochim. Acta A* **1982**, *38*, 791-796.
- [128] E. Hernando, R. R. Castillo, N. Rodríguez, R. G. Arrayás, J. C. Carretero, *Chem. Eur. J.* **2014**, *20*, 13854-13859.
- [129] L. Chu, X. C. Wang, C. E. Moore, A. L. Rheingold, J. Q. Yu, *J. Am. Chem. Soc.* **2013**, *135*, 6344–16347.
- [130] J. F. King, J. Y. L. Lam, S. Skonieczny, *J. Am. Chem. Soc.* **1992**, *114*, 1743-1749.
- [131] L. Cardelli, L. Greci, P. Stipa, C. Rizzoli, P. Sgarabotto, F. Ugozzoli, *J. Chem. Soc., Perkin Trans. 2* **1990**, 1929-1934.
- [132] L. Chen, H. Lang, L. Fang, M. Zhu, J. Liu, J. Yu, L. Wang, *Eur. J. Org. Chem.* **2014**, 4953-4957.
- [133] R. L. Shriner, M. T. Goebel, C. S. Marvel, *J. Am. Chem. Soc.* **1932**, *54*, 2470-2476.
- [134] A. Yasuhara, M. Kameda, T. Sakamoto, *Chem. Pharm. Bull.* **1999**, *47*, 809-812.
- [135] C. W. Y. Chung and, P. H. Toy, *Tetrahedron* **2005**, *61*, 709–715.
- [136] C. Almansa, J. Alfón, A. F. de Arriba, F. L. Cavalcanti, I. Escamilla, L. A. Gómez, A. Mirrales, R. Soliva, J. Bartrolí, E. Carceller, M. Merlos, J. García-Rafanell, *J. Med. Chem.* **2003**, *46*, 3463–3475.
- [137] S. Caddick, J. D. Wilden, D. B. Judd, *J. Am. Chem. Soc.* **2004**, *126*, 1024-1025.
- [138] a) S. Bollanti, P. Di Lazzaro, F. Flora, L. Mezi, D. Murra, A. Torre, *High Power Laser Science and Engineering* **2015**, *3*, e29; b) P. Zuppella, A. Reale, A. Ritucci, P. Tucceri, S. Prezioso, F. Flora, L. Mezi, P. Dunne, *Plasma Sources Sci. Technol.* **2009**, *18*, 025014.
- [139] D. Merli, L. Pretali, E. Fasani, A. Albini, A. Profumo, *Electroanal.* **2011**, *23*, 2364-2372.

- [140] W. R. Heineman, P. T. Kissinger, in *Laboratory techniques in electroanalytical chemistry*, ed. P. T. Kissinger, W. R. Heineman, Dekker, New York, **1996**, 51-126.
- [141] D. Madea, T. Slanina, P. Klán, *Chem Commun* **2016**, 52, 12901-12904.
- [142] a) P. Klahn, H. Erhardt, A. Kotthaus, S. F. Kirsch, *Angew. Chem. Int. Ed.* **2014**, *53*, 7913-7917; b) C. T. Hoang, F. Bouillère, S. Johannesen, A. Zulauf, C. Panel, A. Pouilhès, D. Gori, V. Alezra, C. Kouklovsky, *J. Org. Chem.* **2009**, *74*, 4177-4187.
- [143] S. Stavber, M. Jereb, M. Zupan, *Chem. Commun.* **2002**, 488-489.
- [144] R. Zhu, B. Wang, M. Cui, J. Deng, X. Li, Y. Ma, Y. Fu, *Green Chem.* **2016**, *18*, 2029-2036.
- [145] a) D. Ravelli, S. Protti, M. Fagnoni, *Acc. Chem. Res.* **2016**, *49*, 2232-2242; b) S. Protti, D. Ravelli, M. Fagnoni, A. Albini, *Chem. Commun.* **2009**, 7351-7353.
- [146] N. V. Kirij, A. A. Filatov, G. Yu. Khrapach, Y. L. Yagupolskii, *Chem. Commun.* **2017**, *53*, 2146-2149.
- [147] S. Mizuta, I. S. R. Stenhagen, M. O'Duill, J. Wolstenhulme, A. K. Kirjavainen, S. J. Forsback, M. Tredwell, G. Sandford, P. R. Moore, M. Huiban, S. K. Luthra, J. Passchier, O. Solin, V. Gouverneur, *Org. Lett.* **2013**, *15*, 2648-2651.
- [148] T. Kino, Y. Nagase, Y. Ohtsuka, K. Yamamoto, D. Uraguchi, K. Tokuhisa, T. Yamakawa, *J. Fluorine Chem.* **2010**, *131*, 98-105.
- [149] Y. Wu, H.-R. Zhang, R.-X. Jin, Q. Lan, X.-S. Wang *Adv. Synth. Catal.* **2016**, *358*, 3528-3533.
- [150] K. A. Jacobson, D. Shi, C. Gallo-Rodriguez, M. Manning Jr., C. Müller, J. W. Daly, J. L. Neumeyer, L. Kiriasis, W. Pfeleiderer, *J. Med. Chem.* **1993**, *36*, 2639-2644.
- [151] K. Hirota, M. Sako, H. Sajiki, *Heterocycles* **1997**, *46*, 547-554.

- [152] K. Natte, R. V. Jagadeesh, L. He, J. Rabeah, J. Chen, C. Taeschler, S. Ellinger, F. Zaragoza, H. Neumann, A. Brückner, M. Beller, *Angew. Chem. Int. Ed.* **2016**, *55*, 2782-2786.